Targeting Ectopic Hsp90 in Breast Cancer

by

Jared James Barrott

Department of Pharmacology and Cancer Biology
Duke University

Date:_____

Approved:

_____
Timothy A. J. Haystead, Supervisor

_____
H. Kim Lyerly

_____
Dennis Thiele

_____
Bernard Mathey-Prevot

Dissertation submitted in partial fulfillment of
the requirements for the degree of Doctor
of Philosophy in the Department of
Pharmacology and Cancer Biology in the Graduate School
of Duke University

2014

ABSTRACT

Targeting Ectopic Hsp90 in Breast Cancer

by

Jared James Barrott

Department of Pharmacology and Cancer Biology
Duke University

Date:_____

Approved:

_____
Timothy A. J. Haystead, Supervisor

_____
H. Kim Lyerly

_____
Dennis Thiele

_____
Bernard Mathey-Prevot

An abstract of a dissertation submitted in partial
fulfillment of the requirements for the degree
of Doctor of Philosophy in the Department of
Pharmacology and Cancer Biology in the Graduate School of
Duke University

2014

Abstract

On the surface heat shock protein 90 (Hsp90) is an unlikely drug target for the treatment of any disease, let alone cancer. Hsp90 is highly conserved and ubiquitously expressed in all cells. There are four major isoforms encoded by distinct genes and together they may constitute 1–3% of the cellular protein. Genetic deletion results in nonviable phenotypes in some organisms, and there are no recognized polymorphisms suggesting an association or causal relationship with any human disease. With respect to cancer, the proteins absence from some recent high profile articles underlines the perception that it is an unlikely bona fide target to treat this disease. Yet, to date, there are 17 distinct Hsp90 inhibitors in clinical trials for multiple indications in cancer. The protein has been championed for over 20 years by the National Cancer Institute as a cancer target since the discovery of the antitumor activity of geldanamycin. Rather than focus on the intracellular inhibition of Hsp90, we have shifted our aim to the differences of Hsp90 between cancer and normal tissue, namely its extracellular expression.

My graduate thesis work has focused on the characterization of a series of novel small molecule imaging agents (fluor-tethered Hsp90 inhibitors) that enable the specific detection of ectopically expressed Hsp90 on tumor cells. We believe that these molecules will have a large impact in the near future on the diagnosis and treatment of metastatic breast cancer as well as other cancers. This hypothesis is based on recent findings in the

clinical literature that have linked upregulation of Hsp90 with poor outcomes in multiple subtypes of breast cancer. Additionally, several papers have also reported an association of the expression of extracellular Hsp90 and metastatic progression in several human cancers. Hsp90 is currently considered by some as a cutting edge cancer drug target. The Haystead lab synthesized a series of tethered Hsp90 inhibitors that were modified with fluorophores and other imaging moieties in such a way as to preserve the binding to Hsp90 and enable detection through non-invasive imaging techniques. In a series of cell-based, live animal and biochemical studies we demonstrated that these molecules are highly selective for Hsp90 and can be used to specifically recognize intact tumor cells expressing ectopic Hsp90. Furthermore, we also observed that once bound to ectopic Hsp90, our tethered-inhibitors are actively internalized and this process can be blocked with Hsp90 antibodies. These findings have two implications; first, Hsp90 is undergoing active cycling at the plasma membrane; second, the finding that once bound to surface Hsp90 our fluor-tethered inhibitors can be internalized despite their polar nature. These results suggest a new therapeutic strategy that will enable specific delivery of tumor killing agents (e.g. ^{131}I or metabolic poisons) to metastatic cells. This is unique because the use of small molecule inhibitors and not antibody- or nanoparticle-based payload delivery strategies offers advantages in formulation, cost and reproducibility.

In addition to payload delivery possibilities, we also show the utility of the tethered-inhibitors diagnostically by demonstrating their use in the detection of tumors in mouse models of human breast cancer. As a result of our animal studies, we believe our molecules in their present form could be used to address a currently unmet need in the early diagnosis of aggressive breast cancer and discriminating this from more indolent forms.

Furthermore, the tethered Hsp90 inhibitors have been used to make ligand affinity chromatography resins that have facilitated the discovery of other unique Hsp90 expressions and functions associated with cancer. We have found a pool of Hsp90 that is misfolded as determined by affinity chromatography depletion and a leftward thermal stability shift in the population of Hsp90 that flows through the ligand affinity resins. Differential trypsin digest patterns detected by mass spectrometry reveal also that the native protein has sites that are more accessible to trypsinization. This could have further implications in treating and detecting differences between cancerous tissues and normal tissues by designing an antibody that recognizes the exposed portions of the misfolded Hsp90. Together this body of work illustrates that not only is Hsp90 different in total expression levels in cancers, but is ectopically expressed and misfolded so as to provide other opportunities for therapeutic intervention that improve the safety for more clinical applications.

Dedication

I dedicate this work to my loving and supporting wife and children.

Contents

List of Tables

List of Figures

List of Abbreviations

Hsp90	heat shock protein 90
Grp94	glucose-regulated protein 94
TRAP1	tumor necrosis factor receptor associated protein 1
TPR	tetratricopeptide repeat
CHIP	C-terminus of Hsp70 interacting protein
Hop	Hsp70/Hsp90 organizer protein
Cyp40	cyclophilin 40
FKPB	FK506-binding protein
Aha1	activator of heat shock 90kDa protein ATPase homolog 1
HSF	heat shock factor
HDAC	histone deacetylase
Ppt1	Palmitoyl-protein thioesterase 1
PP5	Protein phosphatase 5
CK2	Casein kinase 2
Swe1	saccharomyces wee1 homologue
Yes	Yamaguchi Sarcoma Viral Oncogene Homolog 1
DNA-PK	DNA-dependent protein kinase
B-Raf	v-raf murine sarcoma viral oncogene homolog B1
PKA	protein kinase A

eNOS	endothelial nitric oxide synthase
ER	estrogen receptor
Her2	human epidermal growth factor receptor 2
Bcr-Abl	breakpoint cluster region-Abelson
MMP-2	matrix metalloproteinase-2
tPA	tissue plasminogen activator
mDia2	diaphanous-related formin-3
RhoA	Ras homolog gene family member A
ALK	anaplastic lymphoma kinase
CML	chronic myelogenous leukemia
CLL	chronic lymphocytic leukemia
NSCLC	non-small cell lung carcinoma
IHC	immunohistochemistry
FRET	fluorescence resonance energy transfer
ECFP	enhanced cyan fluorescent protein
EYFP	enhanced yellow fluorescent protein
FAD	flavin adenine dinucleotide
SCID	severe combined immunodeficiency
PEG	polyethylene glycol
PET	positron emission tomography

RDH12	retinol dehydrogenase 12
PERK	protein kinase RNA-like endoplasmic reticulum kinase
XBP-1	X-box binding protein 1
ATF6	activating transcription factor 6
TNF	tumor necrosis factor
DMSO	dimethyl sulfoxide
APC	antigen presenting cell
CTL	cytotoxic T lymphocytes
MHC	major histocompatibility complex
DMA	dimethyl amiloride
LRP1	low density lipoprotein receptor-related protein 1
TGFα	transcription growth factor alpha
EMT	epithelial-mesenchymal transition
Hif-1α	hypoxia inducible factor 1 alpha
AD	Alzheimer's disease

Acknowledgements

First and foremost, I would like to thank and acknowledge the dedicated companionship of my wife, Keri, throughout these years of graduate school. She has been my anchor in the many ups and downs of graduate school and scientific research, always reminding me of my long-term goals and what is most important in life. I want to thank her for the joy she brings me by raising four beautiful children: Elise, Packer, Spencer and Taylor. They have been a great source of motivation to press forward when times get tough.

Secondly, I want to thank Tim for giving me opportunities that were challenging and rewarding and having confidence in my abilities despite my shortcomings. Additionally, Tim has always been easy to talk to about science and life, and I always left with a greater enthusiasm for science as I caught glimpses of the vision he frequently shared for his research. He is truly a visionary scientist.

Next, I would not have enjoyed my experiences in the Haystead lab as much if not for the exceptional individuals that I was able to interact with daily. I want to thank Yazan for his meticulous details and protocols. I want to thank Lauren for picking up the project and carrying on the exciting findings of Hsp90 biology in cancer. Also I appreciate Matt for inheriting the "Brittany curse," because I was sure that if anyone would catch that bad luck it would be someone as accident prone as me. Guess not. Aaron has been a true friend both in and out of the lab and for that I am deeply grateful.

I want to thank Dave and Dave for their positive contributions and optimism for my project. They have also acted as surrogate big brothers and were willing to help with many aspects of my life. Last but not least in the lab, I want to thank Phil for being my chemistry tandem throughout this project. The daily doses of Phil have kept me grounded at all times and has given me an example of someone who is passionate about learning and sharing knowledge with others (we just wish you would not have shared the rule of three with Tim).

To the many collaborators on this project, I am indebted to your services. Many hands make light work, and this project could not have taken off the way it did without members of the Lyerly lab, specifically Takuya Osada, members of the Zalutsky lab, specifically Ganesan Vaidyanathan, and the Ramanujam lab.

I am also very appreciative of the members of my thesis committee who have given so graciously of their time and ideas to make this project better. Dr. Lyerly has given me unwavering support, resources and training throughout my project. Dr. Thiele has been an excellent mentor and teacher, and I want to thank him for including me in his social circles. Dr. Mathey-Prevot has mentored me through class grant proposals and given great classroom instruction in regard to cancer signaling networks.

Finally, I would be remiss if I did not thank my parents and my wife's parents for their emotional and financial support. Without their contributions and encouraging words, graduate life would have been vastly different.

1. Introduction

Undoubtedly, any protein or gene of interest that has relevance to cancer will receive superfluous recommendations to pursue it pharmacologically. Heat shock protein 90 (Hsp90) is no exception. With each new interaction and publication about Hsp90 there is augmenting enthusiasm to pursue clinical applications. The fact of the matter is that Hsp90 inhibitors are being pursued and advancing through clinical trials and their applications toward multiple cancers are expanding. Despite these successes, a few recent high-profile articles on the mechanisms of cancer have overlooked this already established therapeutic target, and it does not appear to be an anomaly with the authors of these cancer reviews[1,2]. Many cancer pharmacologists are often blindsided by the clinical trial data or even the notion that one could target an abundant chaperone protein, such as Hsp90 that has no known disease-linked polymorphisms[3,4]. On the surface this seems reasonable, how could one pharmacologically target a protein that is essential for normal cell viability and has a documented interactome that involves over 400 putative clients and over a dozen cellular pathways and processes?

Because it was hard to envision any clinical success at first, the application of Hsp90 inhibitors was relinquished to purely academic exercises as pharmaceutical companies considered it inconsequential. However, despite the high abundance and pleiotropic effects of Hsp90 protein-protein interactions, Hsp90 inhibitors have advanced into clinical trials. Counterintuitively, the aspects that at first made Hsp90

inhibitors seem inappropriate are now demonstrating advantages over single target therapies, and the potential of combination therapies that include Hsp90 inhibitors should effectively prevent or prolong the development of cancer drug resistance that is commonly seen with tyrosine kinase inhibitors and other target-based therapies[5-7].

To underline the improved successes of Hsp90 inhibitors, we highlight results published for ganetespib, an Hsp90 inhibitor developed by Synta Pharmaceuticals (Lexington, MA, USA). In in vitro tumor cytotoxicity studies, it was shown that a five minute exposure to ganetespib at 1 μM (a readily achievable plasma level in vivo) was sufficient to induce cell death within 72 hours. This suggests that a brief exposure to Hsp90 inhibitors results in a permanent and lasting effect on the cell. These observations extend to animal studies. A single weekly dose of 100-150 mg/kg for 3 weeks resulted in 50-90% tumor reduction in solid and hematological xenograft models[8]. Most importantly, in recent clinical studies it was also shown that once weekly ganetespib treatment in patients with non-small cell lung carcinoma (NSCLC) resulted in a 50% overall response rate[9,10]. Development of ganetespib in many ways is therefore a good example of how second generation synthetic Hsp90 inhibitors are surpassing their first generation geldanamycin-based counterparts. Ganetespib not only shows increased efficacy and improved formulation over the geldanamycins, but also significantly reduced cardiovascular and hepatotoxicity side effects[8]. In our view such consistent advances are a testament to the validity of Hsp90 as a druggable target. While safety for

off target effects is being improved and desired tumor effects continue to progress, the mechanisms for Hsp90 targeting in tumors over Hsp90 found in normal tissue is less understood.

1.1 Hsp90, the basics

To frame this thesis, I offer a brief overview of the basics of Hsp90 and its known biology and then address the distinguishing characteristics of Hsp90 between cancer cells and normal cells. Hsp90 plays an essential role in maintaining cellular protein homeostasis by acting as a molecular chaperone to aid in folding as well as in intracellular trafficking of its protein clients[11,12]. It is expressed as a 90 kDa protein (Hsp90α 732 aa; Hsp90β 724 aa) in the cytosol and the nucleus and contains an N-terminal ATP binding domain that is essential for most of its cellular functions[13]. ATP hydrolysis is thought to drive various conformational changes within Hsp90 and this process is highly regulated by interactions with co-chaperones and possibly a variety of posttranslational modifications (Table 1)[12,14]. Through these mechanisms the apparent ubiquitous cellular chaperone functions of Hsp90 are thought to be acutely regulated.

Much effort has been seen in the past two decades to characterize the specific protein interactions with other proteins termed co-chaperones. Co-chaperones assist Hsp90 throughout its conformational cycling that is required for its normal function, act as substrate recognition proteins and even provide additional enzymatic activity. The predominant class of co-chaperones is the tetratricopeptide repeat domain (TPR)-

containing proteins, which bind the MEEVD motif found in the C-terminus of Hsp90[15-18]. Among the co-chaperones with a TPR domain are CHIP, Hop, Cyp40, FKPBs and PP5. While most co-chaperones facilitate the recruitment of other substrate proteins, some of these co-chaperones add enzymatic functionality to the chaperone complex as is the case for the isomerases, phosphatases, and ligases[19-21]. Other co-chaperones that interact with Hsp90 via alternative domains are Aha1, which enhances the function of Hsp90 by stimulating its ATPase activity[22,23]. The co-chaperone that is most implicated in facilitating tumorigenesis is Cdc37 because it associates with mutant kinases that drive cancer progression[24]. Recently it was shown that the Hsp90-Cdc37 complex binds two-thirds of the kinome to varying degrees, while at the same time demonstrating negligible interactions with ligases and transcription factors[25]. Another co-chaperone that is responsible for the complexing of nuclear hormone receptors and Hsp90 is p23. However, its interactions are not as limited as Cdc37, as p23 has been found in a broad range of Hsp90-client complexes[26-29]. Unlike the activating co-chaperone, Aha1, the co-chaperones Cdc37, p23, and Hop inhibit ATPase activity. These co-chaperones therefore add another layer of regulation of this multifaceted master chaperone, underling the complexity of the Hsp90 chaperone cycle and its folding functions. Hsp90 is also regulated transcriptionally, primarily through direct interactions with the transcription factor HSF[30]. Despite its high level of expression in normal cells, cellular stresses such as

heat shock (37°C to 42°C) have been reported to induce Hsp90 protein levels by as much as two fold[31].

Two other immediate family members, Glucose Regulated Protein 94 (Grp94) and TNF Receptor Associated Protein 1 (TRAP1), share sequence similarity in the ATP binding domain and are also thought to act as cellular chaperones to promote protein stability and folding either in the mitochondria (TRAP1) or endoplasmic reticulum (Grp94), albeit they do not exemplify the same complexity and vast interactions that Hsp90 exhibits[32]. Like Hsp90, Grp94 and TRAP1 contain an N- terminal ATP binding domain and ATPase activity that is also necessary for cellular function[33-36]. Unlike Hsp90, the list of client proteins interacting with either Grp94 or TRAP1 is much more limited and less well defined. Several groups have proposed that Grp94 and TRAP1 are additional potential targets that can be exploited as cancer chemotherapies, although selective inhibitors of these proteins have yet to show clinical promise.

A surprising and common finding with most Hsp90 inhibitors is their selectivity for certain tumor cells and not other cells. With few exceptions in vivo, most cancer cells are more sensitive to Hsp90 inhibition than non-transformed cells and non-toxic doses demonstrate anticancer activity. In animals and humans, Hsp90 inhibitors consistently accumulate in tumors whereas they are rapidly cleared from plasma and do not appear to enter most tissues[37-43]. One notable exception may be the retina. Although idiosyncratic in nature, a reversible ocular toxicity has been observed in some patients

with some but not all Hsp90 inhibitors[44]. Generally this occurs at higher dosing or after prolonged exposure and manifests as a loss of night vision. Drug withdrawal or dose reduction usually reverses the symptoms. However, the idiosyncratic nature of the phenomenon suggests that the mechanisms of drug accumulation in the retina may be different from tumor cells and perhaps related to some underlying eye pathology in patients that are most susceptible. Alternatively, the structural variations of different Hsp90 inhibitors permit varying degrees of cellular uptake, with the retina being more susceptible than most other tissues. The fact that certain tumor cells preferentially absorb Hsp90 inhibitors strongly suggests that specific mechanisms exist within these cells that contribute to the druggability of Hsp90. One early hypothesis suggested that in tumor cells Hsp90 preferentially exists in chaperone complexes and these multiprotein complexes were reported to exhibit a higher affinity for Hsp90 inhibitors as well as higher ATPase activity[45]. Experiments with affinity resins based on immobilized Hsp90 inhibitors suggest a large imbalance of Hsp90 to its co-chaperones in both normal and transformed cells[46,47]. A simple mechanism that could explain the drug accumulation may be that tumor cells simply express more Hsp90 than normal cells. Certainly, transformation has been shown to induce expression of Hsp90 at the protein level and this can also be measured in tumors isolated from patients. However, even in the most extreme case the fold inductions are 2-3 fold at best at the protein level. As discussed, in normal cells Hsp90 is thought to constitute 1-2% of the cellular protein and

many believe that high expression of Hsp90 is evolutionarily conserved. Indeed, normal Hsp90 expression levels beg the question as to why tumor cells would need to induce more expression of the protein. We align our theory with others that the abundance of Hsp90 is evolutionarily conserved for a purpose and not wastefully guarded to bewilder scientists. If we can come to an understanding of the mechanisms that accentuate the tumor differences, Hsp90 inhibitors could be universally employed to fight the constantly evolving battle on cancer.

In this introduction I will discuss the mechanisms that differentiate tumor Hsp90 from the Hsp90 that is abundantly expressed in normal tissues, thereby making it a druggable cancer target. The three mechanisms, not mutually exclusive, that are the most important in distinguishing Hsp90 in cancer cells from Hsp90 in non-transformed cells are (1) the induction of Hsp90 mRNA and protein (2) the activation of the protein through either client association or post-translational modifications (3) the localization to ectopic cellular compartments (Figure 1). As we understand more clearly the mechanistic differences in tumor biology and normal cellular biology regarding Hsp90, the remaining hurdles for Hsp90 inhibitors to enter routine clinical practice will be overcome. For reviews on the current status of clinical applications of Hsp90 inhibitors see the following[37,48-53].

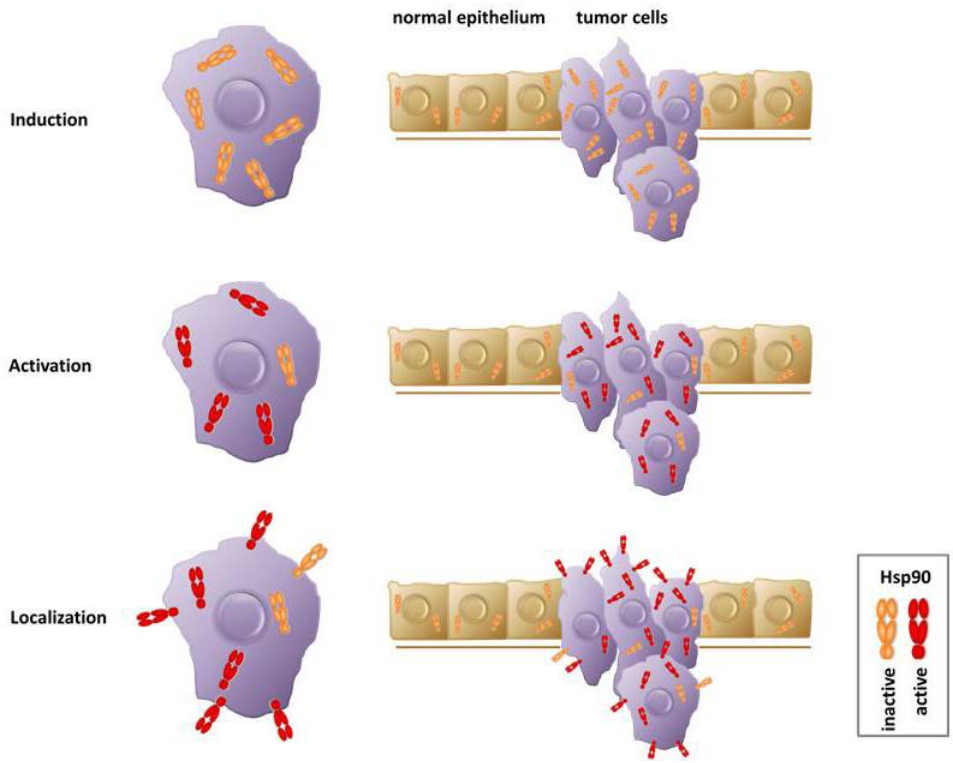

Figure 1: Differential patterns of expression of Hsp90 in cancer

1.2 Induction

First, we look at the differential expression of Hsp90. Few will argue that Hsp90 is overexpressed in tumors 2-3 fold higher than corresponding non-tumorigenic tissue, but even under basal conditions Hsp90 is abundant comprising 1-3% of the total cellular protein[46,51,54,55]. Hsp90 is upregulated in response to cellular stress imposed by heat, hypoxia and nutrient deprivation, which are commonly associated with the tumor microenvironment. Thus it has been proposed that Hsp90 upregulation in tumors is

essential to surviving the harsh microenvironment by allowing unstable mutations to persist that drive tumor malignancy[56].

In one of the strongest cases for clinical applications, hormone and protein kinase dependent breast cancer, Hsp90 expression levels have been well characterized and correlated to patient outcome of survival. First, Hsp90 expression in the breast has been recently evaluated immunohistochemically (IHC) for various types of tissue: normal, pre-malignant, and malignant. Hsp90 was shown to be expressed at higher levels in cancer tissues compared to non-cancer tissues[57]. Also Pick and colleagues performed IHC analysis of breast cancer cell lines and 655 primary breast cancers, including 331 ER^+ and 324 ER^- tumors, and found detectable Hsp90 expression in all of the breast cancer cell lines and in 90% of primary breast cancers. In addition, they reported that high expression of Hsp90 is associated with poor prognosis[58]. Because of the recognition of specific molecular subtypes of breast cancer, biostatisticians at Duke evaluated Hsp90 gene expression from profiles of over 4,000 breast cancer patients from 23 publically available gene expression databases, annotated with overall survival data from over 1,000 patients. They found a normal distribution of Hsp90 expression, and confirmed that high expression of Hsp90 was associated with a poor overall survival[59]. It has also been shown in melanomas, leukemia, and human colonic carcinoma, that Hsp90 is elevated in the transformed and even more malignant tumors[60-62]. Elevated levels are

also being detected in the serum of patients with non-small cell lung cancer and prostate cancer[63,64].

Based on these studies it is believed that high expression of Hsp90 represents an important oncogenic signaling node for malignant behavior in cancer and detecting upregulation or activation of Hsp90 in cancer cells could be an early indicator of malignant behavior. However, increased Hsp90 expression is not sufficient to explain the mechanisms that drive tumorigenicity. One discrepancy is that even though Hsp90 is elevated in breast tumors compared to normal breast tissue, there are other normal tissues such as the bladder, spleen, and brain that express higher Hsp90 in the ratio of total Hsp90:total protein[55,65]. This leads to the argument that there is something unique about the protein in cancer cells that distinguishes it from Hsp90 found in normal tissue. With hundreds of putative client proteins and over 30 sites where post-translational modifications can occur, one can easily envision a scenario where tumor Hsp90 proteins are poised to behave differently than normal Hsp90.

1.3 Activation

Hsp90 is implicated in cancer cell survival and growth through its transient interactions with client proteins. Over 400 clients have been thought to be identified thus far and many of these are involved in mediating signal transduction pathways that govern cellular growth, apoptotic evasion, differentiation, and metastasis[25,66-68]. For a

current and comprehensive list of reported Hsp90 protein interactions visit the Picard lab's website at http://www.picard.ch/Hsp90Int/index.php.

Due to the fact that Hsp90 inhibitors preferentially target tumors, one may infer that these drugs target a subset pool of Hsp90, and this subset exhibits a high affinity conformation of Hsp90 for the inhibitors. One possibility is that Hsp90 exists in a multichaperone complex with transformation-specific oncoproteins, such as classical mutant kinases, Her2 and Bcr-Abl. These proteins may represent a small fraction of the client proteins regulating the transformed phenotype. The latent Hsp90 complexes regulating normal misfolding processes and comprising at any time the majority of total cellular Hsp90 may not be effectively inhibited by these drugs at the relatively nontoxic doses used. Such an interpretation leads to the hypothesis that, under normal conditions, Hsp90 interacts with client proteins in a dynamic manner regulated by low-affinity binding and release of ATP and ADP. Upon mutation or deregulation, which is characteristic of the cancer phenotype, many of these client proteins may display unusually stable association with Hsp90, representing the active and druggable state.

A 2003 Nature paper by Kamal et al claimed that Hsp90 in tumors exist entirely in multi-chaperone complexes and that when Hsp90 is in these specific complexes it has higher ATPase activity and a 100-fold higher affinity for the inhibitor 17-AAG[45]. However, one incorrect assumption was that all Hsp90 has an equal opportunity of binding ATP or its mimetics that are immobilized to a bead. We and others have shown

that only a fraction (20-30%) of Hsp90 binds to ATP or its ligands. Radiolabeled PU-H71 also only labeled 30% of the Hsp90 in MDA-MB-468 cells and only half that in CML cells[46]. As far as co-chaperone involvement, Kamal et al demonstrated that when Hsp90 was reconstituted in vitro with Hsp70, Hsp40, Hop, and p23, the highest ATPase activity was observed. Moulick et al also showed that Hsp90 recognized by immobilized ligand precipitated the co-chaperones Hsp70, Hsp40, Hop, and Hip and that these co-chaperones were not found in the fraction of the antibody-isolated Hsp90, but they were found in the flow through[45,46]. It is thus hypothesized that the population of Hsp90 that binds to the ligand also exists in complex with several co-chaperones, but the "inactive" pool does not exist with co-chaperones. In their in vivo analysis they found that mouse tumors when compared to corresponding normal tissue do not differ that much in total Hsp90 levels as determined by western blotting. However, their ATPase activity was higher and their affinity for Hsp90 inhibitors was more[45], thus supporting that transformation and malignancy cannot be explained solely by the elevated expression of Hsp90. On the other hand, efforts to replicate this work have failed to show the exclusive complex of Hsp90 found in cancer. In regard to the complex having a higher affinity for Hsp90 inhibitors, it is believed to be an artifact of non-specific binding to the affinity resin. Our lab has shown that non-specific binding to an Hsp90 affinity resin decreases upon extending the ligand away from the immobilized bead. Hsp90 was cleanly and competitively eluted from the affinity resin[47], suggesting an alternative

hypothesis that when Hsp90 is in complex with an inhibitor that targets the ATP-binding domain, co-chaperones that should be in stoichiometric abundance are displaced and not recovered.

The studies to elucidate the client-chaperone interactions for Hsp90 are incomplete and provide little rationale for these interactions. For example, Hsp90 does not recognize an amino acid sequence that is common among the vast array of putative client proteins, nor do proteins within the same family that are structurally similar interact with Hsp90 in a comparable manner, such as is the case with EGFR and Her2. In the many criticisms that have been offered for the various approaches of identifying the Hsp90-client interaction, whether it is by immunoprecipitation, yeast two-hybrid assays, or mass spectrometry analysis, a recent study attempted to circumvent previous obstacles by expressing tagged potential client proteins (i.e. kinases, ligases, and transcription factors) with essential co-chaperones in order to study the interactions in a quantifiable manner. While no specific recognition sequence or structure was determined, the researchers concluded that a co-chaperone, Cdc37 in this case, provided a recognition of an as yet undefined fold and the thermal and conformational stability determined the extent of the interaction of Hsp90 with many of its kinase clients[25]. Cynically, one could also conclude from this study that any denatured protein is more likely to interact with Hsp90 than properly folded ones. Certainly the observation that inclusion of protein kinase inhibitors generally reduced binding to Hsp90 supports such

a notion. Expressed protein kinases are generally stabilized in the presence of ATP competitive inhibitors as reflected by an increase in thermal stability. In our experience, studies that use assays relying on affinity pull downs to study protein-protein interactions are fraught with artifacts and designing the appropriate controls to prove that interactions are real is not easy. Our own experience in the development of affinity resins targeting Hsp90 revealed the importance of carrying out appropriate controls in discriminating proteins that bind directly to Hsp90 versus those that are non-specific. We have shown that changing the linker that is used to immobilize an Hsp90 inhibitor can dramatically affect the patterns of proteins recovered from a cell extract (see page 81). One could conclude for example from the resin shown in the decane linker lane that this resin recovers a large amount of Hsp90 clients in addition to Hsp90. However, by blocking binding of Hsp90 itself to the affinity media by including a free Hsp90 inhibitor in the cell extract prior to mixing with the affinity resin shows that although recovery of Hsp90 is blocked, none of the other proteins are affected showing these are artifacts and have nothing to do with Hsp90[47]. Ultimately this has led us to develop a media that clearly recovers only Hsp90 and very little else including co-chaperones. We are somewhat perplexed by the absence of the Hsp90 interactome with this affinity resin, despite the observation that it clearly recovers Hsp90 in a competitive manner. Our own conclusions from these studies is that the Hsp90 interactome should be revisited using more rigorous controls such as including Hsp90 inhibitors in control extracts to

eliminate non-specific binding to the resin surface. We feel that such studies are likely to shorten the stable interactome considerably.

Having suggested that affinity based approaches might lead to misidentification of clients; other approaches examining client fate in the presence of an Hsp90 inhibitor may be more informative. Many studies that try to establish Hsp90 client associations evaluate the fate of the putative client after Hsp90 inhibition. Most often cited is the degradation of a given client, while those proteins that persist are thought not to be chaperoned by Hsp90. The best example of this phenomenon is the degradation of Her2 in breast cancer cell lines treated with Hsp90 inhibitors. We can acknowledge that by Western blot we can confirm recovery of Her2 with Hsp90 on our most selective Hsp90 resin[47]. Importantly, this recovery is blocked by the inclusion of an Hsp90 inhibitor in the cell extracts prior to mixing with the affinity media. We do note however, that the ratio of active drug bound Hsp90 recovered relative to Her2 is at least two orders of magnitude higher (Hsp90:HER2). As suggested in studies by Lindquist and colleagues, Hsp90 interacts with its clients transiently or with low affinity, at least in the drug bound state[25]. Client degradation approaches also have their caveats, for example it is common knowledge that the fate of unfolded proteins varies as some are degraded with differing kinetics and others form more stable aggregates when improperly folded. Thus, the lack of sensitivity to Hsp90 inhibition cannot fully explain the interactions or discredit client interactions. Additional caveats in establishing clients is that only a

fraction of Hsp90 is considered active due to its ability to bind inhibitors in its ATP-binding pocket leaving the remaining Hsp90 pool to continue its chaperoning functions.

With many uncertainties in the reported clients and no clear way to establish a transient interaction for a protein that is otherwise stable without the chaperoning functions of Hsp90, the nature of defining a general activated state of Hsp90 in cancer will continue to be difficult to attain. However, much progress is being made in the differences in cancer Hsp90 compared to normal tissue Hsp90 in regards to its post-translational modifications. These modifications are now demonstrating their effects in ATPase activity, as well as localization, which in turn are affecting the association Hsp90 has with other proteins. For a comprehensive list of reported modifications see Table 1. Hsp90 modifications that influence localization are highlighting some of the stronger differences that are being observed in cancer cells over normal tissue.

Table 1: Reported posttranslational modifications for Hsp90 and their effects on protein function

Modification	Hsp90α Residue	Enzyme	Result
4-HNE, 4-ONE	C572		Decreased client association[69]
Acetylation	K294	HDAC6	Decreased client association[70]
Acetylation	K69, K100, K292, K327, K546, K558	p300, HDAC6	Increased inhibitor binding, increased extracellular expression[71-75]
Dephosphorylation		Ppt1/PP5	Decreased chaperone function[76]
Phosphorylation	Y309	SRC	VEGFR2-induced angiogenesis[77]
Phosphorylation	S231, S263	CK2	Increased apoptosome formation, decreased client association[78,79]
Phosphorylation	Y38	Swe1/Wee1	Increased client association, decreased inhibitor binding[80,81]
Phosphorylation	T36	CK2	Decreased ATPase activity, increased inhibitor binding[82,83]
Phosphorylation	Y197	Yes	Decreased co-chaperone association[84]
Phosphorylation	Y309	Yes	Increased co-chaperone association[84]
Phosphorylation	T5, T7	DNA-PK	Increased extracellular expression[85,86]
Phosphorylation	T		$P2X_7$ receptor repressor[87]
Phosphorylation	S263	B-Raf	unknown[88]
Phosphorylation	S460	PKA	unknown[89]
Phosphorylation	T90	PKA	Increased extracellular expression, decreased client association[90,91]
S-nitrosylation	C597	eNOS	Decreased chaperone function, decreased ATPase activity[92,93]
Ubiquitination			Decreased client association[94]

1.4 Localization

The emphasis of distinguishing tumorigenic Hsp90 from normal Hsp90 is being placed in the field of client association. Post-translational modifications are thought to influence the association of Hsp90 with its clients, and in the past decade, the community of Hsp90 has begun to reveal how post-translational modifications affect the localization of Hsp90. More importantly, they have shown that ectopic localization can lead to the progression of a more malignant phenotype of most cancers.

No longer is Hsp90 being considered to reside exclusively in the intracellular milieu, but can be found on the surface membrane of a variety of cancer cells, as well as being secreted into the extracellular space[60,95]. The fact that cell surface Hsp90 is higher in some cancer cells than normal cells makes it an even more attractive target to destabilize metastatic pathways that are dependent on surface Hsp90 for invasion and migration. Since the initial screen in 2004 that implicated Hsp90 in cell invasion and migration, multiple researchers have shown that blocking or neutralizing secreted Hsp90 has had an inhibitory effect on these metastatic behaviors[96,97]. While we still do not understand the mechanisms responsible for Hsp90 extracellular expression, certain environmental stresses and growth factors have been shown to stimulate its secretory pathways[98,99]. The secretion of Hsp90 also appears to be influenced by the post-translational modifications, such as acetylation and phosphorylation[72,85].

The presence of Hsp90 outside the cell was first discovered in 1986 when a mouse tumor-specific antigen was found to be a heat shock protein, now recognized as Hsp90[100]. In 2004, it was published that Hsp90 was discovered in a functional screen looking at cell surface proteins that are necessary for cell invasion, but due to the cellular abundance of Hsp90 it was first viewed as an artifact. However, the screen was validated and Hsp90 was determined to be biologically important in the mechanisms of cell invasion as it was established that it interacts with and activates matrix metalloproteinase-2 (MMP2)[96]. Also in 2004, it was observed that in flow analysis of malignant melanoma that isolated tumor cells exhibited surface expressed Hsp90[60]. In the same year it was reported that surface Hsp90 plays a role in the migration of developmental neurons. Both Hsp90α and β are expressed on the surface of rat primary neural cells and antibodies against Hsp90 inhibited cell motility and lamellapodia formation. In this study crude measurements were made to determine the relative expression of surface Hsp90. Ratios of surface to total levels of Hsp90 were obtained and surface Hsp90 represented < 10% of total cellular Hsp90[101]. Others have shown that tumor cell lines excrete Hsp90 into the conditioned medium and the lack of other classical intracellular proteins such as actin and tubulin argues that the Hsp90 does not come from lysed cells. In one study of dying cells, acrylamide-induced necrosis leads to extracellular release of Hsp90 and increased HSF1 activity. Extracellular Hsp90 could be considered a danger signal to the immune system that something is detrimental to the

cells[102]. However, it is unknown what external cues trigger the excretion of Hsp90 in necrotic cells.

Because intracellular Hsp90 plays a key role in proteomic homeostasis, it begs the question, are its chaperoning functions required outside the cell or does it play a different role altogether? It is known that intracellular misfolded proteins have three possible fates: chaperoning, proteolysis or aggregation. It appears that extracellular proteins require chaperoning as well. Compared with intracellular fluid, extracellular fluids have a lower protein concentration, 6% in plasma and 2% in interstitial fluid, as opposed to 30% in cytosol[103]. It is thought that extracellular Hsp90α functions with the co-chaperones, Hsp70, Hsp40, Hip, Hop, and p23, to assist in the cleavable activation of MMP-2 and can do it independently of ATP, an important feature for performing its function in an environment where ATP is drastically reduced[104].

Normal cells secrete Hsp90 but only when they are subjected to a compromised environment, such as heat, ROS, gamma-irradiation and injury released growth factors, whereas tumor cells constitutively secrete Hsp90[98]. Early researchers proposed that Hsp90 is secreted by a non-canonical secretory pathway because Hsp90 lacks the conventional signal peptides in secretory proteins as well as post-translational modifications such as N-glycosylation. Also Hsp90 is not localized to the ER and Golgi apparatus and Hsp90 secretion is resistant to BrefeldinA treatment, a classical inhibitor of ER/Golgi dependent secretion[105]. Indeed it has been demonstrated that Hsp90 is

excreted through the exosome pathway[98,106]. McCready et al showed that exosomes harvested from MDA-MB-231 cells were applied to other invasive cell lines in a wound healing assay and both exogenous exosomes and recombinant Hsp90 stimulated faster migration into the scratched area. Conditioned medium was immunoprecipitated for Hsp90α and 10 client proteins were identified by mass spectrometry. The complex of interest was Hsp90:AnnexinII:tPA:plasminogen, which results in the activation of plasmin, a key protein in tumor invasion and cancer metastasis[106]. Why however, is some Hsp90 targeted for exosomal secretion while the majority remains in the cell? Additionally, secretion of Hsp90 does not appear to be isoform specific as first speculated, with the recent finding of Stellas et al. who showed breast cancer cells also secrete the β isoform[96,98,99,107].

Some speculated whether or not the numerous possibilities for protein modification distinguish Hsp90 for secretion. Knockdown of HDAC6 results in increased acetylation which in turn decreases ATP binding and chaperone activity in Hsp90. Seven lysine residues on Hsp90α revealed hyperacytelation by mass spectrometry (Table 1), and acetylation increased 17-AAG binding to Hsp90, whereas K294 acetylation in the middle domain affects co-chaperone binding. Hyperacetylated Hsp90 was found extracellularly and promoted in vitro breast cancer cell invasion. Additionally, an antiactyl lysine-69 Hsp90α antibody markedly inhibited the cell's invasiveness. P300 is the putative histone acetyl transferase responsible for acetylating

Hsp90α. The Hsp90α K292Q mutant showed increased binding to ATP whereas the other K to Q mutations at the other sites showed decreased binding. However, all the acetylated mimetics demonstrated increased binding to biotinylated-geldanamycin[72]. While acetylation appears to play a role, others suggest that it is the phosphorylation of T5 and T7 of Hsp90α and others suggest that it is a C-terminal truncation[85,90]. It was shown that the secreted Hsp90 is a C-terminal truncated form and its secretion was regulated by the C-terminal EEVD motif via interacting with proteins containing TPR domains. It was also demonstrated that the secretion of Hsp90 was determined by the phosphorylation status at residue Thr-90, regulated by protein kinase A and protein phosphatase 5. It was further demonstrated that the secretion of Hsp90 is a prerequisite for its pro-invasive function and blocking the secreted Hsp90 resulted in significant inhibition of tumor metastasis. Meanwhile, the level of plasma Hsp90 was positively correlated with tumor malignancy in clinical cancer patients[90].

While the precise mechanisms by which Hsp90 is targeted for exosomal secretion remain unclear, it is well established that extracellular Hsp90 plays pivotal roles in driving a non-motile tumor cell to become motile and invasive. Hsp90 facilitates each step in the three step model for tumor invasion: degradation of the extracellular matrix, adhesion, and migration of the cancer cells[108]. These events most likely are coordinated with intracellular chaperoning functions that drive the cell to become more malignant. These observations were made in context of Hsp90 inhibition and its effects on

cytoskeletal architecture and remodeling during cell motility and cell invasion. Hsp90 inhibition lead to decreased cell motility associated with a decrease in filopodia, lamellipodia and tough cortical actin bundles and resulted in less ruffling. The Hsp90 inhibition was also associated with a loss of mDia-2 and a decrease in RhoA, both necessary for the formation of lamellipodia and generation of contractile force. Hsp90 inhibition stimulated an increase in the pull down of actin in the soluble fraction with Hsp90. These observations suggested an increased interaction of Hsp90 with the soluble form of actin (G-actin) and αB-crystallin upon Hsp90 inhibition, which might be responsible for the decreased actin tread-milling at the cell periphery. Actin-ECFP and actin-EYFP showed a 50% reduction in FRET when inhibited with 17-AAG, and 17-AAG treatment resulted in an 80% decrease in inverse cell invasion for MDA-MB-231-GFP cells. Inhibition of Hsp90 also leads to a decrease in surface Hsp90 expression[109]. In light of the many advances in studying extracellular Hsp90, several questions remain: How do the extracellular cues communicate with the exosomal trafficking machinery to send Hsp90 out of the cell? Do the extracellular cues selectively cause Hsp90 secretion and leave other exosome-housed proteins behind or do they simply trigger secretion of the exosome vesicles as a whole? What percentage of total intracellular Hsp90 gets secreted?

One of the most important questions that we can ask pharmacologically is whether the surface expression of Hsp90 can be exploited to increase the safety threshold of future Hsp90 inhibitors. Our laboratory has explored the hypothesis that

expression of surface Hsp90 may contribute to the tumor selectivity of many Hsp90 inhibitors. This hypothesis was driven by our data using cell impermeable Hsp90 inhibitors tethered to fluorophores showing that a portion of ectopically expressed Hsp90 was reinternalized causing drug accumulation[110]. By extension of this observation, it is conceivable that many leading inhibitors of Hsp90 preferentially enter tumor cells through a similar mechanism and may have been fortuitously optimized to do so. Such a statement is not without possibility. From our own experience in the discovery of Hsp90 inhibitors, although our initial high throughput leads were identified by elution of native Hsp90 bound to an ATP affinity column, all molecules were subsequently evaluated for biological activity in cell-based assays[41]. These assays comprised a combination of growth inhibition and evidence of the mechanism of action including inhibition of Her2 expression, induction of Hsp70, Akt and S6 phosphorylation. Generally at this stage compounds that caused overt cell toxicity would have been considered second tier and not pursued further. Such a path would have most likely have been pursued by other groups developing Hsp90 inhibitors. It will therefore be interesting to test whether Hsp90 inhibitors that have higher cLogP values, and are thus more freely diffusible, are more toxic to normal cells compared with our current armamentarium of clinically active Hsp90 inhibitors. This finding would have great significance because the development of Hsp90 inhibitors that only penetrate

cells through interactions with surface Hsp90 could have vastly improved safety profiles enabling the therapeutic window of this class of drugs to be extended.

1.5 Combination Therapy

Typically when Hsp90 inhibitors are successively dosed to animals bearing human tumors, the tumors stop growing. However, when the inhibitor is withdrawn the tumors tend to start growing again[41]. Generally the same phenomenon occurs in patients with solid tumors being treated with a variety of structurally unrelated Hsp90 inhibitors. These observations are consistent with the role of the protein in maintaining tumor growth and suppression of these pathways by Hsp90 inhibitors. For these reasons Hsp90 inhibitors may have limited use as a monotherapy. Although, more recent observations suggest that certain tumor types may be more responsive to Hsp90 inhibition than others and monotherapy may be sufficient to promote tumor reduction, and even cellular death. In recent Phase II studies with ganetespib alone, an encouraging response rate of 50% in NSCLC patients whose tumors contained ALK translocations was observed[111]. Instead there is however great excitement in the field for using Hsp90 inhibitors in combination with either existing chemotherapeutics or more cutting edge drugs like Herceptin, lapatinib or Gleevec. Fadden et al shows that a combination of the drug SNX5422 and Herceptin not only shrinks the tumors dramatically and persistently (even after withdrawal), but it is also synergistic[41]. The argument for combination therapy is in the evidence that genome sequencing of human

cancers reveals numerous driver mutations within any one individual cancer[112,113]. Intratumor heterogeneity may foster tumor evolution and adaptation and hinder personalized-medicine strategies that depend on results from single tumor-biopsy samples[114]. Hsp90 inhibitors can play a unique role in preventing drug resistance in tumors because oncogenes rely heavily on Hsp90 to chaperone their otherwise unstable conformation due to their mutations. This dependence has been termed oncogene addiction. Because numerous mutant oncoproteins are "addicted" to Hsp90 activity, an inhibitor to Hsp90 has the ability to affect multiple targets and pathways, which can prevent oncogene switching, a major mechanism for developing resistance[115,116].

Hsp90 inhibitors have the potential to circumvent or diminish the drug resistance seen in the use of target-based therapies, but because cancers evolve, resistance to Hsp90 inhibition is also a real possibility. However, the silencing of co-chaperones such as p23, Aha1, or Cdc37, has been shown to cause dramatic sensitization to Hsp90 inhibition[117-119]. Because Hsp90 inhibition allows the trimerization and activation of HSF1, and because elevated HSF1 is linked to stages of oncogenesis, there are efforts to find inhibitors to HSF1 that can be used in conjunction with Hsp90 inhibitors to minimize the negative effects of Hsp90 inhibition[120,121]. As a result of HSF1 activation, Hsp70 transcription is dramatically upregulated, which is often used as readout in cell based assays for efficacy of an Hsp90 inhibitor. However, Hsp70 induction is another chaperone that can drive oncogenesis in many tumors. Researchers

have shown a therapeutic value for targeting Hsp70 because tumors overexpress the inducible form over the constitutive form[122]. Therefore, combination therapy that inhibits both Hsp90 and the inducible Hsp70 could be formidable method of treating cancer by eliminating the unwanted effect of Hsp70 induction.

1.6 Conclusions

While some are still not cognizant to the advances of Hsp90 inhibitors in the clinic, others, including members of the Hsp90 community, still question whether or not any of the now 17 Hsp90 inhibitors will successfully exit clinical trials and enter the market. We think the day will come that Hsp90 inhibitors will be commonplace in the clinic and that in the oncological application of Hsp90 inhibitors, these drugs will be used as first line chemotherapeutics in combination with other potent anti-cancer therapies to prevent or prolong the development of drug resistance. In the immediate term, combination therapy involving an Hsp90 inhibitor and cutting edge targeted therapies clearly holds the greatest promise. If the consistent synergisms in efficacy and tumor elimination observed in animal combination studies with drugs such as Herceptin hold true in human trials maybe we are well on the way to seeing actual "cures" rather thinking about merely halting disease progression over the shorter term. Beyond combination therapy, as we have discussed, other aspects of Hsp90 biology may render it even more druggable. Exploring the differences in Hsp90 between cancer cells and normal tissues may reveal additional strategies on how to target Hsp90 and how to

improve its therapeutic window. One of these in our sights is the role of ectopically expressed Hsp90 in metastatic progression. Although yet to be demonstrated in human biopsy samples, clearly, if there is a correlation between expression of ectopic Hsp90 and metastatic progression, this is likely to be of both diagnostic importance as well as therapeutic. If expression of ectopic Hsp90 correlates with poor outcomes it could be used as an early biomarker to discriminate indolent forms from aggressive disease. We are particularly excited by the prospect of developing Hsp90 inhibitors that only target ectopically expressed Hsp90 as a means to improve the selectivity of Hsp90 inhibitors and deliver tumor-killing payloads to tumor cells. On top of all these tangible possibilities for extending Hsp90s therapeutic potential is the co-chaperone/chaperone machinery of associated proteins regulating and regulated by Hsp90. Once bona fide clients are established and validated, one could envision strategies that could selectively inhibit these protein-protein interactions, thus potentially making Hsp90 therapy highly targeted and disease specific.

Finally, from a pharmacologist's perspective, there are lessons to be learned from the development of Hsp90 as a cancer target that are pertinent to 21st century drug discovery. Clearly, new therapies to treat cancer are not always going to be obvious as has been the case in the past i.e. one must not assume that a "hall mark of cancer" involves a point mutation and that alone signifies a usable target. Not all targets are going to be "Gleevec type stories". If we make the assumption that this is the case we are

likely to miss the boat on some great opportunities. A second lesson is that although an Hsp90 drug has yet to be brought to market, there is clearly a ground swell of independent data that strongly indicate that this will happen soon, despite some side effect concerns such as retinal toxicities. This ground swell is self-evident in the form of the numbers of independently derived inhibitors that are currently being advanced clinically. Within these independent paths we count an extraordinary six distinct structurally diverse scaffolds upon which the current clinical armamentarium of Hsp90 inhibitors is currently derived. In future drug discovery efforts involving unconventional targets where we don't have obvious genetic data to validate a target we should look for similar trends to assure pharmaceutical companies that such targets should not be ignored.

2. Experimental Procedures

2.1 Studies with HSP90 antibodies

MCF7 and MCF10A cells were cultured and fixed in wells using 4% PFA/PBS. Successively, cells were incubated in blocking solution (5% goat serum, 0.2% Na Azide, PBS) with or without 0.3% Triton X-100 for 1 hour. After blocking with or without the detergent, cells were incubated with a polyclonal antibody for Hsp90 at 1:100 (sc-7947, Santa Cruz Biotechnology, Santa Cruz, California). Cells were sequentially incubated with a goat-anti-rabbit Alexa Fluor 488-conjugated antibody at 1:1,000 (A-11008, Life Technologies, Grand Island, New York). Cells were imaged using the Olympus IX 71 epifluorescence microscope. To evaluate ectopic expression of HSP90, HSP90 antibody was incubated with live MCF7cells (2.5 hours), then 100 nM of HS-27 was added. Concurrently, cells were stained with DAPI and goat-anti-rabbit Alexa Fluor 568 secondary antibody (A11011, Life Technologies, NY) at 1:1,000 and incubated the cells for one hour at 37°C. Cells were washed in PBS and imaged using the Olympus IX 71 epifluorescence microscope. Ratios of cells that retained HS-27 at the cell periphery to cells that internalized HS-27 was calculated and plotted against the antibody mass.

2.2 Anion exchange chromatography

Samples from either cell or tissue lysates underwent buffer exchange using 30K or 10K filter devices. Lysis buffers were exchanged for 25 mM Tris-HCl and 1 mM DTT. Samples were centrifuged (13,000 rpm, 10 minutes), then passed through a 0.2 μm

syringe filter. Next the supernatants were loaded onto a Pharmacia mono Q anion-exchange SMART column (0.1 X 1.0 cm) that has been previously equilibrated in 25 mM Tris-HCl, 1 mM dithiothreitol buffer, pH 7.4 as described[123]. The column was eluted using a linear salt gradient over 80 minutes (100 μL/minute) to 1 M NaCl in the same buffer. Samples were fractionated into an opaque plate that was read for fluorescence on the multi label plate reader. Peak fractions of fluorescence were passed over a cleavable affinity resin to purify Hsp90 as described[47].

2.3 IVIS Kinetic mouse imaging

All protocols using mice were approved beforehand by the IACUC at Duke University and strictly adhered to throughout the studies. SCID mice bearing MDA-MB-468 tumors were anesthetized with ketamine. Mice received tail vein injections or abdominal injections and imaged post injection at the indicated time using an IVIS Kinetic imager (Caliper Life Science, MA) as part of the Optical Molecular Imaging and Analysis shared resource in the Duke Cancer Institute. The following filters were used for the corresponding small molecule inhibitors (emission/excitation): HS-27 (468/GFP), HS-105 (468/GFP), HS-69 (640/Cy5.5), HS-70 (745/ICG).

2.4 Tissue Harvest and Analysis

The following mouse tissues were taken immediately post mortem: blood, brain, eyes, heart, kidney, liver, lung, spleen, and tumor. With the exception of the blood, the tissues were rinsed in PBS and blotted followed by image analysis using the IVIS kinetic

imager. Tissues were stored on dry ice or at -80°C. For analysis of tissue lysates using SMART mono Q fractionation and multi label fluorescent reader, tissues were dounced in mono Q buffer (25 mM Tris-HCl, 1 mM DTT). We centrifuged the samples and transferred supernatants to be analyzed for fluorescence and protein concentration.

2.5 Fluorescence spectroscopy of drug uptake

SCID mice bearing MDA-MB-468 tumors were anesthetized with ketamine and received tail vein injections of drug. Using an optical spectroscopy instrument and a fiber optic probe the fluorescence spectrum of the FITC-conjugated drug was measured in vivo at 6, 24, 48, 72 and 96 hours post injection[124]. With optical spectroscopy, tissue is illuminated using light of interest and the reflected light is analyzed to study the morphology and biochemical composition of the underlying tissue. The pen-shaped fiber optic probe has a diameter of approximately 2 mm and was placed in gentle contact with the tumor or adjacent normal site. Incident light at 490 nm corresponding to FITC excitation was delivered through the probe into tissue and resulting longer wavelength fluorescent light was collected. Although 490 nm does not correspond to maximal absorption by FITC, this wavelength was used to minimize fluorescent contributions from flavins (FAD) which fluoresces in the same wavelength range. Measured fluorescence spectra were corrected for tissue absorption and scattering using an intrinsic fluorescence recovery model described in the literature[125]. Briefly, the model calculates the tissue optical properties that are a function of light scattering and

absorption and uses these properties to correct distortions in the measured fluorescence. The intrinsic fluorescence model has been shown to accurately recover fluorophore concentrations in tissue-mimicking phantoms[126]. In addition, the intrinsic fluorescence calculated using this model has been used to monitor intra-tumor drug concentrations in vivo and shown to be strongly correlated with concentrations measured using HPLC[127]. Because optical spectroscopy measures wavelength-dependent fluorescence, the background fluorescence can be accurately measured prior to injection. This allows monitoring of the fluorophore concentration in vivo and determination of when the fluorescent tether has cleared from the tumor.

2.6 Active Hsp90 depletion using affinity resin chromatography

MDA-MB-468 cell lysate was diluted to 1 mg/mL in low stringency wash buffer and 1 mL was added to 1 mL of the Hsp90 affinity resin at 50% slurry. For three consecutive washes fresh resin was used and 25 μL of flow through (< 3%) was set aside for flow through analysis. The resin was washed thoroughly with low stringency wash buffer and then Hsp90 was eluted off with 10% SDS. Both flow through and resin samples were characterized by 1D SDS-PAGE and silver staining. In a separate experiment, flow through and resin samples were incubated with 100 nM HS-27 and then washed using a 10K kDa filter. Samples were concentrated and analyzed on a multilabel plate reader for fluorescence.

For the more through-put assay of analyzing active and inactive Hsp90, cell and tissue lysates were diluted in low stringency wash buffer to 0.1 mg/mL and 100 μL was added to 300 μL of prewashed, 50% slurry Hsp90 affinity resin in wells of a 96-well plate with 0.2 μm PDVF membranes on the bottom. The resin was washed three times and the flow through was captured and transferred to the next well of virgin resin. The resin samples were incubated with 5X SDS sample buffer and the flow through was concentrated to 50 μL boiled with 5X SDS sample buffer. All samples were subsequently run out by gel electrophoresis, transferred to PVDF and immunoblotted for Hsp90.

2.7 Ex vivo cell treatment and injection into mice

MDA-MB-468 cells were treated with 5 μM β-escin for 5 minutes. Cells were harvested and treated with either 10 μM HS-70 or PBS. Cells were counted and aliquots of 10 million to 10 thousand cells were made in 200 μL of saline. SCID mice were anesthetized with ketamine and received two flank injections of the treated cells and the control cells. Mice were imaged using the IVIS kinetic imager and average radiant efficiency was measured.

2.8 ^{125}I-labeled Hsp90 inhibitor treatment of cells

Cells were permeabilized by treatment with 5 μM β-escin for 5 minutes. Competition experiments were performed by treatment of cells with 1 μM of HS-10 for 5 minutes prior to exposure to the [^{125}I]HS-111. β-escin and HS-10 were washed away and then cells were incubated in 5 mL of medium with the [^{125}I]HS-111 that had about 10 μCi

of activity per 10 cm dish of cells for 45 minutes. Cells were washed extensively with PBS and then lysed on an ethanol/dry ice bath and harvested in 25 mM Tris buffer and centrifuged. Supernatants were fractionated on a Pharmacia mono Q anion-exchange SMART column and fractions were counted using a PerkinElmer 1480 Wizard 3 gamma counter (Turku, Finland) for 30 seconds per fraction sample.

2.9 Immunoblotting and treatment of cells with fluor-tethered inhibitors

MCF7, MCF10A, BT474, MDA-MB-468, and Huh7 cell lines were cultured under standard conditions. For Western and biochemical studies, following treatments, cells were washed in PBS and flash frozen on dry ice/95% ethanol and extracts prepared as described previously[47]. Western blots were quantified using ImageJ software (National Institutes of Health, Bethesda, Maryland). All protein concentrations were determined by Bradford assay. For cell permeabilization, cells were washed with PBS and incubated in 5 μM β-Escin in Rigors buffer solution at room temperature then treated with 100 μM HS-27[128]. For quantification of fluor-probe uptake, lysates were prepared from washed cells treated with the probe and immediately analyzed for fluorescence on a Victor X2 2030 multilabel reader (Perkin Elmer, Waltham, Massachusetts) using either excitation/emission pairs of 485/535 (fluorescein) or 635/660 (nIR). For fluorescent microscopy, following washing in PBS, cells were imaged in culture using an Olympus IX 71 epifluorescence microscope, and images were acquired using an Olympus DP70 digital camera. Cells were also counterstained with DAPI.

2.10 Determination of inhibitor affinity using immobilized ATP

ATP resin was prepared as described previously[47]. All affinity measurements were determined against lactating pig mammary gland Hsp90[47]. Briefly, mammary gland extract was mixed with ATP resin at ratio of 5 grams of tissue to 1 mL of resin. Following washing, the charged resin was transferred by 50 μL aliquots on a PVDF membrane filter plate. Various tethered Hsp90 inhibitors were added at the indicated concentrations and the filter plates were placed on top of a microtitre plate and centrifuged (1 min, 3,000 X g). Following elution with the nucleotides, the eluted proteins were characterized by 1D SDS-PAGE and silver staining. The gels were analyzed by densitometry and regions of the gel containing Hsp90 excised analyzed in a 4700 AB systems MALDI TOF TOF mass spectrometer as described[47] .

2.11 Flow cytometry of cultured cells and excised tissues

Cells were seeded into 24-well plates at 1 x 10^5 cells/well the day before the assay. β-escin at 5 μM was prepared with HS-27 at 100 nM. Following media aspiration and washing with PBS, the cells treated with 0.05% Trypsin/EDTA for 5 minutes then harvested by centrifugation (1,200 rpm, 5 minutes). Cells were resuspended in 1% BSA/PBS buffer and analyzed by flow cytometry on a BD FACSCalibur using CellQuest software (Becton Dickinson and Company, San Jose, California). In competition experiments performed cells were first incubated with HS-10 (10 μM, 5 minutes), followed by aspiration and incubation with HS-27. For flow analysis of HS-27 uptake

into tumors and other tissues, the excised tissues were harvested, minced and digested with trypsin as described[129].

2.12 Heat shock treatment

Cells that underwent heat shock treatment were incubated at 42°C for 1 hour and returned to an incubator at 37°C for 18 hours.

2.13 pH effect on HS-27 fluorescence

Phosphate buffered saline was adjusted to pH 1 to 14 and 5 μM of HS-27 was added to each condition and fluorescence was measured in an opaque plate on a multilabel plate reader with the filter pair of 485 excitation and 535 emission.

2.14 Mass Spectrometry Protein Identification

Visible bands were excised from the gel manually and cut into small pieces approximately 1mm x 1mm. These gel pieces were washed (x3) with water, then washed (x2) with 1:1 acetonitrile: 100mM ammonium bicarbonate. To further prepare the gel pieces for digestion, the gel pieces were then dehydrated in 100% acetonitrile. After removing all acetonitrile, 30μL of porcine trypsin (Promega) at a concentration of 20 μg/mL was added to the gel pieces. The gel pieces were then kept on ice for approximately 1 hour to allow for the trypsin to remain inactive as it enters the gel. Following this, the gel pieces were incubated at 37°C overnight (approximately 12-16 hours). Following digestion, the supernatant was transferred to a second tube, and acetonitrile was added to the gel pieces to complete the extraction of digested peptides.

This extract was added to the first supernatant and this combined solution, containing the extracted peptides was frozen and lyophilized. The peptides were resuspended in 5 μL of 1:1 acetonitrile:0.5% aqueous formic acid immediately prior to spotting on the MALDI target.

For MALDI analysis, the matrix solution consisted of alpha-cyano-4-hydroxycinnamic acid (Aldrich Chemical Co. Milwaukee, WI) saturating a solution of 1:1:0.01 acetonitrile: 25mM ammonium citrate: trifuoroacetic acid. Approximately 0.15 μL of peptide solution was spotted on the MALDI target immediately followed by 0.15 μL of the matrix solution. This combined solution was allowed to dry at room temperature. MALDI MS and MS/MS data was then acquired using the ABI 4700 TOFTOF Mass Spectrometer (Applied Biosystems Inc., Framingham, MA). Resultant peptide mass fingerprint and peptide sequence data was submitted to the NCBI database using the Mascot search engine to which relevance is calculated and scores are displayed.

2.15 Mammary Gland Tissue Collection

Lactating mammary tissue was collected at the local abattoir from 2 Yorkshire sows ages 1.5-and 2.5 years. The mammary tissue of only active glands was dissected away from skin and underlying muscle, flash frozen and stored at -80°C until processed. Weaning occurred on day 7 of lactation for sow 1, 2 hours prior to collection and on day 18 of lactation for sow 2, 18 hours prior to tissue collection.

Table 2: Lactating pigs' biographical data

	Date Harvested	Breed	Age (mo)	Time from wean to euthanasia (hr)	Litter size	Days lactating
1	2/01/2010	Yorkshire	17	18	8	18
2	8/31/2010	Yorkshire	30	2	5	7

2.16 Mouse Tissue Extraction

Adult male mice (Mus musculus (house mouse) black 6 strain) were CO_2-asphyxiated and sacrificed. The organs of interest (i.e. pancreas, heart, spleen, kidney, skin, brain, colon, lung, testes, skeletal muscle, liver, adipose, and eye) were quickly excised and washed in ice-cold phosphate-buffered saline. The organs were then frozen in liquid nitrogen and the tissue ground in liquid nitrogen with a mortar and pestle. The liquid nitrogen was allowed to evaporate off and the mass of the tissue was measured. Immediately afterwards, 2.5 X the volume (mL) of extraction buffer [50 mM HEPES, 60 mM $MgCl_2$, 60 mM KCl, 0.2% NP-40, 1 mM DTT, 1 µM Microcystin (Cayman Chemical Company), Complete Mini protease inhibitor cocktail (Roche), pH 7.4] was added to the powdered tissue (gram). The tissue samples were subsequently centrifuged at high speed and the supernatants collected to combine with the affinity resin columns. The protein concentrations were determined for each tissue by Bradford analysis and the tissue sample divided in half.

2.17 Resin Binding

Before binding to the resin, if competition was performed, then half of each sample was pretreated with 1 mM of HS-10 for 1 hour at room temperature. Following the pretreatment, all samples were tumbled with 100 µL of 50% slurry of the Hsp90 affinity resin. After 1 hour of tumbling, the resin was washed 3 X with a low stringency wash buffer [50 mM Tris-HCl, 60 mM $MgCl_2$, 60 mM KCl, 10 mM Citrate, 1 mM DTT, pH 7.4]. After the final wash, the buffer was completely aspirated and replaced with 30 µL of 25 mM dithionite in 100 mM phosphate buffer solution pH 7.4 and tumbled for 1 hour at room temperature. Subsequently, the resin was pelleted and the cleaved linker with the protein was removed and subjected to 2 % SDS denaturation for 10 min at 90°C.

2.18 Protein gel electrophoresis and silver staining

SDS protein samples were loaded in Criterion precast gels (BioRad), 4-15% Tris-HCl and separated at 120 V. Gels were then fixed in 10 % methanol and 5% acetic acid for 20 minutes. Afterwards, the gels were washed 4 X in H_2O, incubated in 0.2 g thiosulfate/500 mL of H_2O for 90 seconds and then washed 3 X in H_2O. The gels were then incubated in 0.9 g silver nitrate/500 mL of H_2O for 20 minutes and washed 3 X in H_2O and finally incubated in a developer solution of 10 g potassium carbonate, 20 mL of the thiosulfate solution, 0.02 % formaldehyde/500 mL of H_2O. The reaction was quenched with 10% methanol and 5% acetic acid just as the background started to stain.

2.19 Pig mammary protein extraction

Frozen pig mammary tissue was ground in liquid nitrogen and stored at -80°C. Pig tissue mass was measured (g) and then 2.5 X volume (mL) of extraction buffer [50 mM HEPES, 60 mM $MgCl_2$, 60 mM KCl, 0.2% NP-40, 1 mM DTT, 1 μM Microcystin (Cayman Chemical Company), Complete Mini protease inhibitor cocktail (Roche), pH 7.4] was added and homogenized on a laboratory blender. The homogenate was centrifuged at 35,000 rpm for 45 minutes at 4°C, and then the supernatant was filtered over silica wool to purify from solid materials. The protein extract concentration was determined by Bradford analysis.

2.20 Thermofluor Assay

SYPRO orange (Molecular Probes, Eugene, OR) was diluted 1:1000 in 25 mM HEPES, 5 mM $MgCl_2$, 10mM KCl (pH 7.5), and purified Hsp90 from the resin or Hsp90 harvested from the flow through after mono Q fractionation was then added to a final dilution of 0.04 mg/ml. Compound or DMSO was then added at the specified concentration and each sample was added as a minimum of three replicates to a 384 well-plate (BioRad, Hercules, CA). A melt curve protocol (25°C to 90°C, increasing 0.5°C and a plate reading every 30 seconds) was run on a CFX384 TouchTM Real-Time PCR Detection System (BioRad, Hercules, CA) to determine the midpoint of the protein unfolding transition or Tm. GraphPad Prisim4 (La Jolla, CA) was used to normalize the

melt curve and to calculate the first derivate of the melt curve, with the steepest point of the slope being the Tm.

2.21 Cell culture

BT474 cells were maintained in RPMI-1640 supplemented with 10% fetal bovine serum and incubated at 37°C in 5% CO_2. MDA-MB-468, MCF7, SKBr3, Huh7 and HEK 293T cells were maintained in DMEM supplemented with 10% fetal bovine serum and incubated at 37°C in 5% CO_2. MCF10A cells were maintained in DMEM/F12 (1:1) supplemented with 5% horse serum, 20 μg/mL EGF, 500 ng/mL hydrocortisone, 100 ng/mL cholera toxin, 10 μg/mL insulin and incubated at 37°C in 5% CO_2.

2.22 Determination of tissue affinity for HS-27

Cell lysates and tissues were harvested and protein concentration was measured by Bradford assay. 2000 μg of total protein was added to 96-well 10K cutoff filter plates and the indicated amount of HS-27 was added and incubated for 15 minutes with gentle agitation. Sample wells were subsequently washed with low stringency wash buffer until negligible fluorescence was observed in the flow through. Each sample well was then punctured with a pin to allow samples to flow through to an opaque catch plate, wherein fluorescence was measured on a multilabel fluorescent plate reader using the 485 excitation and 535 emission filter pair.

3. Extracellular Hsp90 for tumor detection

Hsp90 inhibitors have demonstrated unusual selectivity for tumor cells despite its ubiquitous expression. This phenomenon has remained unexplained but could be influenced by ectopically expressed Hsp90 in tumors. We have synthesized novel Hsp90 inhibitors that can carry optical or radioiodinated probes via a PEG tether. We show that these tethered inhibitors selectively recognize cells expressing ectopic Hsp90 and become internalized. The internalization process is blocked by Hsp90 antibodies, suggesting that active cycling of the protein is occurring at the plasma membrane. In mice, we show exquisite accumulation of the fluor-tethered versions within breast tumors with very high sensitivity. Cell-based assays with the radiolabeled Hsp90 inhibitor showed picomolar accumulation that was detected by gamma counting . Our findings show that fluor-tethered or radiolabeled inhibitors targeting ectopic Hsp90 can be used to detect breast cancer malignancies through non-invasive imaging.

3.1 The breast tumor detection paradigm

The current paradigm for detection and treatment of breast cancer is based on clinical evaluation and anatomic imaging, usually with mammography or less commonly breast magnetic resonance imaging (MRI), followed by biopsy and surgery or surgery plus radiotherapy. Other imaging modalities, such as ultrasound or position emission tomography (PET), are not routinely used for screening although they have specific indications and potential[130]. While both mammography and MRI demonstrate

excellent sensitivity for detecting tissue abnormalities, they lack sufficient specificity for unequivocally distinguishing malignant tissue from benign tissue[131]. The question remains as to whether pre-malignant molecular markers can be used non-invasively to detect aggressive cancers.

It is clear that anatomic changes are not the earliest cancer-related transformations. Instead, breast cells with malignant and lethal potential are characterized early on by activated oncogenic signaling nodes. These signaling nodes have been classified into a broad set of characteristics termed the "Hallmarks of Cancer" and are candidate molecular markers of malignant behavior[2]. Unfortunately, these signaling nodes have been difficult to detect in vivo, particularly when confined to small clusters of cells, as in early stage disease. To date, strategies to visualize these signals in vivo, such as using ^{18}FDG-PET to detect increased glucose uptake, have not achieved the sensitivity or specificity required to appreciably improve breast cancer screening and diagnosis[132].

Hsp90 is a signaling node that could be exploited as a diagnostic molecular marker to distinguish malignant breast cells from normal tissues[133]. Hsp90 has an essential role in cellular homeostasis by chaperoning client proteins. Over 400 putative Hsp90 clients have been identified and many of these regulate signaling pathways governing cellular growth and differentiation[46,66,68,134,135]. Hsp90 and its family members, Grp94 and TRAP1, contain an N-terminal ATP-binding domain with ATPase activity

that is necessary for cellular function[33]. Hsp90 is regulated both translationally and post-translationally, the latter affecting both ATPase activity and intracellular location[14]. Direct evidence for Hsp90's participation in oncogenic protein folding/stability in vivo comes from studies with Hsp90 inhibitors that bind competitively to its ATP-binding domain resulting in the degradation of its oncogenic clients[41,136,137]. This phenomenon has also been demonstrated in human tumor biopsies from patients undergoing Hsp90 inhibitor therapy[138]. To date, there are 17 different Hsp90 inhibitors targeting its ATP-binding site in clinical development for multiple indications in cancer[52,53,138,139].

Recent studies have linked high expression of Hsp90 with poor prognosis in malignant breast tumors[58,59]. The role of Hsp90 in mediating malignant behavior may be the result of oncogene driven factors that alter its normal cellular behavior[56]. Hyperactivation is postulated to result in an increased affinity for ATP and Hsp90 inhibitors and the expression of ectopic Hsp90[97,140]. If oncogenically activated Hsp90 precedes malignant behavior in vivo, we reasoned that this could be used diagnostically[96,104,106]. We therefore developed a series of Hsp90 inhibitors tethered to fluorophores or radioiodine to detect Hsp90 in vivo. When injected into mice bearing human breast tumors, the fluorophore versions are exquisitely targeted to tumors. We show that this targeting is achieved through interactions with ectopic Hsp90, which is undergoing active internalization along with the bound probes. This finding suggests

new roles for Hsp90 in which the protein is not only trafficked to the plasma membrane but also reinternalized.

3.2 Synthesis and Development of Probes Selectively Targeting Ectopic Hsp90

We have also developed a cleavable tethered Hsp90 inhibitor and demonstrated its use as an affinity resin[47]. When bound to the tethered ligand, Hsp90 could be recovered along with one of its established oncogenic clients, Her2, in a competitive manner (Figure 42). To extend our tethered ligands utility, we synthesized several versions tethered to a variety of fluorophores and other molecules to facilitate the detection of Hsp90 in vivo (Figure 2, Appendix A and Table 3).

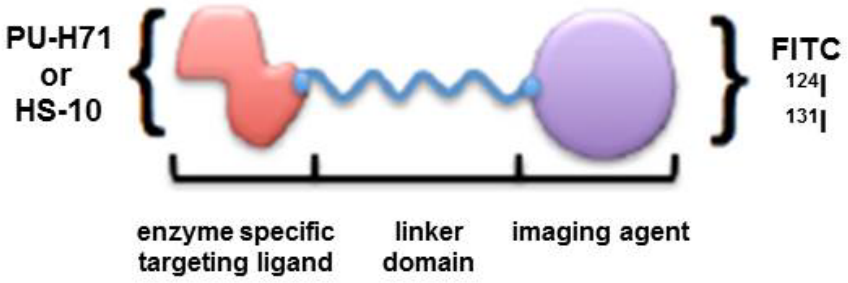

Figure 2: Generic structure of tethered Hsp90 inhibitors

In binding studies against immobilized ATP, the tethered inhibitors showed reduced affinity for native Hsp90 (K_d HS-27, 288 nM; HS-69, 49 nM; HS-70, 42 nM) in comparison to the parent compound (HS-10, 3 nM) (

Table 3 and Figure 3)[41,141]. Proteins from a pig mammary gland were loaded onto an ATP media resin and eluted with HS-10 or HS-27 (n = 3, ±SEM).

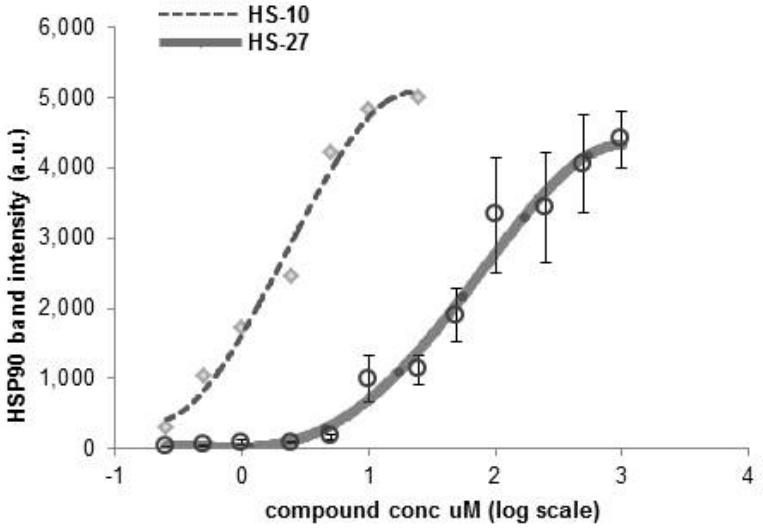

Figure 3: Hsp90 affinity for HS-10 and HS-27

Despite some reduction in affinity, the addition of the tethered components was found to increase specificity by eliminating binding to Grp94 (Figure 4). Both non-conjugated HS-10 and PU-H71 showed non-selectivity between Hsp90 isoforms by eluting both Hsp90 (bottom arrow) and Grp94 (top arrow). Grp94 is no longer eluted when molecules are tethered to HS-10 at 100 μM. HS-105 is a control compound with no ligand for Hsp90.

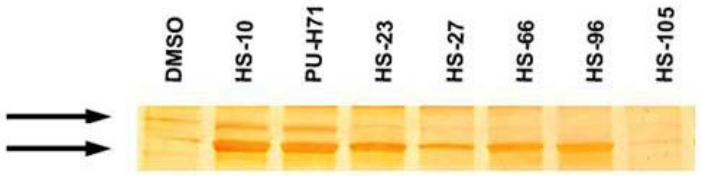

Figure 4: Hsp90 selectivity with tethered Hsp90 inhibitors

Previous work had also shown that the addition of the tether at the ortho-position of the parent ligand reduced the specificity towards recombinant and native TRAP1[47]. These findings suggest that the added steric bulk due to the presence of the tether and added fluorophore, for example, interferes with the ATP-binding site of Grp94 and TRAP1, but not Hsp90. Similar specificity was also observed by adding various non-fluorescent molecules to the tethers, such as ferrocene, iodinated benzylamine or an additional Hsp90 inhibitor, to create a bifunctional inhibitor (Figure 4, Table 3).

Table 3: Hsp90 and Her2 tethered inhibitors: names, descriptive features and structures for compounds

Designation name	Feature	Structure
HS-10	parent ligand	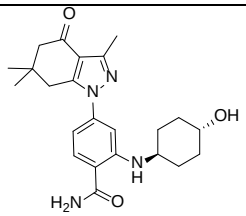
HS-23	ligand + linker	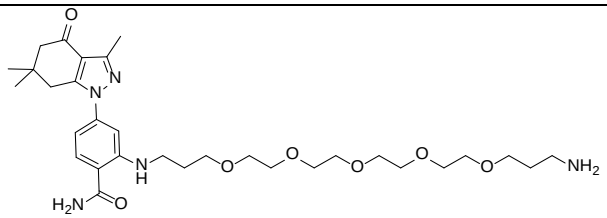
HS-27	ligand + FITC	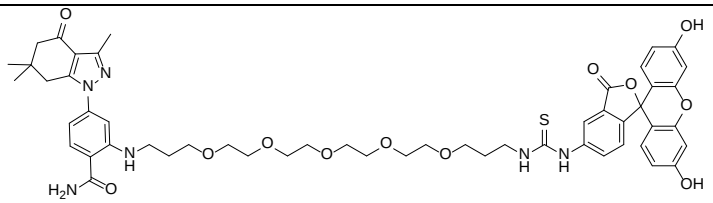
HS-32	bis-ferrocene	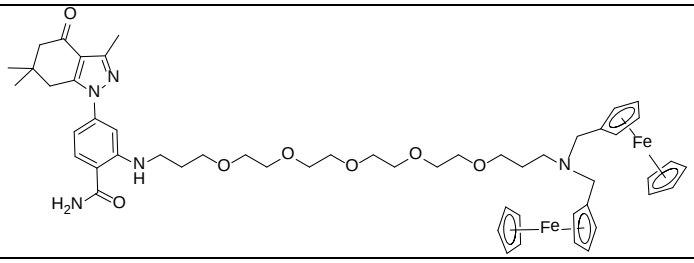
HS-42	lapatinib + fluorescein	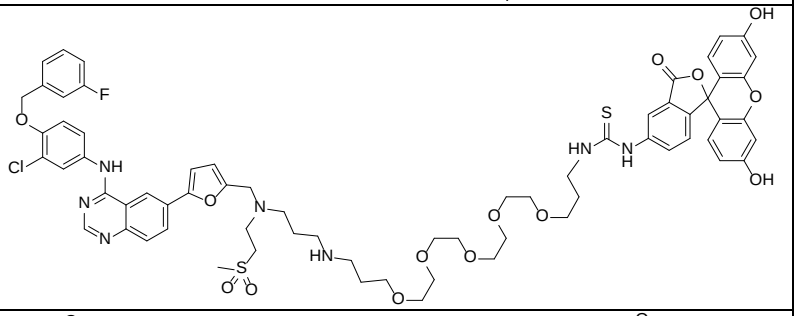
HS-66	double ligand	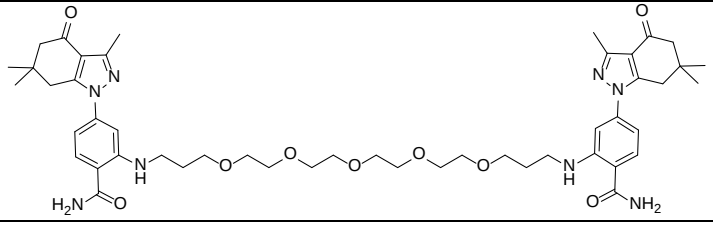

HS-69	ligand + nIR (645)	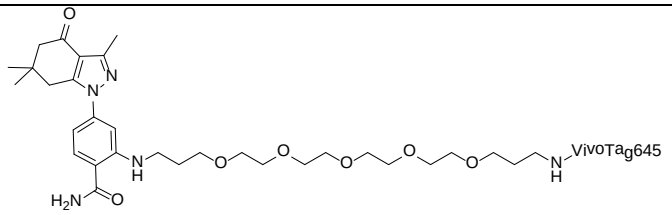
HS-70	ligand + nIR (800)	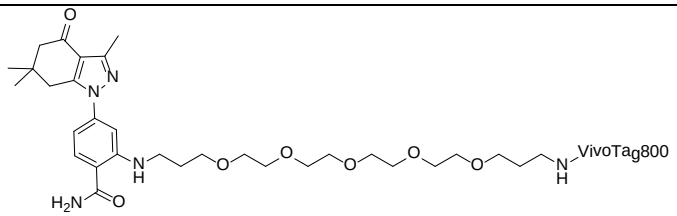
HS-96	ligand + biotin	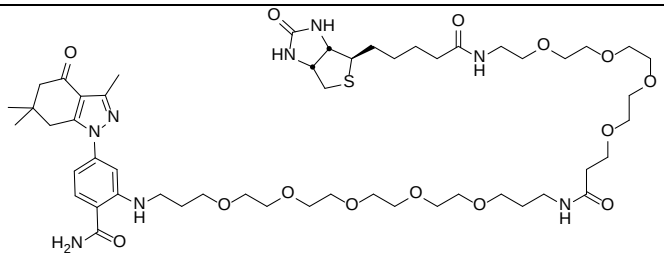
HS-105	FITC derivative w/o ligand	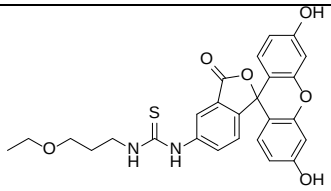
HS-111	Iodine-containing ligand	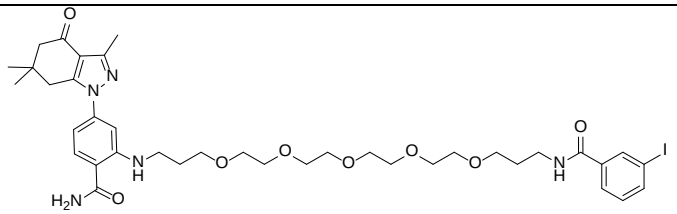

Next, we evaluated the specificity of the fluor-probes in several transformed cell lines by fluorescent microscopy. These cell lines were selected to represent each of the major breast cancer classification schemes: $Her2^{+}$, ER^{+}, triple negative breast cancer, and a non-tumorigenic immortalized breast epithelial cell line (Table 4).

Table 4: Breast cell line classifications

Cell line	subtype	ER*	PR*	Her*	source	tumor type
BT474	Luminal	+	+	+	primary tumor	invasive ductal carcinoma
MCF7	Luminal	+	+	-	pleural effusion	metastatic adenocarcinoma
MCF10A	Basal B	-	-	-	reduction mammoplasty	fibrocystic disease
MDA-MB-468	Basal A	-	-	-	pleural effusion	metastatic adenocarcinoma

Figure 5 shows that HS-27 at 100 μM is internalized by breast cancer cell lines, which correlate to the established malignancy of the cell lines (scale bar, 50 μm). Remarkably, HS-27 does not label Huh7 cells, a hepatocarcinoma cell line, despite the latter cell line having higher total cellular levels of Hsp90 as determined by immunoblotting (Figure 6).

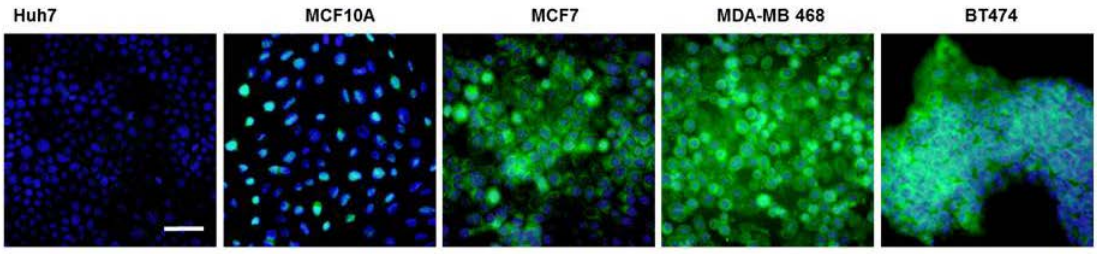

Figure 5: Tissue culture cell lines demonstrate variable responses to HS-27

Immunoblotting of Hsp90 and Her2 was performed in several cancer cell lines. Cell lysates were harvested and analyzed by Western blotting. Hsp90 was highest in Huh7 cells and the same amongst BT474, MCF7, and MDA-MB-468 and less in the non-tumorigenic breast cancer cell line MCF10A. Additionally, only BT474 cells demonstrated the presence of Her2 in total cell extracts as expected (Figure 6).

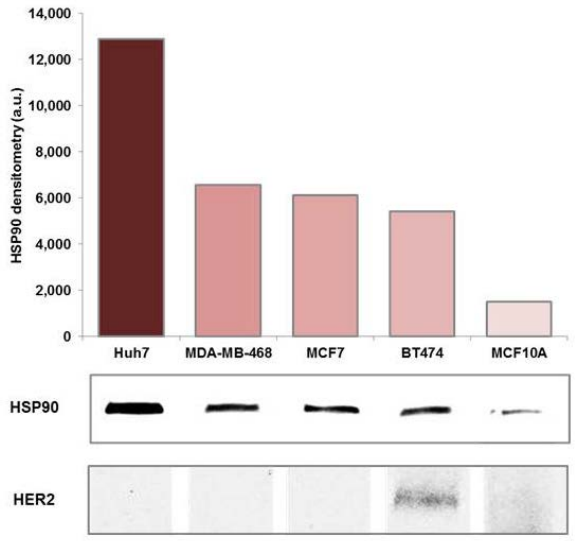

Figure 6: Immunoblots of Hsp90 and Her2 in cell lines

Time course studies at 100 μM HS-27 and titration studies evaluated at 60 minutes showed HS-27 uptake is variable between breast lines in the following order MCF10<<<MCF7<MDA-MB-468<BT474 despite having approximately equivalent levels of total Hsp90 among the latter three, (n = 3, ±SEM) (Figure 7). Interestingly, this uptake order correlates with the relative tumorigenicity of the cells to form tumors in SCID mice[142].

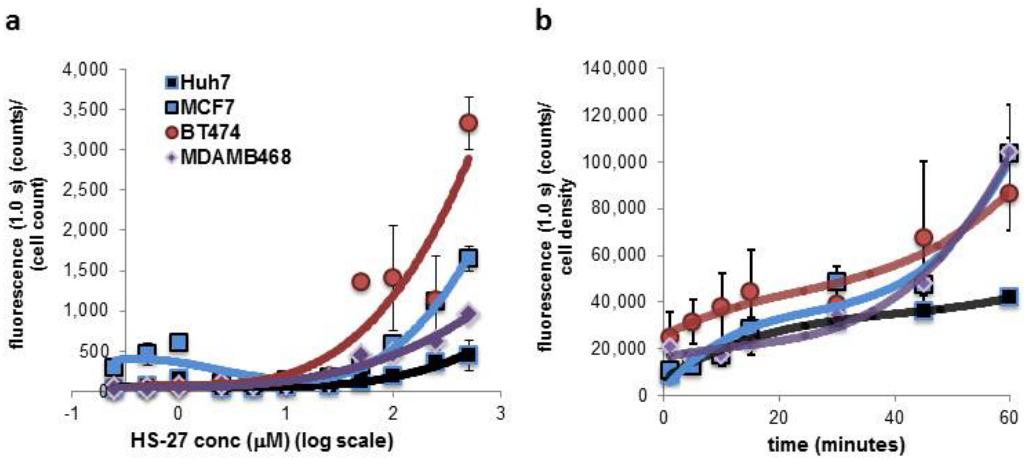

Figure 7: Titration and time course studies of HS-27 in cell lines

Analysis of Her2 levels in BT474 cells show that, once internalized, HS-27 is active as an Hsp90 inhibitor and uptake (green) inversely correlates with Her2 degradation (black) (Figure 8).

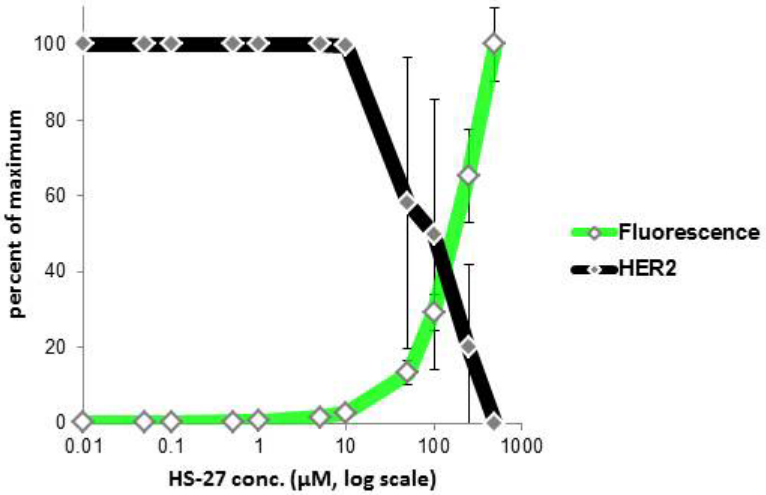

Figure 8: HS-27 uptake in BT474 cells inversely correlates to Her2 degradation

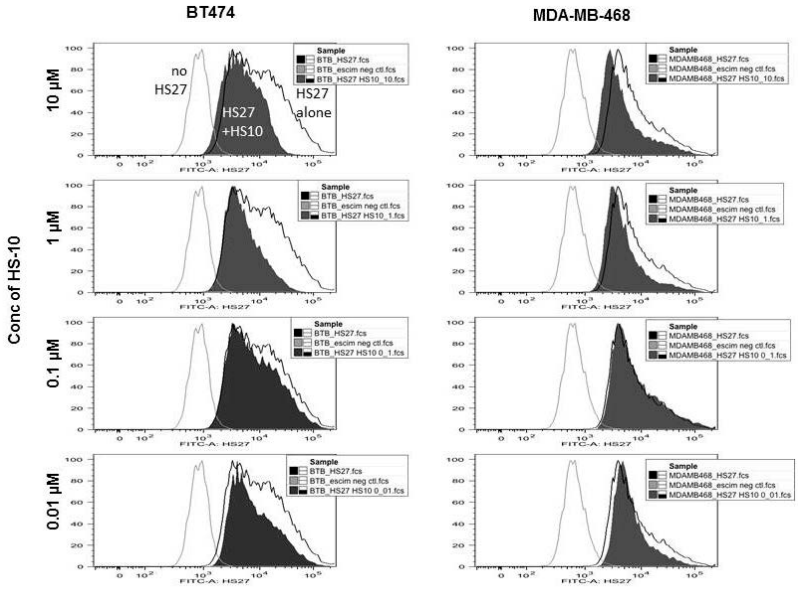

Figure 9: Flow cytometry reveals that HS-10 competes HS-27 in a dose dependent manner in breast cell lines

Competition experiments with the untethered ligand, HS-10 (Figure 9), and comparisons with a control compound FITC-tethered lapatinib, HS-42 (Figure 10), demonstrate that HS-27 uptake and selectivity for the breast cells is Hsp90-dependent. In the case of HS-42, despite sharing a common fluorophore with HS-27, HS-42 (black line) was rapidly absorbed with identical kinetics between BT474 (a) and Huh7 (b) cells (Figure 10). These findings show that the uptake of the two FITC-tethered inhibitors involve different mechanisms that are ligand-dependent. As for HS-42, uptake may reflect binding to EGFR, whereas for HS-27, the apparent mechanism is binding to ectopic Hsp90. This conclusion is consistent with others who have linked extracellular Hsp90 with the metastatic potential of various tumor lines, including breast cancer cells[97,140,143].

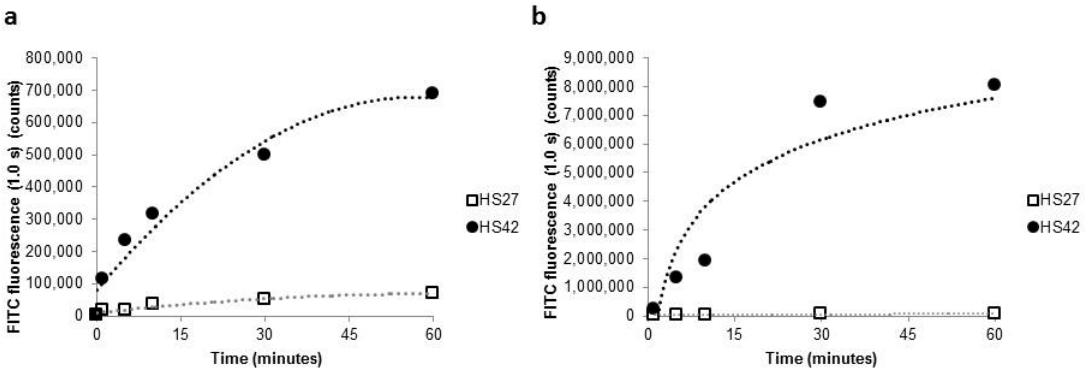

Figure 10: Comparison of HS-27 and HS-42 kinetics in BT474 and Huh7 cell lines

Additional data supporting that the tethered Hsp90 inhibitors bind to ectopically expressed Hsp90 in breast cell lines came from observations with the permeabilizing agents, β-escin and Triton X-100. In the presence of 5 μM β-escin, HS-27 enters MDA-MB-468 and Huh7 cells. To test whether HS-27 was non-specifically labeling permeabilized Huh7 cells, we competed HS-27 binding with a 10-fold excess of HS-10, which blocked binding in both cell lines (scale bar, 50 μm) (Figure 11). These data suggest that Huh7 cells do not express ectopic Hsp90, but they do contain an internal pool of Hsp90 that binds the inhibitor. We also observed other cell lines that were unable to internalize HS-27 without permeabilization, including lymphoma cells purified from patients with CLL, human peripheral blood mononuclear cells or cultured fibroblasts.

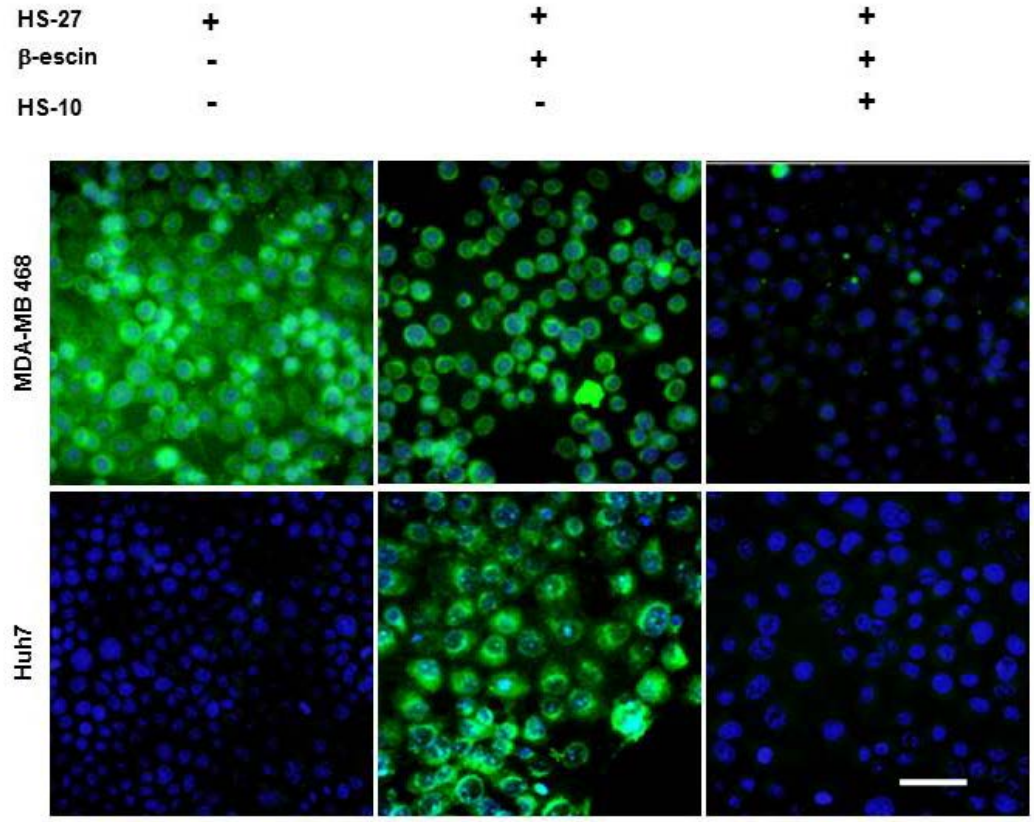

Figure 11: β-escin permeabilization assay points to the role of ectopic Hsp90 in HS-27 internalization

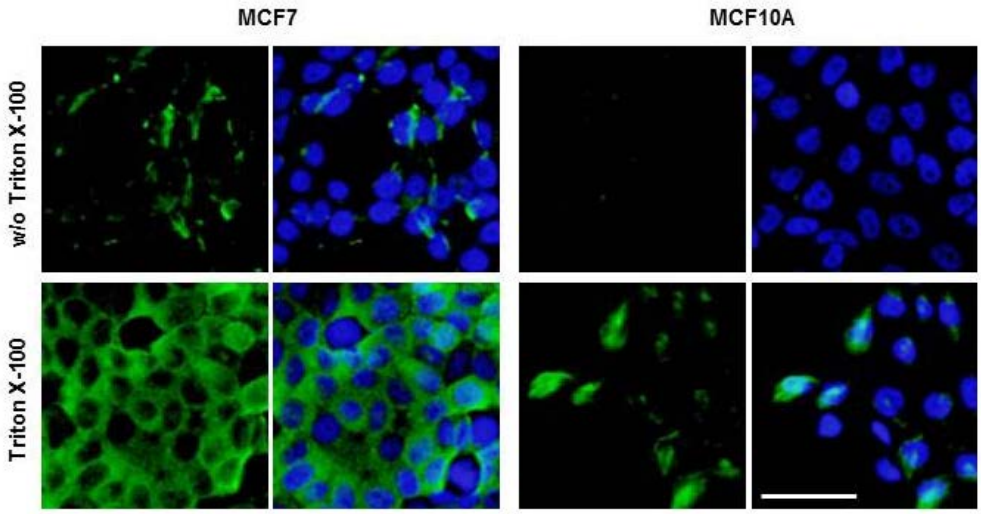

Figure 12: Anti-Hsp90 antibodies label surface Hsp90 in non-detergent conditions in MCF7

Because of its polar nature, HS-27 would not be predicted to enter cells through passive diffusion and the competition studies with HS-10 strongly argue that its internalization requires binding to Hsp90 expressed at the surface. Consistent with this hypothesis, anti-Hsp90 antibodies were found to selectively stain the surface of the more tumorigenic MCF7 cells compared with non-tumorigenic MCF10A cells (scale bar, 50 μm) (Figure 12). These fixed breast cancer cell lines were treated with or without 0.3% Triton X-100 and subsequently stained by immunofluorescence with an anti-Hsp90 antibody. Cells treated with Triton have intracellular pools that are labeled, while non-permeabilized cells exhibit exclusive labeling of surface Hsp90.

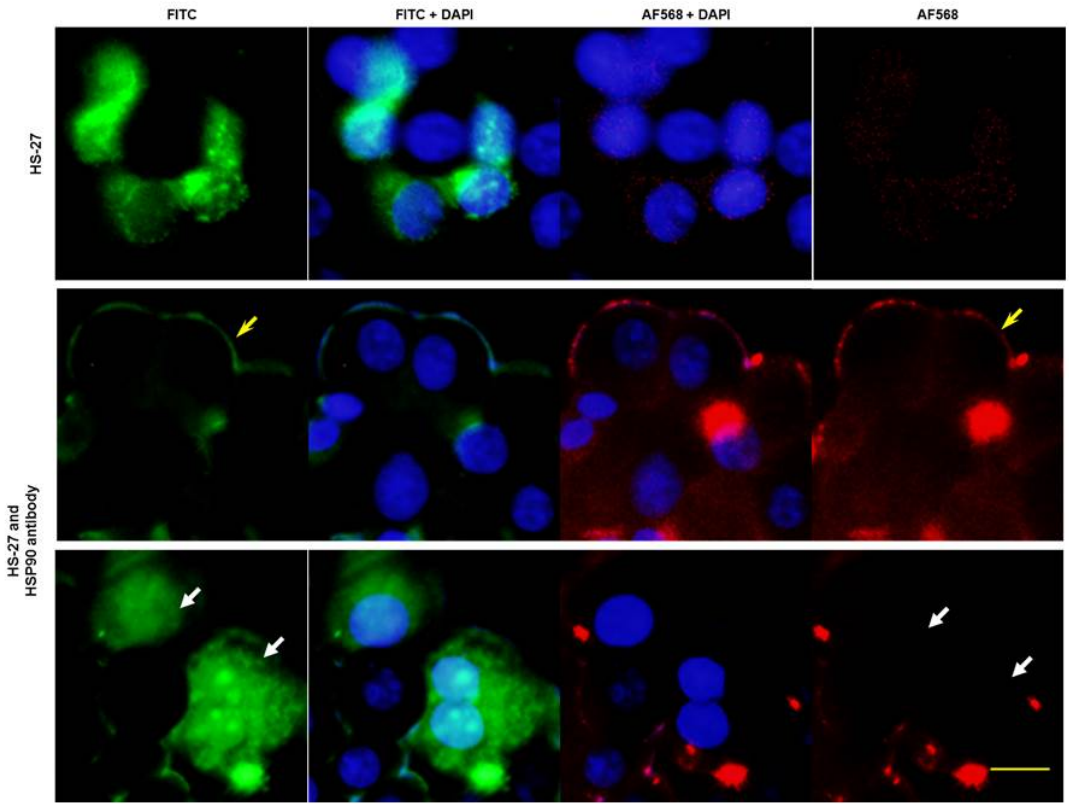

Figure 13: Anti-Hsp90 antibodies block the internalization of HS-27 in MCF7 cells

Additionally, when live MCF7 cells were incubated with anti-Hsp90 antibodies in the presence of HS-27, the probe is retained at the plasma membrane and no longer internalized as shown by co-staining at the surface with the Hsp90 antibody (

Figure 13). The first row is the incubation with HS-27 alone and denotes a single field observed with different filters. Rows 2 and 3 are separate fields of cells incubated with the antibody and HS-27. Row 2 demonstrates peripheral staining of Hsp90 (yellow arrow) by both the antibody (red) and HS-27 (green). Row 3 shows cells that are not labeled with the antibody and have internalized HS-27 (white arrows) (scale bar, 10 μm) (Figure 13).

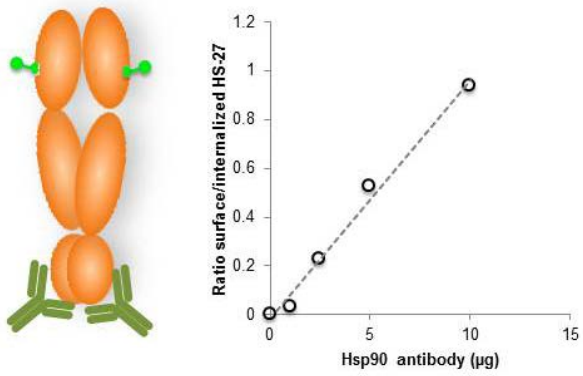

Figure 14: Does-dependent Hsp90 antibody blocking of HS-27 internalization

Importantly, the Hsp90 antibody used in this experiment targets the C-terminal domain of the protein and does not interfere with the HS-27 binding at the N-terminal ATP-binding domain (Figure 14). In antibody titration experiments, the retention of HS-27 at the surface correlates precisely with antibody concentration. At 10 µg/well of antibody, the number of cells that retained HS-27 at the surface to those cells that internalized HS-27 was almost 1:1, whereas the ratio was 1:4 at an antibody treatment of 2.5 µg/well (Figure 14). Collectively our data highlight an unrecognized pathway in which Hsp90 is not only trafficked to the membrane, but actively internalized. The internalization is likely not attributed to general pinocytosis that results in fusion with the lysosomes. Lysosomes have internal pHs of <6, and HS-27 consists of an Hsp90 inhibitor tethered to FITC which loses its fluorescent properties below pH 6.5 (Figure 15). Additionally, we failed to detect the co-localization of HS-27 with Rab5, a marker of early endosomes, by fluorescent microscopy. We posit that the internalization mechanism of HS-27 is active endocytosis yet Rab5-independent.

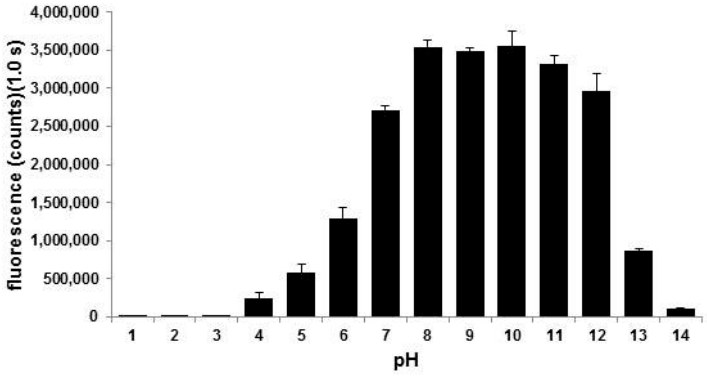

Figure 15: HS-27 fluorescence is pH dependent

As aforementioned, Hsp90 is thought to be constitutively secreted only from tumor cells[90,98,106]. To detect the presence of secreted Hsp90, we added 10 μM HS-27 to media harvested from BT474, MCF7 and Huh7 cells, and removed the free probe by ultrafiltration. BT474 and MCF7 exhibited substantial recovery of fluorescence compared to Huh7, which is consistent with the former cells actively secreting Hsp90 (Figure 16).

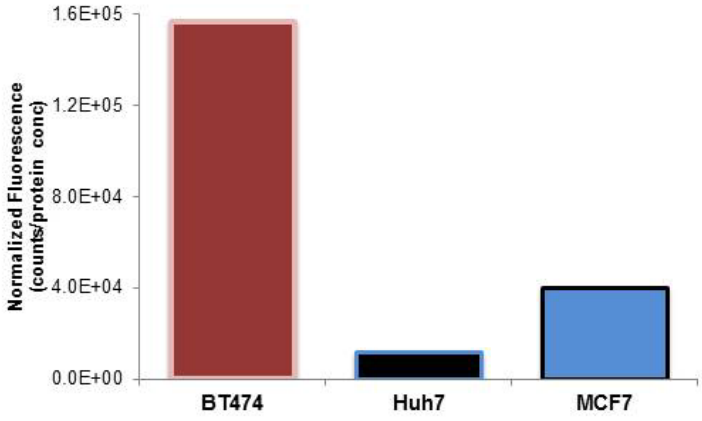

Figure 16: HS-27 binds to Hsp90 in the conditioned medium of cultured cells

To examine whether extracellular Hsp90 was sufficient to facilitate HS-27 uptake into Huh7 cells, MCF7 cells were co-cultured with Huh7 cells and incubated with HS-27. Figure 17 shows that the presence of locally secreted Hsp90 from MCF7 cells is not sufficient to promote subsequent reuptake into the Huh7 cells. This suggests that Huh7 cells lack the machinery (e.g. receptor) necessary for the active internalization of HS-27 bound to Hsp90.

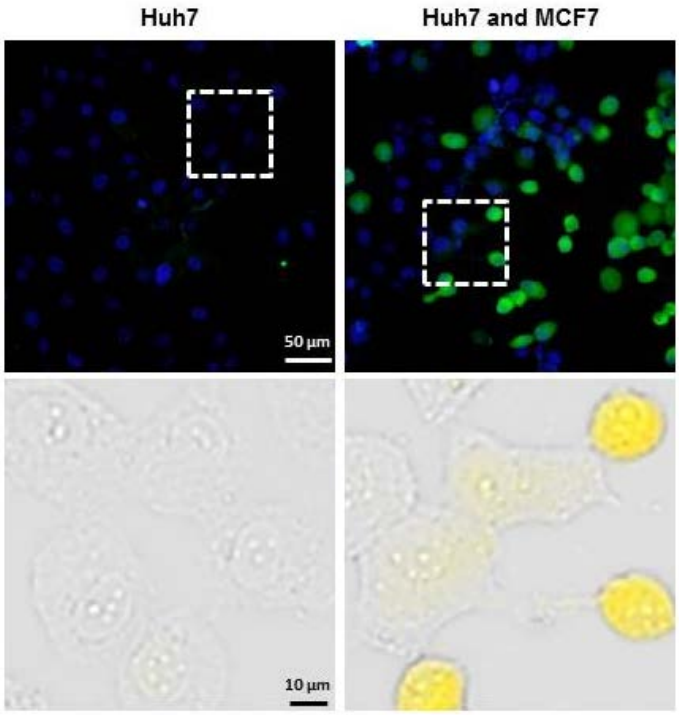

Figure 17: Co-culture of Huh7 and MCF7 cells treated with HS-27

3.3 Fluor-tethered Hsp90 Inhibitors are Selective for Active Hsp90 in vitro

Our probes can discriminate between various cell lines, but recent data suggest that there are distinct populations of active and inactive Hsp90 within a given cell[45,46]. To test if our probes also discriminate between these cellular pools in vivo, we first isolated these pools using affinity chromatography. Briefly, cell extracts from MDA-MB-468 cells were passed over virgin immobilized Hsp90 ligand beads three times. The "active pool" binds and the "non-active pool" flows through the resin (Figure 18)[47]. Once separated, the resin bound extract and flow through were incubated with HS-27 and unbound probe was filtered away. Fluorescence was measured on a multi label plate reader (n = 3, ±SEM student t-test P value < 0.005). Hsp90 from the resin-bound pool demonstrated HS-27 binding that was 15.5-fold higher than inactive Hsp90 in the flow through.

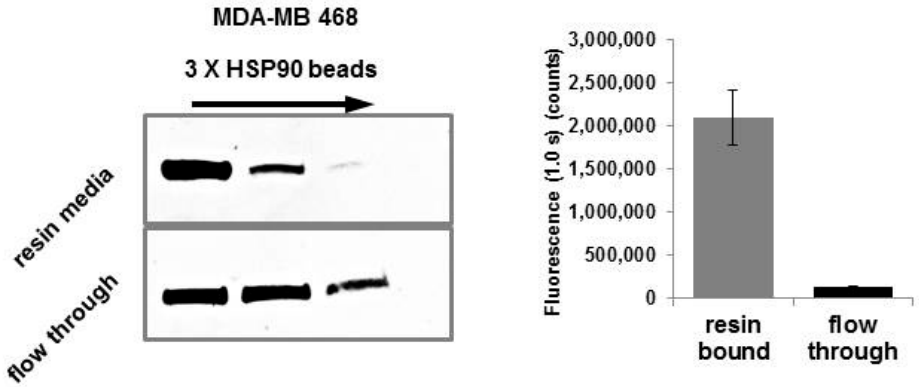

Figure 18: Active Hsp90 depletion using affinity resin chromatography

To further characterize the HS-27 bound active pool of Hsp90, we separated either purified Hsp90 (from lactating pig mammary gland) or BT474 cell extracts incubated with HS-27 by micro-anion-exchange chromatography. In the extracts from the BT474 cells, we expected to see multiple column fractions with fluorescence in the breast cancer cell extract, consistent with multiple interactions of active Hsp90 with its respective client proteins. However, and in most cases, only a single peak of fluorescence was observed, which correlated precisely with the migration of purified pig mammary Hsp90 bound to HS-27 (Figure 19a).

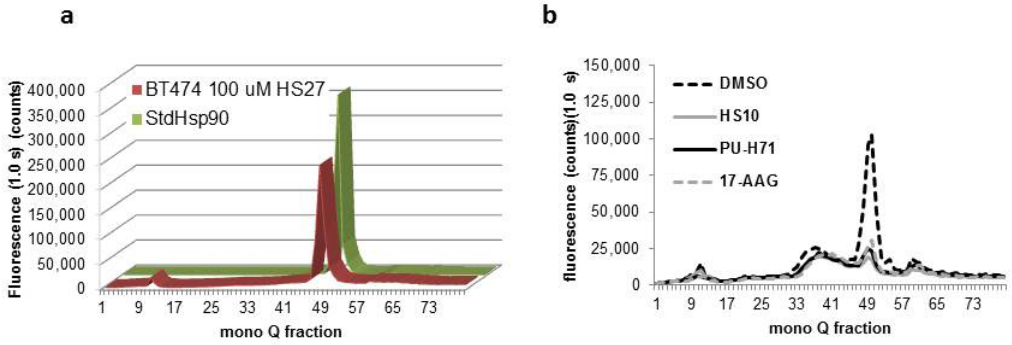

Figure 19: Mono Q fractions of HS-27 treated cells and purified Hsp90

Furthermore, we competed the binding of HS-27 with three structurally distinct Hsp90 inhibitors: HS-10, PUH71 and 17-DMAG. MCF7 cells were incubated with the non-fluorescein Hsp90 inhibitors, followed by HS-27. Equal competition was observed with the three Hsp90 inhibitors compared to the DMSO control treatment (Figure 19b). The presence of Hsp90 in the single peak was confirmed after column fractions containing fluorescence were passed over the cleavable Hsp90 affinity resin followed by

SDS-PAGE, silver staining and mass spectrometry (Figure 20). Collectively, these biochemical data strongly argue that the only intracellular target for HS-27 is an active pool of Hsp90 that is largely devoid of client proteins. These data are consistent with previous work by our laboratory using Hsp90 small molecule affinity resins showing that the ligand bound form is not associated in vivo with multiple clients as previously thought [47].

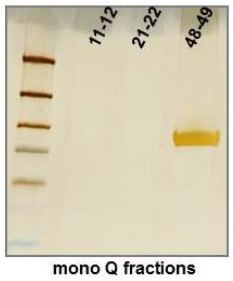

Figure 20: Hsp90 protein present in corresponding HS-27 fractions

We next explored whether the probes could be used to measure acute activation of Hsp90 in cells in response to heat stress. We show that heat stress produces a consistent 1.2-fold increase in fluorescence eluting in the 49th fraction of MCF7 (a) and MDA-MB-468 (b) cell lines (Figure 21).

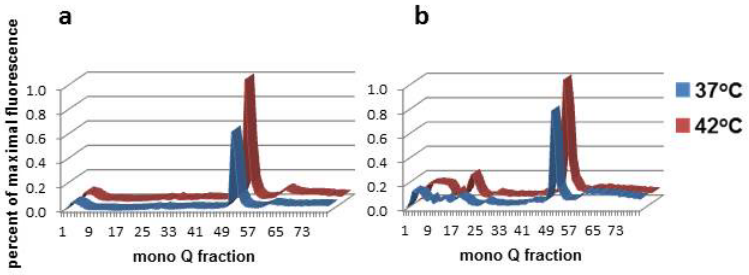

Figure 21: Mono Q fractions of heat shocked cells treated with HS-27

We then examined if the probe could be used to quantify the amount of activated Hsp90 distributed in normal tissues by adding HS-27 to homogenized mouse tissue extracts and then fractionating the tissue extracts chromatographically. Mouse tissues were harvested from BALB/C mice and lysed tissues were incubated with HS-27. After clearing away the unbound probe, samples were analyzed by anion exchange chromatography. Tissues were ordered from lowest expressing tissues to highest. We show that homogenized tissues contain diverse levels of active Hsp90 which also elute as a single peak (Figure 22).

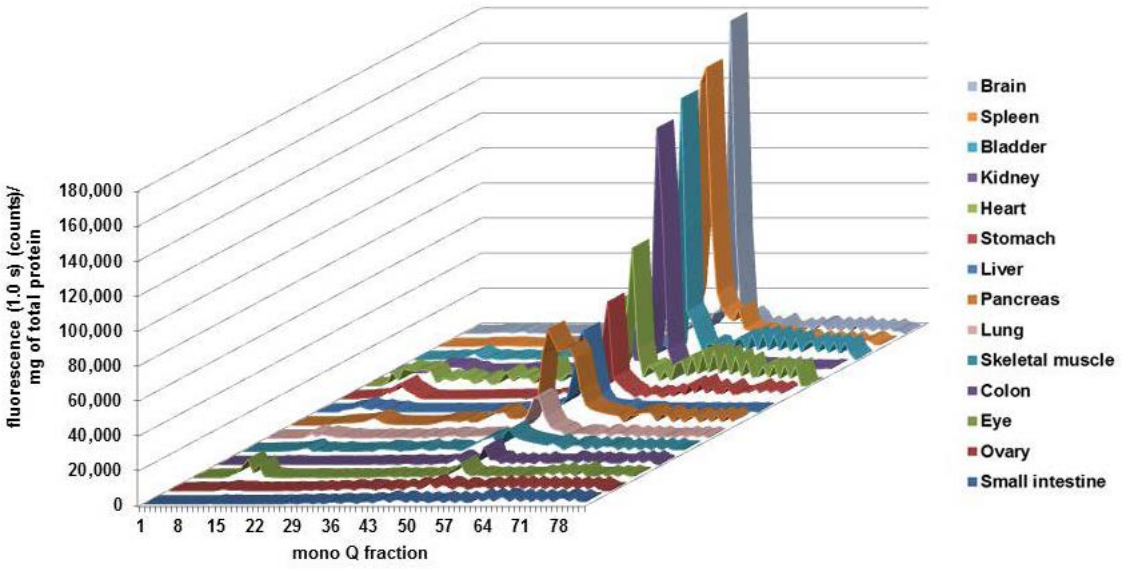

Figure 22: Mono Q fractions of mouse tissues homogenates exposed to HS-27

The significance of these observations is that non-tumorigenic tissues contain an active pool of Hsp90, and in brain, spleen, bladder and kidney the levels were especially high. Irrespective of this finding, only intact cells expressing ectopic Hsp90 are capable of internalizing the fluor-tethered inhibitors. We suggest that malignant tumor cells express ectopic Hsp90 and that this pool of Hsp90 can be used to discriminate malignancies in vivo over normal tissues or more benign tumor cells. We also conclude that although the probe can reflect the tumorigenic state, the drug-bound version must have a low affinity for client proteins in stark contrast to the conclusions reported by others[46].

3.4 Fluor-Tethered Hsp90 inhibitors Specifically Target Human Breast Tumors in Mice

To test if fluor-tethered Hsp90 inhibitors might be exploited to selectively visualize malignancies non-invasively, we injected the probes into mice bearing breast tumor derived xenografts in their right flanks. With MDA-MB-468 xenografts, we detected the tumor mass within 5 minutes post intravenous tail injections either with HS-27 or the near infrared (nIR) HS-69 and HS-70 versions in a IVIS Kinetic fluorescent imager (Perkin-Elmer, Inc.). In the case of HS-27, the tumor is clearly visible through the fur and discriminated from the natural background fluorescence normally observed at 520 nm (Figure 23). With nIR versions, post injection, the probe was observed in the extremities (i.e. ears, nose, and paws) and eyes reflecting the circulating unbound probe in the blood pool. This was not visible with the fluorescein versions because of the light scattering at 520 nm.

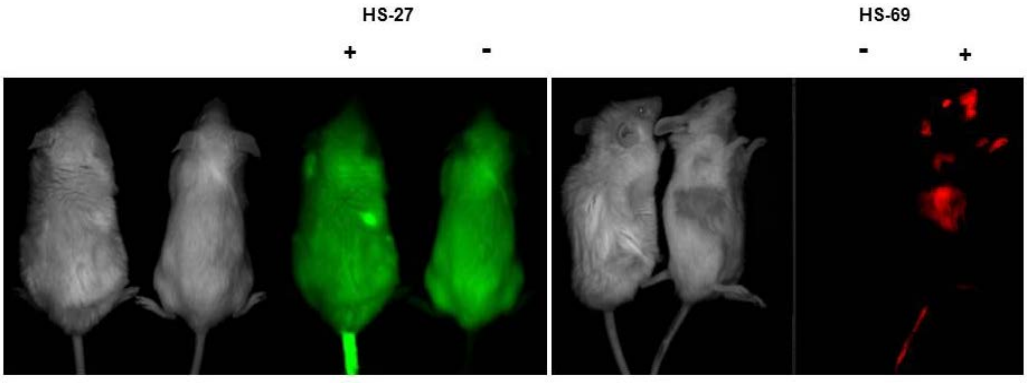

Figure 23: Non-invasive imaging of mouse xenograft tumors after post injection of HS-27 or HS-69

All fluor-tethered Hsp90 inhibitors demonstrated dose-dependent accumulation of the small molecules in the tumors (Figure 24a,b). With HS-27, an 8-fold increase was consistently observed over control tumors in mice that did not receive HS-27. With both nIR probes, we achieved a 150-fold increase at the tumor site due to the low background signal at 660 nm or 800 nm. HS-27 (green), HS-69 (red), and HS-70 (dark red) were injected in 1 mg doses into mice and tumors excised. Tumors were compared to non-tumor areas (left flank) and control tumors (n = 3; ±SEM) (Figure 24c,d).

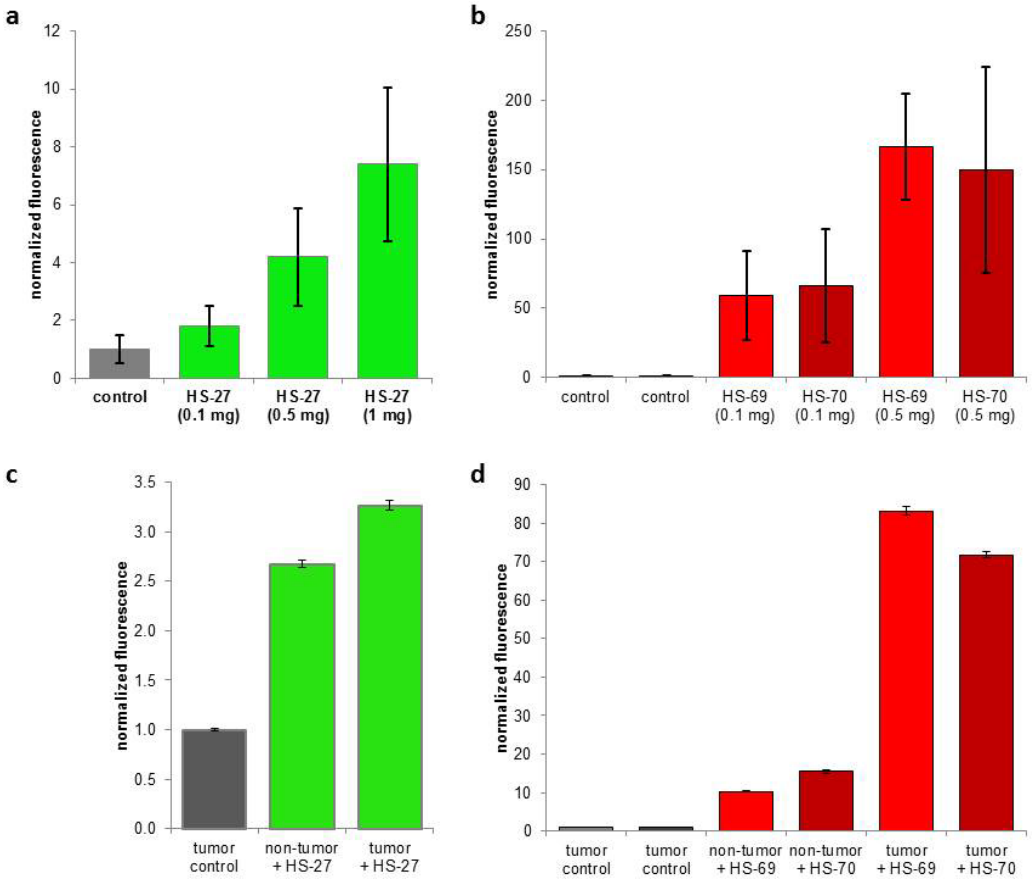

Figure 24: Dose-dependent uptake and specificity of fluor-tethered Hsp90 inhibitors

Pharmacokinetic studies by various methods show dose dependent uptake of either the visible or nIR forms, peaking within the tumor mass by 30 minutes and with a detectable signal remaining for up to 72 hours (Figure 25). In the case of Figure 25b, non-tumorigenic tissues displayed no fluorescence over the course of 96 hours.

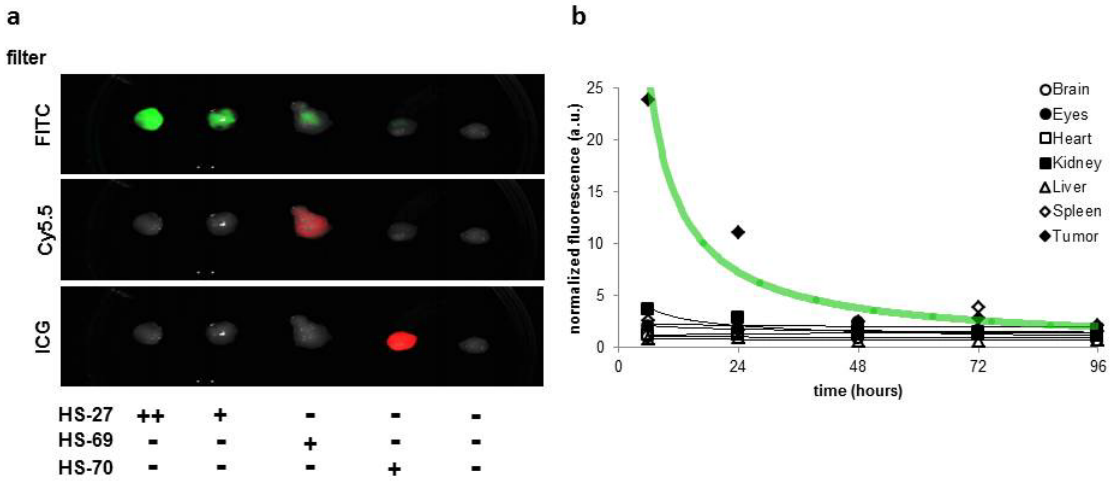

Figure 25: Dose-dependent uptake and pharmacokinetics of fluor-tethered Hsp90 inhibitors

We specifically looked at earlier time points and different methods of administration of HS-27. We found that highly vascularized tissues such as the lungs exhibited high fluorescence at earlier time points, but by 30 minutes the signal from non-specific binding was cleared from the organ (Figure 26a). There was no biological difference in HS-27 kinetics, whether we injected the animals intravenously (i.v.) or intraperitoneally (i.p.). The liver did show greater accumulation in earlier time points in the i.p. injection of HS-27, but again it is quickly cleared from the tissue (

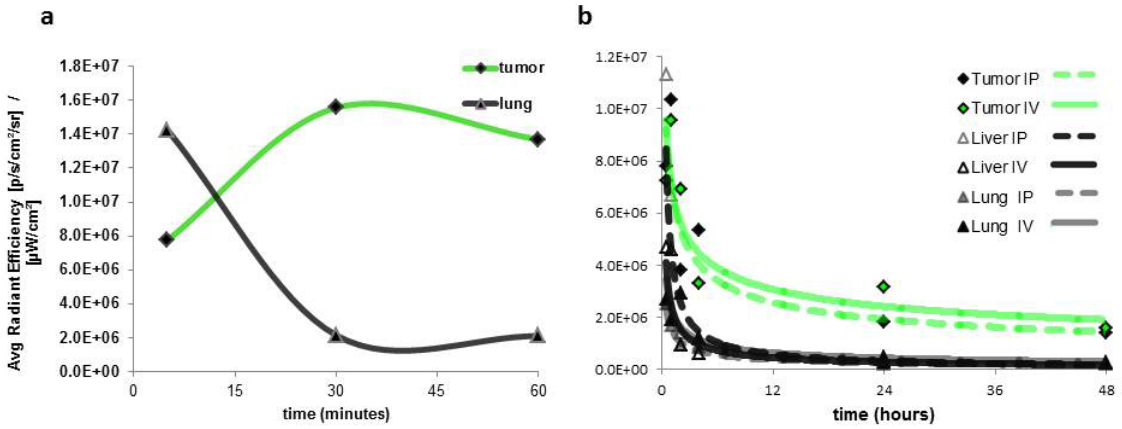

Figure 26b).

Figure 26: Pharmacokinetics of HS-27 and effects of the route of administration

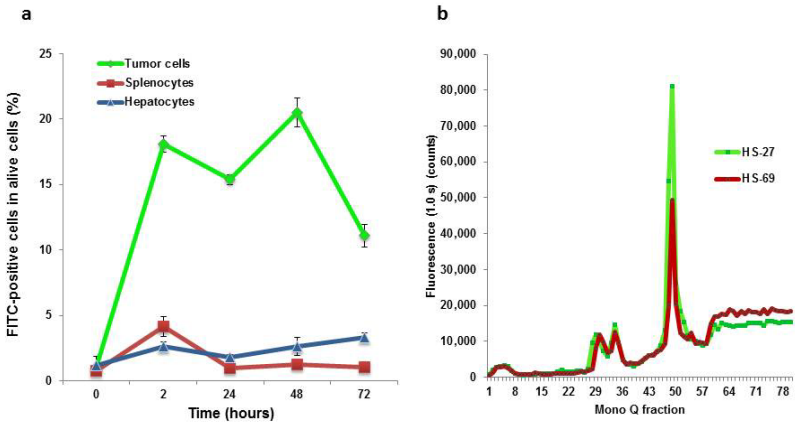

Figure 27: Flow analysis and mono Q detection of HS-27 and HS-69 in tumors

As a test of tumor selectivity in vivo, the Lyerly lab simultaneously harvested tumor cells, splenocytes and hepatocytes from SCID mice bearing MDA-MB-468 tumors over the course of 72 hours and analyzed the viable cells by flow cytometry for the presence of HS-27. Figure 27a shows specific uptake of the probe by tumor cells, while splenocytes and hepatocytes did not. To test whether the probes were binding to Hsp90 in vivo, or just accumulating in the tumors because of a blood pooling effect, excised tumor lysates were fractionated chromatographically. As shown in Figure 27b a single major peak of fluorescence was observed that contained Hsp90.

Pharmacokinetic studies over 96 hours by optical spectroscopy performed by the Ramanujam lab more elegantly confirmed selective uptake of the tethered inhibitors. In this in vivo approach, a spectral pen was placed either at the tumor site or an adjacent skin patch, and the fluorescence spectrum measured from 500-620 nm. Figure 28 shows the signature spectrum of fluorescein at the tumor site and not at the adjacent skin sites

over a period of 6-24 hours post injection. Spectra were corrected for the effects of scattering and absorption from the tissue.

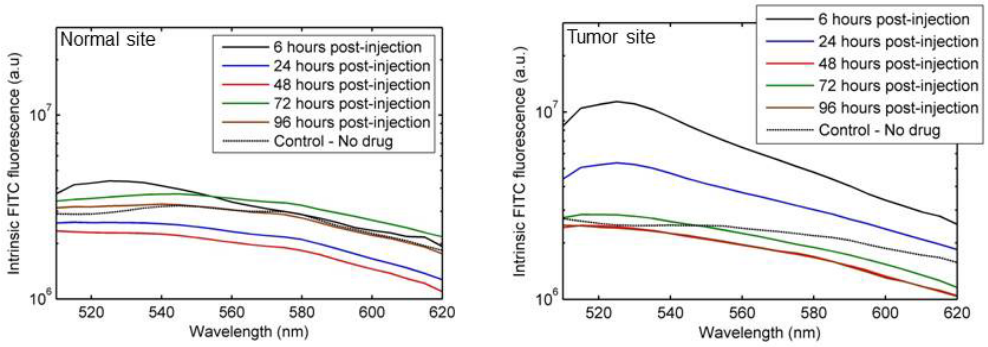

Figure 28: Optical scanning for fluorescence in xenograft mice injected with HS-27

To ensure that the in vivo probe accumulation within the tumor was ligand-dependent, a control compound HS-105 was synthesized. HS-105 consists of the fluorophore and tether, minus the ligand. In affinity chromatography studies against Hsp90 bound to immobilized ATP, HS-105, showed no affinity for the protein, and therefore any tumor retention would be non-specific (Figure 29a). In Figure 29b, HS-27- and HS-105-injected SCID mice were compared in tissues and xenografts. Excised tissues were measured for average radiant efficiency after 24 hours post injection. Tumors show retention of HS-27 whereas the lungs display a slight retention of HS-105.

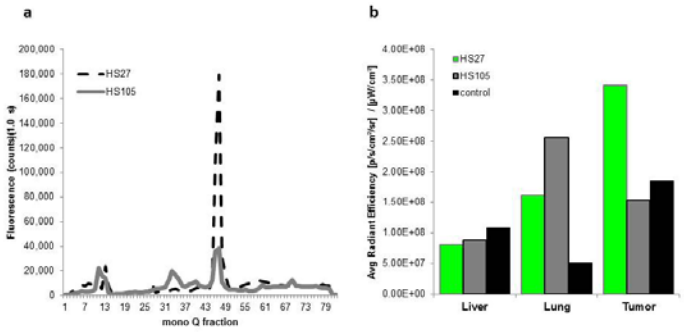

Figure 29: HS-27 shows tumor specificity and the compound without ligand, HS-105, does not

Using IVIS kinetic imaging, HS-27 was detected through the skin in live animals at one hour, whereas HS-105 was below detection (Figure 30). In more detailed necropsies, by 24 hours we found no trace of HS-105 by fluorescence whereas HS-27 was still present within the tumor (Figure 30).

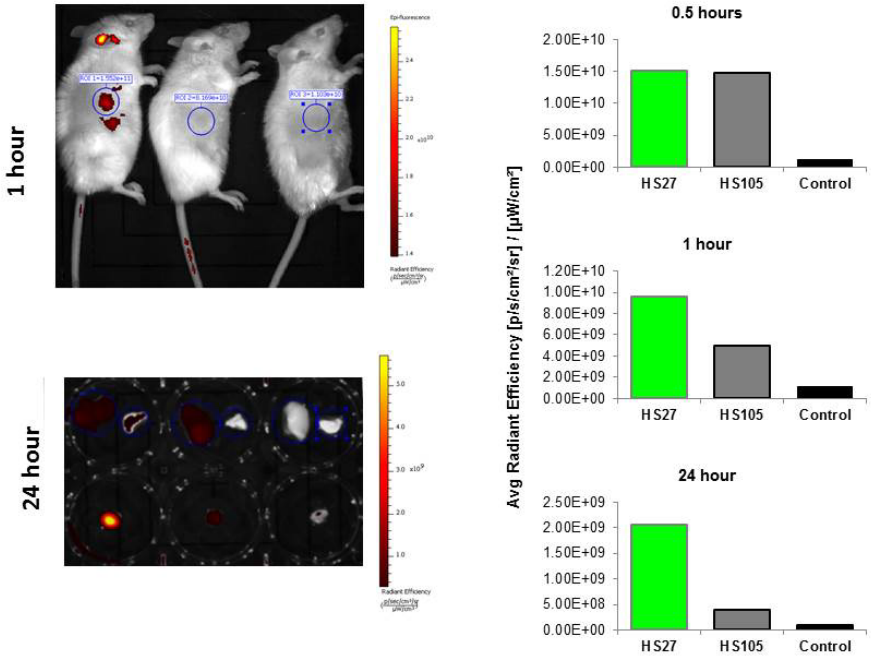

Figure 30: HS-27 retention in the tumor is dependent on the Hsp90 ligand

Next we sought to quantify the amount of HS-27 accumulation in the tumor by comparing the average radiant efficiency in the tumor to a standard curve of HS-27 concentrations measured by the IVIS kinetic imager. We calculated that in a cohort of 5 mice, the mean accumulation of HS-27 was 6.5 μM ±2.6 (SEM) at 24 hours. To test the utility of fluor-tethered Hsp90 inhibitors as potential means of non-invasive early tumor detection, the Lyerly lab designed an assay to test the sensitivity of the nIR version, HS-70, in mice. MDA-MB-468 cells were treated ex vivo with HS-70 or control (untreated). A fixed number of cells were injected in an equal volume to the right flank of SCID mice. We found that HS-70 could be detected at as little as 100,000 cells (Figure 31).

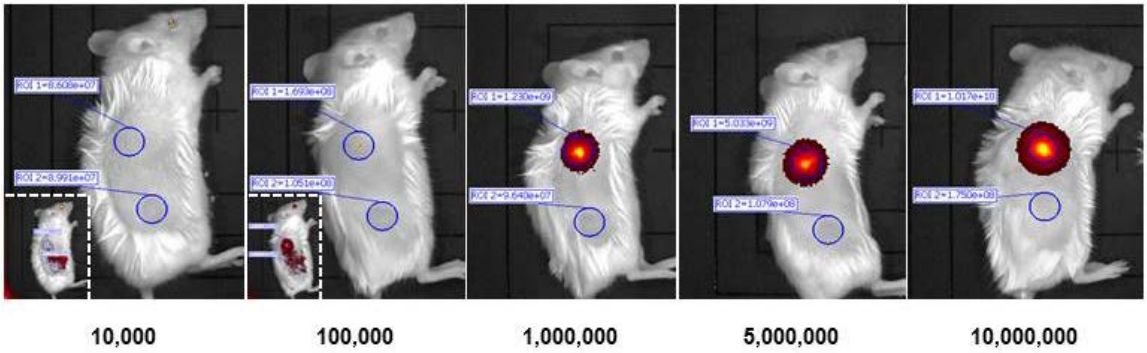

Figure 31: Ex vivo labeling of MDA-MB-468 cells with HS-70 and in vivo detection

Current imaging approaches by MRI or PET/CT are estimated to reliably detect tumor masses at 1 cm^3 with an estimated cell mass of ~10 million cells[144,145]. By these criteria, 100,000 cells would suggest that nIR probes could theoretically detect masses as low as 0.01 cm^3.

Based upon our findings with the nIR probes, an obvious application for early malignancy detection would be surface tumors in which upregulation of Hsp90 has been indicated, such as head and neck, colorectal, bladder and melanoma[139,146]. Because nIR probes are limited to 3-4 cm in tissue depth, to enable whole body imaging we investigated an alternative approach using tethered Hsp90 inhibitors capable of carrying the radioisotope ^{125}I ([^{125}I]HS-111). Picomolar amounts of [^{125}I]HS-111were added to either MCF7, BT474 or Huh7 cells and as observed with the fluor versions, the breast cancer cells exhibited uptake above Huh7 cells (data not shown).

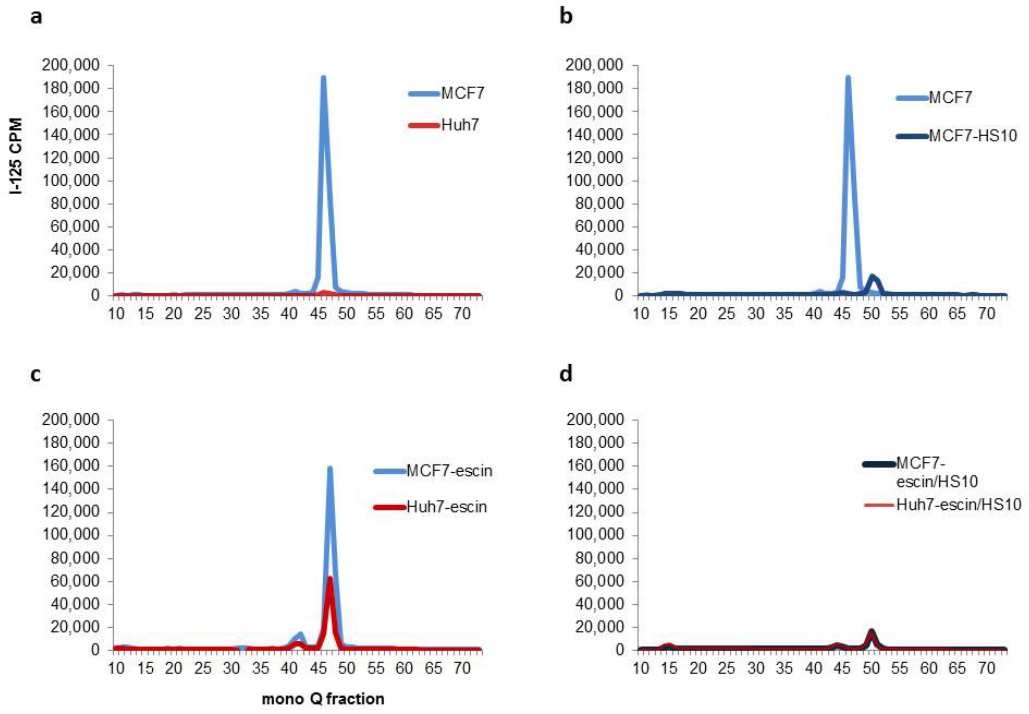

Figure 32: Radiolabeled Hsp90 inhibitor, HS-111, recognizes cell lines with ectopic Hsp90

Uptake of [^{125}I]HS-111into MCF7 and Huh7 cells was then characterized after chromatographic fractionation and the probe was detected by its radioactivity. As observed with the fluor-tethered versions, in MCF7 cells, the majority of the radioactivity migrated as a single peak, in stark contrast to Huh7 cells which showed no peak recovery (Figure 32a). Importantly, the signal in MCF7 cells was effectively competed by the free ligand, HS-10 (Figure 32b). As with the fluor versions, β-escin permeabilization of Huh7 cells permitted the labeling of Hsp90 with [^{125}I]HS-111in a competitive manner (Figure 32c,d).

Importantly, HS-111 behaves similarly to the fluor-tethered versions in terms of its selectivity towards the breast cancer cell lines and entry to these cells also clearly requires active internalization through binding to ectopic Hsp90. Interestingly, HS-111 is more potent than the fluor versions in Her2 knock down assays suggesting faster kinetics of internalization and performed most closely to HS-10, the parent untethered compound. This is likely due to the differences in added steric bulk of the attached imaging moieties. HS-111 consists of a benzalamide moiety of 121.1 Da, whereas HS-27 carries a bulky fluorescein moiety of 389.0 Da. Similarly, a lower rate of entry was observed with HS-96, a biotin-tethered Hsp90 inhibitor, which is considered to not passively diffuse across cell membranes (Figure 33).

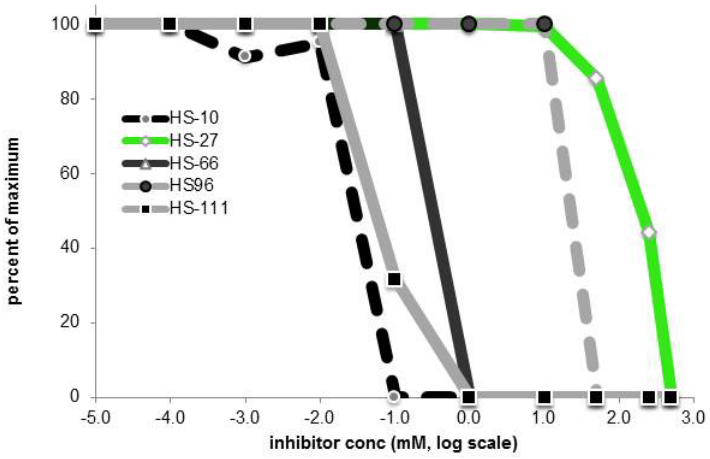

Figure 33: Her2 degradation as a predictor of Hsp90 inhibitor internalization

These data strongly suggest that one can readily manipulate the entry rate of tethered inhibitors into cells expressing ectopic Hsp90 by changing the properties of the tethered imaging moiety. The finding that tethered inhibitors with structurally diverse imaging prosthetic groups only enter cells expressing ectopic Hsp90, and at variable rates, discredits the possibility that the entry of the tested probes occurs only through simple diffusion.

3.5 Conclusions

Our data have shown that an important frontline cancer target, Hsp90, can be exploited through its role in the oncogenic process as a diagnostic marker for real-time imaging of metastatic status. This observation represents somewhat of a paradigm shift in the way we currently view cutting edge therapeutic targets such as Hsp90, and the concept could be extended to other therapeutic targets. Tethered Hsp90 inhibitors as imaging agents potentially add an element of diagnostic detail that cannot be garnered

from expression analysis or deep sequencing techniques. Specifically for Hsp90, these techniques do not measure the activation state of the protein or its localization, two important parameters linked to disease progression in breast cancer[46,97]. The urgency to exploit this approach is made more relevant by the recent landmark studies of Gerlinger et al. who demonstrated the degree to which tumors exhibit phenotypic heterogeneity, even within the same tumor[114]. Because expression analysis and deep sequencing only represent a fraction of a tumor's global heterogeneous expression pattern at a single time point, these findings signal the limited utility of these approaches to stratify and diagnose tumors. However, because tumor growth requires the continued activation of signal pathways, then perhaps the development of fluor-tethered and other imaging inhibitors targeting proteins like Hsp90, or constitutively activated oncogenes like Her2, can offer a new alternative strategy to more accurately stratify disease progression through real-time, non-invasive imaging.

If expression of ectopic Hsp90 signifies metastatic behavior in vivo, the fluor- or ^{125}I-carrying-tethered Hsp90 inhibitors could be used in conjunction with current biopsy practice to diagnose aggressive tumors. This would simply involve histological examination to determine probe uptake following microdose administration prior to the biopsy procedure. Moreover, non-invasive whole body PET imaging could be employed using ^{124}I-containing tethered versions. The PET based approach is attractive because one could simultaneously determine the fate and distribution of the tethered inhibitor in

all tissues and in real-time. If PET analysis of a ^{124}I-carrying-version showed highly selective targeting to the tumor in any one individual, one could proceed to a ^{131}I version (which emits cytotoxic β-particles) with the goal of achieving complete body-wide tumor ablation without unwanted damage in normal tissues. The known μM accumulations of Hsp90 inhibitors (5-20 μM) within tumors and established protocols for the treatment of thyroid cancers with ^{131}I should help accelerate the development of such treatment strategies[41].

The importance of ectopically expressed Hsp90 to the metastatic process has been established in a variety of ways including using a functional proteomic screen[96] and a non-cell permeable form of geldanamycin (DMAG-N-oxide) and anti-Hsp90 antibodies, both of which block cellular migration in metastatic tumor lines[107,140,143,147,148]. The observation that fluor-tethered versions are selectively internalized by binding to ectopically expressed Hsp90 has revealed new roles for the protein in vivo. Although the expression of surface Hsp90 appears to be connected to cell migration and metastasis, the molecular mechanism by which ectopic Hsp90 signals to the tumor cell to promote these events is not known. Both migration to the surface and reinternalization of Hsp90 could involve low copy clients, which may provide a means of signaling that promotes cellular migration and metastasis. This conclusion is supported by anti-Hsp90 antibodies that blocked reinternalization of Hsp90 as reflected by inhibition of HS-27 uptake into MCF7 cells. Irrespective of ectopic Hsp90 roles in metastatic progression, the knowledge

that the protein is reinternalized could be exploited to improve the safety margins of existing Hsp90 therapeutics or selectively deliver chemotoxic payloads to tumor cells. Compared to other cancer therapeutics, Hsp90 inhibitors are generally well tolerated by humans although some dose limiting side effects have been observed such as night blindness[44].

To many, the fact that inhibition of Hsp90 can be used therapeutically at all may seem paradoxical. After all, Hsp90 is thought to represent 1-3% of the expressed protein in most cells. This paradox is made even more extraordinary in the light of biochemical studies shown herein, with the finding that extracts from normal tissues contain considerable levels of active Hsp90. Various explanations have been offered in the past concerning the extraordinary selectivity of various Hsp90 inhibitors for tumor cells, including the idea that tumor cells express an oncogenically activated form of Hsp90 with a higher affinity for Hsp90 inhibitors[45]. Our results suggest that the expression of ectopic Hsp90 may play a substantial role in the entry of Hsp90 inhibitors in general. This finding also suggests that in addition to tumor imaging, it may be possible to extend the therapeutic window of Hsp90 inhibitors by developing a range of molecules that do not passively diffuse across the plasma membrane, but can only enter cells expressing ectopic Hsp90.

4. Hsp90 affinity and selectivity

While most of the applications of Hsp90 tethered inhibitors appear to have promising clinical applications, conjugating Hsp90 inhibitors to sepharose beads has allowed us to uncover some fundamental Hsp90 biology, especially as it pertains to cancer. As stated in the introduction, we hypothesize that the three main differences in Hsp90 between cancer cells and normal tissues are (1) the induction, (2) the ectopic expression of Hsp90 on the cell membrane, (3) the activity or affinity of Hsp90 for ATP and its mimetics. For the remainder of this dissertation, I will focus on the activity and affinity of Hsp90 in cancer. Unlike others that use recombinant proteins, we have shown that native Hsp90 and Grp94 can be isolated and examined biochemically for activity and affinity. Additionally, using the unique tools of fluor-tethered Hsp90 inhibitors and Hsp90 affinity resins, we can test and refute previous claims about the differences of affinity found in normal tissue compared to tumors. We observed that one of the major differences is the conformation of Hsp90 in cancer cells. In cancer cells, there is a pool of Hsp90 that does not bind Hsp90 affinity resins and exhibits lower melting temperature despite being full length.

4.1 Resin synthesis and evaluation

A challenge in developing an affinity resin lies in choosing an appropriate ligand and devising chemistry that allows linker attachment without disrupting binding affinity. A structural analog of HS-10 in complex with the N-terminal domain of human

Hsp90 revealed the parts of the molecule which are solvent exposed and suggested a variety of substitutions likely to be tolerated at site number 1 (

Figure 34a,b)[40]. Further analyses suggested that replacing the trimethoxyphenyl group with a linker on a 3-methylpyrazole analog would provide a good balance of potency and ease of synthesis. Therefore, a fluoro-compound was initially synthesized. This intermediate provided a reactive center for the attachment of linkers and allowed for facile synthesis of a potent inhibitor, HS-10, for competition studies[40].

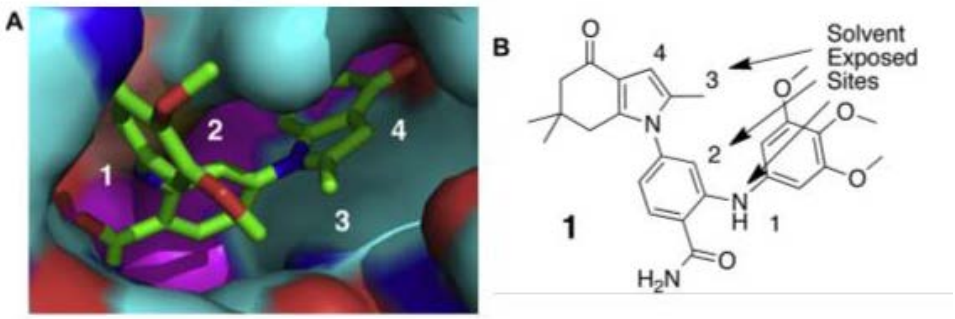

Figure 34: Hsp90 inhibitor in ATP binding pocket of Hsp90

Affinity resins were prepared by reaction of the inhibitor–linker construct with activated affinity media, CNBr-activated Sepharose™ 4B according to the manufacturer's instructions. Ligand was added at 1–10 μM/gram of resin in minimal methanol. Dr. Phil Hughes tried a commonly used linker that has the more hydrophobic n-decane linker to prepared affinity resin A and we analyzed its ability to selectively capture Hsp90 from pig mammary gland extract, a tissue shown to be high in ATP binding proteins including native forms of Hsp90, Grp94 and TRAP1 (Figure 35).

Figure 35: Purinome elution from ATP resin using 1 μM ATP

The resin was incubated in the protein solution then washed with a high salt buffer. The bound proteins were removed via an SDS boil procedure, separated by SDS–PAGE electrophoresis, located by silver staining and identified using mass spectrometry sequencing[149]. A large number of proteins, including Hsp90, were retained. Resin A proved capable of capturing Hsp90 and additional proteins, particularly in the competition experiments with HS-10 (Figure 36, lane A). This may be the result of enhanced and nonspecific hydrophobic interactions of proteins with the linker. We next examined affinity resin B using the short PEG-like 8 atom linker-construct. While the lane minus HS-10 appeared to have less non-specific binding, (Figure 36, lane B); however, the initial hypothesis that proteins other than Hsp90 might be clients was negated when a competition experiment, performed by pre-incubating the protein solution with HS-10 showed clean exclusion of Hsp90, but not the other proteins (Figure 36, lane B).

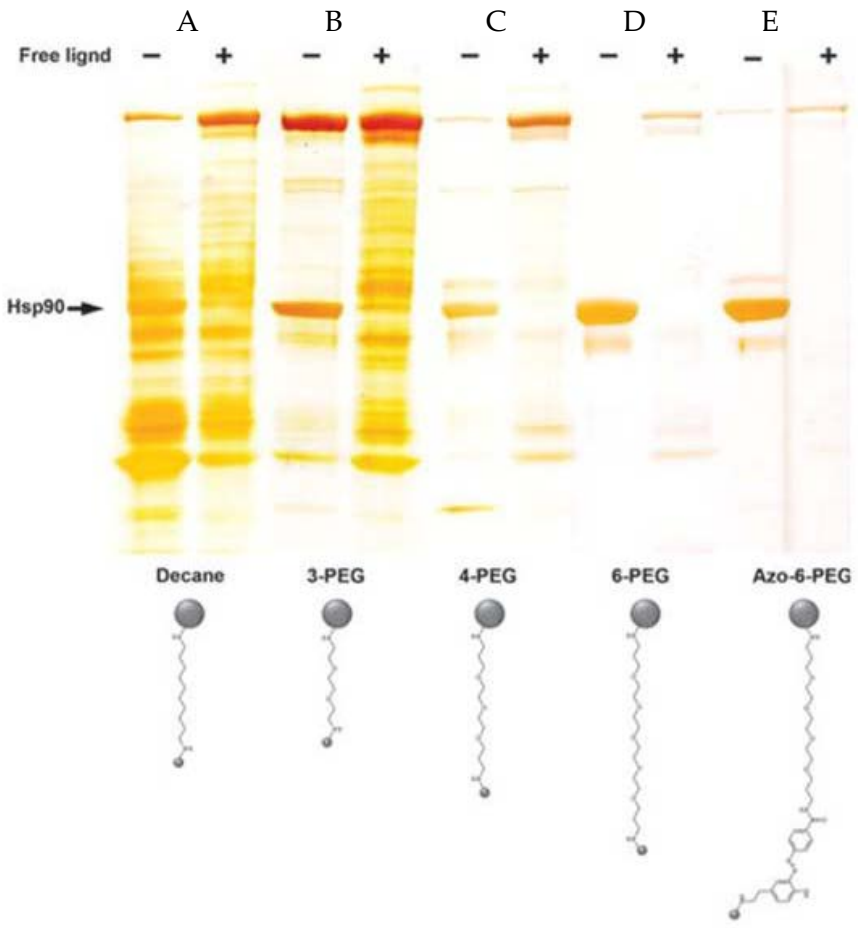

Figure 36: Hsp90 affinity resins and competition

We investigated another intermediate length PEG-like 13 atom linker and prepared affinity resin C. Although it was more selective than resins A and B, some nonspecific binding was observed (Figure 36, lane C). We next examined longer, more hydrophilic linkers that allowed the ligand to extend farther away from the Sepharose surface (Figure 37). Affinity resin D was prepared using the polyethylene glycol (PEG)-like 19-atom linker-construct. The capture experiment was repeated and an intense band of Hsp90 was eluted with SDS (Figure 36, lane D). Importantly, competing with HS-10

showed complete blocking of Hsp90 binding as well as several N-terminal fragments. MS analysis demonstrated that all of the recovered proteins were Hsp90 or proteolytic fragments of the protein, suggesting that resin D is selective for Hsp90 over Grp94 and TRAP1. As mentioned previously (Figure 35), the pig mammary gland tissue contained adequate levels of Grp94 and TRAP1 to be detected by MS when eluted from an ATP resin with 1 μM ATP. All further experiments were therefore conducted with resin D, also referred to as HS-23 sepharose resin.

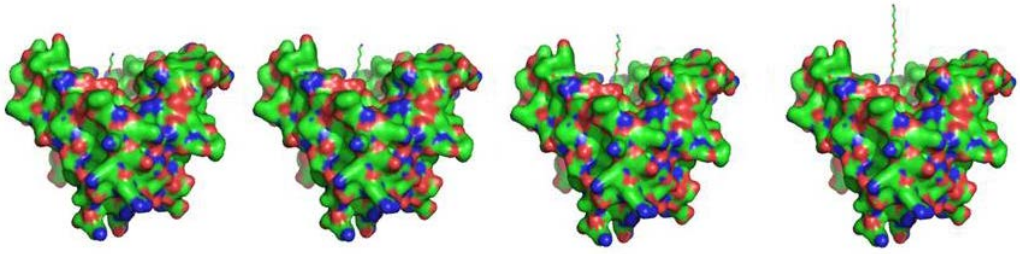

Figure 37: Hsp90 affinity resins with different linkers modeled with homodimers of Hsp90

4.2 Cleavable linker

An important goal of our studies was to derive a probe that could be used to convincingly isolate Hsp90 under mild physiological conditions in association with potentially weakly associated client proteins. Although we can block Hsp90 recovery on our resins by competing with HS-10 or other Hsp90 inhibitors (e.g., geldanamycin or PU-H71)[150,151], we were unable to elute Hsp90 bound to the affinity media without denaturing the protein. A linker that could be broken under non-denaturing conditions was needed. Recently, Verhelst et al reintroduced an azo-linker, which can be cleaved

under mild non-denaturing conditions with sodium dithionite solution[152,153]. This linker was synthesized using the published procedure and coupled to our ligand-construct, and through a two-step synthesis affinity resin E was derived. Following exposure to pig mammary gland extract and treatment of the resin with 25 mM sodium dithionite/100 mM Phosphate buffer pH 7.4, the eluted proteins were identified by MS as described earlier. The retained protein profile (Figure 36, lane E) is essentially identical to resin D, except that the proteins are recovered under non-denaturing conditions.

4.3 Nonspecific binding

One observation in these experiments (Figure 36) is that the binding of Hsp90 to each of the resins seems to lower the level of non- specific binding, effectively protecting the resin. With each of the affinity resins (A–E), addition of HS-10 to the protein mixture completely blocked Hsp90 binding allowing recovery of other proteins, especially abundant proteins such as fatty acid synthase (240 kDa). Although binding of these proteins is clearly not Hsp90 related their recovery illustrates the challenges of using affinity media to study interactions with Hsp90. Even with a highly optimized ligand, our results illustrate the extent to which affinity based strategies in defining Hsp90 clients can lead to incorrect conclusions. To define physiologically relevant associations with Hsp90, it is necessary to demonstrate competitive binding with a free ligand. Competition experiments should be carried out using a selective inhibitor of Hsp90 in

the cell/tissue extract prior to exposure to the affinity resin. Under these conditions, recovery of Hsp90 and any associated proteins should be selectively blocked. Proteins recovered in the presence of the free ligand are likely to be non-specific.

4.4 Selectivity evaluation

The finding that neither Grp94 nor TRAP1 was recovered by the HS-23 sepharose resin suggests that HS-23 is highly selective for Hsp90. To explore this selectivity in a somewhat reverse fashion, we tested the elution of pig mammary gland proteins from a gamma phosphate linked ATP Sepharose resin with HS-10, HS-23 and compared them to other known potent Hsp90 inhibitors: 17-AAG, PU-H71, and SNX2112 (Figure 38)[40,151,154].

Figure 38: Elution of Hsp90 and Grp94 from the ATP-sepharose resin

This ATP resin has been used in our lab for several years to study purine-binding proteins and to discover novel Hsp90 inhibitors[41,155]. It can be used to test ligand binding selectivity against all other purine utilizing enzymes expressed in cells. The ATP resin

was charged with the pig mammary gland extract and aliquots were distributed into individual wells. Proteins eluted from the wells with increasing amounts of the indicated compound were analyzed as described earlier (Figure 39).

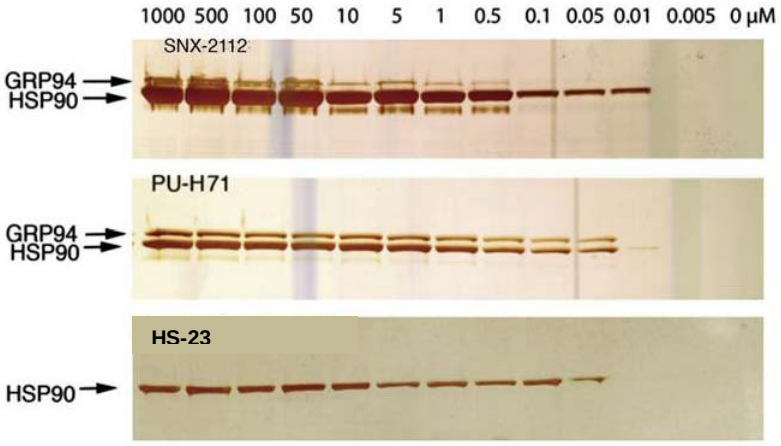

Figure 39: Elution of pig mammary gland protein from ATP-sepharose resin with SNX-2112, PU-H71 or HS-23

Compound PU-H71 demonstrates strong potency towards both Hsp90 and Grp94, whereas SNX2112 shows weaker affinity for Grp94 and HS-23 shows essentially no elution of Grp94. Examination of the crystal structures of Hsp90 and Grp94 with various ligands provided no obvious clue as to why HS-23 would display a greater binding selectivity for Hsp90 over Grp94 compared to the other known Hsp90 inhibitors. It may be that the hydration of the PEG linker attached to HS-23 gives rise to a relatively larger, more sterically demanding structure, which precludes binding to Grp94.

4.5. Grp94 purification

It was possible to use this differential selectivity to purify Grp94. Pig mammary gland extract was passed through cleavable HS-23 sepharose resin, efficiently removing Hsp90, directly onto the ATP-resin. Elution of the ATP resin with PU-H71 gave clean Grp94 when analyzed by SDS–PAGE, silver staining and mass spectrometry (Figure 40).

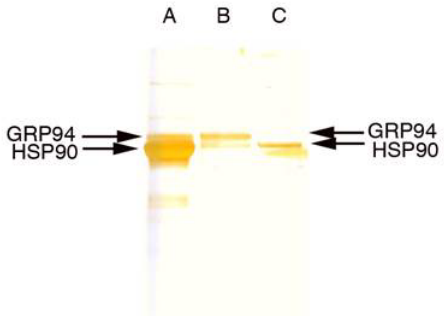

Figure 40: Purification of Grp94 from Hsp90

In (A) the pig mammary gland purinome was captured on ATP resin then eluted with PU-H71 releasing Grp94 and Hsp90 as expected. In (B) pig mammary gland extract was first passed through cleavable HS-23 sepharose resin and the flow through was then applied to ATP sepharose resin. The ATP sepharose resin was then eluted with 10 μM PU-H71 to yield pure Grp94. In (C) cleavable HS-23 sepharose resin was eluted with 30 mM sodium dithionite to yield Hsp90.

4.6 Proteomic studies

To test cleavable HS-23 sepharose resin as a proteomics tool we surveyed mouse organs to determine both Hsp90 expression levels between tissues and to define novel client proteins. Physiological conditions were used to preserve weak binding

interactions with Hsp90. To demonstrate specificity, extracts were mixed with resin cleavable HS-23 sepharose resin ± HS-10. As seen in Figure 41A, each mouse tissue yielded a prominent protein at 90 kDa of varying abundance as well as a distinct pattern of proteins of varying molecular weight. In most instances, inclusion of HS-10 in the extract blocked recovery of the 90 kDa protein as well as the additional proteins (Figure 41B). As expected, the 90 kDa protein was identified by mass spectrometry as Hsp90 (α and β isoforms). Surprisingly, many of the other proteins in the gel were either N-terminal fragments of Hsp90 or dimers of the holoenzyme (Figure 41).

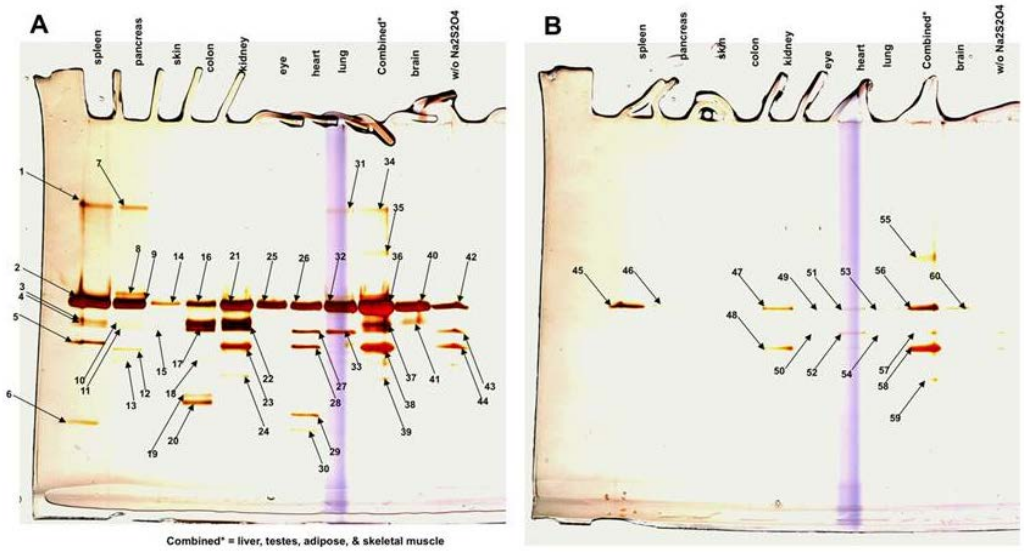

Figure 41: Proteomic survey of mouse tissues with the cleavable HS-23 sepharose resin[1]

Some proteins do appear to be potential clients of Hsp90 and show tissue specific associations including delta(3,5)-delta(2,4)-dienoyl-CoA isomerase, NADPH-dependent retinol dehydrogenase/reductase, acetyl-CoA acyltransferase and glycogen debranching enzyme. Two proteins, epoxide hydroxylase and glutaryl-CoA dehydrogenase, are tentatively identified as novel clients, since recovery of these proteins was not

[1] Tissue extracts were prepared from the indicated tissues and applied to a fixed volume of resin E (100 µl) in the absence (A) and presence (B) of HS-10 (100 µM). Following washes at physiological ionic strength the bound proteins were eluted with 30 mM dithionite and characterized by SDS–PAGE (4–15% acrylamide), silver staining and mass spectrometry. Key: 1–22. Full length Hsp90a/b or N terminal fragments of Hsp90a/b; 23. Epoxide hydroxylase; 24.Glutaryl-CoA dehydrogenase; 25. and 26. Hsp90a/b; 27. Hsp70; 28. Epoxide hydroxylase; 29. Delta(3,5)-delta(2,4)-dienoyl-CoA isomerase; 30. 3,2-trans-Enoyl-CoA isomerase/NADPH-dependent retinol reductase; 31 and 32. Hsp90a/b; 33. Hsp70; 34. Hsp90a/b; 35. Glycogen debranching enzyme; 36 and 37. Hsp90a/b; 38. Epoxide hydroxylase; 39. 3-Ketoacyl-CoA thiolase/3-ketoacyl-CoA thiolase; 40–42. Hsp90a/b; 43. Hsp70; 44. Epoxide hydroxylase/liver carboxylesterase 31; 45–47 Hsp90a/b; 48. epoxide hydroxylase; 49–51. Hsp90a/b; 52. Albumin; 53. Hsp90a/b; 55. Albumin; 56. CAZ-associated structural protein 1/Ankrd11 protein; 56. Hsp90a/b; 57. Albumin; 58. Epoxide hydroxylase; 59. Glutaryl-CoA dehydrogenase; 60. Hsp90a/b. Combined consisted of a mixture of striated muscle, liver, testis and adipose tissue. The lane w/o dithionite was eluted with SDS. This gel is a representative example of using resin E against tissue extracts.

completely blocked by HS-10. Their recovery may be explained by the presence of residual Hsp90 co-elution. Figure 41B also shows, as observed earlier, a few proteins were still non-specifically recovered from some tissues, even in the presence of HS-10, including albumin, CAZ-associated structural protein 1 and Ankrd11 protein. Their recovery underscores the necessity of including a competition control with the free ligand to directly demonstrate Hsp90 dependence of the co-isolation. As a positive control, we confirmed that we could use cleavable HS-23 sepharose resin to find Her2; a known client of Hsp90. Extract from the breast cancer cell line BT474 was added to the resin ± HS-10. Cleavage of the linker with dithionite and analysis by SDS–PAGE and silver staining showed only Hsp90. However, Western blot analysis clearly showed the presence of Her2 (Figure 42). Neither Hsp90 nor Her2 were seen in the sample competed with HS-10.

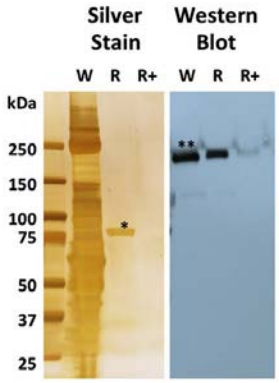

Figure 42: Proteomic analysis for Her2/Hsp90 interactions using the cleavable HS-23 sepharose resin

4.7 Conclusions

We reported the development of a novel affinity probe, cleavable HS-23 sepharose resin, for the selective recovery of Hsp90 in native complex with its physiologically relevant client proteins. Our ligand is the first reported affinity reagent that only binds Hsp90 and shows no affinity for Grp94 and TRAP1 at the limits of silver staining and mass spectrometry analysis. Therefore, cleavable HS-23 sepharose resin enables the study of native client proteins selective for Hsp90 independent of other chaperones. The development of cleavable HS-23 sepharose illustrates the complexities of utilizing affinity approaches to study native protein–protein interactions. Clearly, linker choice is critical to avoid artifacts. Study of Hsp90 is particularly challenging because interactions with its clients may be weak and readily disrupted under stringent, non-physiological conditions. Before assigning a particular protein as a client or co-chaperone of Hsp90, it is essential to also perform a co-isolation experiment with the appropriate competition control. Any proteins recovered under competing conditions are probably artifacts and unlikely to be a client or co-chaperone of Hsp90. In proteomic studies of mouse tissues using cleavable HS-23 sepharose, Hsp90 was recovered either alone or in association with novel client proteins. Recovery of the putative clients was authenticated by the competition experiments with HS-10. Interestingly, the majority of the recovered clients are associated with the metabolism of various lipids namely delta(3,5)-delta(2,4)-dienoyl-CoA isomerase, acetyl-CoA acyltransferase, NADPH-

dependent retinol reductase and epoxide hydroxylase 2. Delta(3,5)-delta(2,4)-dienoyl-CoA isomerase and acetyl-CoA acyltransferase are peroximal enzymes participating in β-oxidation of long chain fatty acids. Delta(3,5)-delta(2,4)-dienoyl-CoA isomerase isomerizes 3-trans,5-cis-dienoyl-CoA to 2-trans,4-trans-dienoyl-CoA functioning as an auxiliary step of the fatty acid β-oxidation pathway, enabling the metabolism of unsaturated fatty acids in mammals. NADPH-dependent retinol reductase (RDH12) has activity toward 9-cis and all-transretinol and is involved in the metabolism of short-chain aldehydes. The enzyme forms 11-cis-retinal from 11-cis-retinol during regeneration of the cone visual pigments. Mutations in the RDH12 are associated with retinitis pigmentosa type 53[156,157]. Retinitis pigmentosa is characterized by retinal pigment deposits as well as loss of rod photoreceptor cells with some secondary cone photoreceptor loss. The condition is typified by night vision blindness and reduced peripheral visual field. If RDH12 is a client for Hsp90, loss of expression of the protein in the eye could explain some of the idiosyncratic visual side effects anecdotally reported in some patients treated with a variety of Hsp90 inhibitors in clinical trials[44]. This would require that these drugs cross the blood–brain barrier since the retina is contiguous with the central nervous system. Epoxide hydroxylase 2 and its immediate family members have roles in the metabolism of arachidonic and linoleic acid epoxides, as well as, xenobiotics[158]. The finding that epoxide hydroxylase 2 is a client of Hsp90 could explain

some of the anti-inflammatory effects of Hsp90 inhibitors in addition to their indications in cancer[159,160].

The mouse study was used primarily to demonstrate the use of the affinity resin for initial identification of potential client proteins. Further studies are needed to confirm that these proteins are true clients of Hsp90. As shown with the breast cancer cell line, actual client proteins may be present below the detection limits of silver staining or mass spectrometry detection but still be detectable by western blot analysis. A final observation relates to the impact of the linker choice on the performance of an affinity resin. There is a radical difference in the amount of nonspecific binding between using the n-decane linker (resin A) and PEG-6 linker (resin D). We were initially disappointed with the number of clients identified with our affinity media, although we now believe the approach of using a 'clean' cleavable linker along with a quenching agent gives rise to fewer experimental artifacts. It may be worthwhile to reexamine other affinity experiments where hydrophobic linkers are used, beyond the field of chaperone proteins. Judicious linker replacement may show some affinity experimental conclusions to be premature and may yet yield positive results in other previously failed experiments.

5. Hsp90 isoform specific inhibitors

Cancer progression is characterized by rapidly proliferating cancer cells that require increased protein synthesis to contribute to other hallmark phenotypes of cancer[2]. Heat shock proteins are well conserved and abundant proteins that buffer the noxious effects of the often harsh tumor microenvironment by chaperoning unstable or misfolded proteins[49]. The over expression of Hsp90 and its correlation to patient outcome is well documented in a number of cancers[57-63]. Thus, Hsp90 inhibitors have been the recent subject of intense pharmaceutical research in cancer[52,53,138]. All Hsp90 inhibitors that have reached clinical trials bind to the Hsp90 N-terminal ATP-binding pocket and demonstrate pan-Hsp90 inhibition[51,138]. Toxicities and off target effects resulting from Hsp90 inhibition could be attributed in part to the pan-inhibition of its family members Hsp90α and β, Grp94, and TRAP1. Therefore, the design of Hsp90 isoform-specific inhibitors may provide valuable pharmacological tools to dissect the roles of each isoform and may lead to more clinically useful inhibitors.

Cytosolic Hsp90 is the most studied of the isoforms and most experimentation using pan-Hsp90 inhibitors attributes their effects to the inhibition of Hsp90α and β. Cytosolic Hsp90α and β play pivotal roles in cell signaling by chaperoning steroid hormone receptors and proto-oncogenic kinases. The effects are pleiotropic and seem to be growing because of the expanding interactome and ubiquitous expression reported in the literature[66]. Despite these cautionary signs, many inhibitors targeting Hsp90 have

successfully advanced through clinical trials, demonstrating patient responsiveness with higher than expected maximum tolerated doses. The interaction between Hsp90α and β and its clients is thought to be very transient, making it difficult to qualify and quantify any binding[25]. Recently, studies have revealed that inhibitors bound to Hsp90 abrogate binding of most of the putative clients and co-chaperone proteins[47]. While Hsp90α and β are major contributors to the progression of tumorigenesis, Grp94 and TRAP1 make distinct contributions to cancer progression and the development of resistance to chemo and targeted cancer therapies[133].

Grp94 is an Hsp90-like protein that facilitates proper folding of denatured proteins in the lumen of the ER as well as their transport to other organelles including the plasma membrane[161,162]. Unlike Hsp90's clients, Grp94's client proteins exhibit commonalities that make them more predictable interactors. Grp94 recognizes the immunoglobulin domain fold, which is found in many secretory proteins. In addition, every known client of Grp94 contains disulfide bonds, suggesting another way by which Grp94 is able to recognize substrates. A list of these clients is provided in a recent review[163]. While the interactions appear to be more predictable, there are still unknowns in the field of immunology as to how Grp94 binds and presents a wide array of peptides for T cell antigen recognition[164]. Grp94 is often overexpressed in cancers, which also implies it can be used as a candidate biomarker for monitoring tumor progression[165,166]. In cancer, Grp94 is needed to chaperone proteins in the ER that are under the stresses of

acidosis, glucose deprivation, and hypoxia, otherwise an unfolded protein response would be triggered through the PERK, XBP-1, and ATF6 signaling pathways that could result in apoptosis[167]. Grp94 has also been implicated as playing a cytoprotective role in etopside-induced apoptosis by directly interacting with calpain[168]. Inhibitors against Grp94 inhibitors would sensitize tumors to other chemotherapies, shifting the balance from survival to controlled cell death. However these tools are underdeveloped with very few promising leads.

TRAP1 is the mitochondrial isoform of the Hsp90 family that was first identified by its interaction with the intracellular domain of the type I TNF receptor[169]. Subsequent sequence analysis demonstrated that TRAP1 is indeed Hsp75[32]. While its primary cellular residence is the mitochondria, it also localizes to the cytoplasm, ER and nucleus[170-172]. The interactome for TRAP1 is significantly less than Hsp90; however, it does chaperone an important mitochondrial protein, Sorcin, and even the nuclear protein, Rb, that protect cells against apoptosis and oxidative stress[170,173-177]. Through these functions, TRAP1 has been proposed to facilitate chemoresistance by buffering the effects of drug-induced apoptosis in cancer cells[177-179].

Several efforts are being made to design isoform-specific inhibitors and some endeavors are focusing on the differential expression of these isoforms from each other and the ectopic expression found in tumor cells[110,133,180-182]. One recent report by Patel et al, hypothesized that the conformational differences between Hsp90 and Grp94 could be

exploited by a ligand-induced selectivity for the Grp94 ATP-binding pocket. Based on their affinity and selectivity, we synthesized their most potent and selective Grp94 inhibitor, PU-H39[180]. Our goals were to make affinity chromatography resins to proteomically mine for bona fide clients and co-chaperones and to isolate Grp94 for more elegant biochemical assays for comparison to Hsp90. However, PU-H39 did not show potency for Grp94 in our native protein elution assays. Using a combination of affinity chromatography resins, we isolated native Grp94 and Hsp90 and performed thermal stability assays, which confirmed the selectivity of our tethered Hsp90 inhibitors and lack of potency of PU-H39. Tethered Hsp90 inhibitors, such as HS-23, further showed in vivo activity against Her2 and upregulation of Hsp70, whereas the unfolded protein response was only detected in the pan-Hsp90 inhibitors.

5.1 Selectivity of Hsp90 inhibitors in a competitive elution assay

Rather than working with exogenously overexpressed proteins, we looked at endogenous heat shock proteins from a lactating pig mammary gland. This tissue has been shown to express all isoforms of Hsp90[47]. Using a dose titration of inhibitors, we eluted protein from a charged ATP-sepharose resin that had been loaded with homogenized pig mammary tissue. We compared known pan-Hsp90 inhibitors, HS-10 and PU-H71[47,151], to the recently reported Grp94 selective inhibitor, PU-H39[180]. At the level of detection of silver staining, we found predictable patterns of elution of Hsp90

and Grp94 for the pan-Hsp90 inhibitors. However, PU-H39 failed to elute any purine binding proteins from the ATP-sepharose resin (Figure 43).

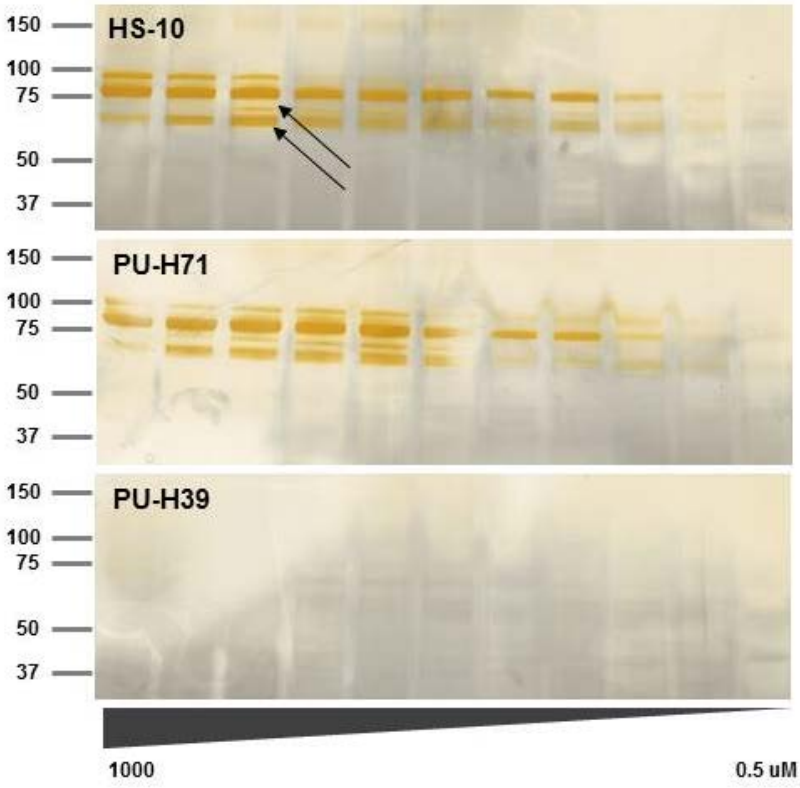

Figure 43: Hsp90 and Grp94 elution from the ATP sepharose resin

Interestingly the lower molecular weight bands (black arrows) were identified as truncated Hsp90 and Grp94. The truncations occurred similarly in the C-terminal end of both proteins (Figure 44).

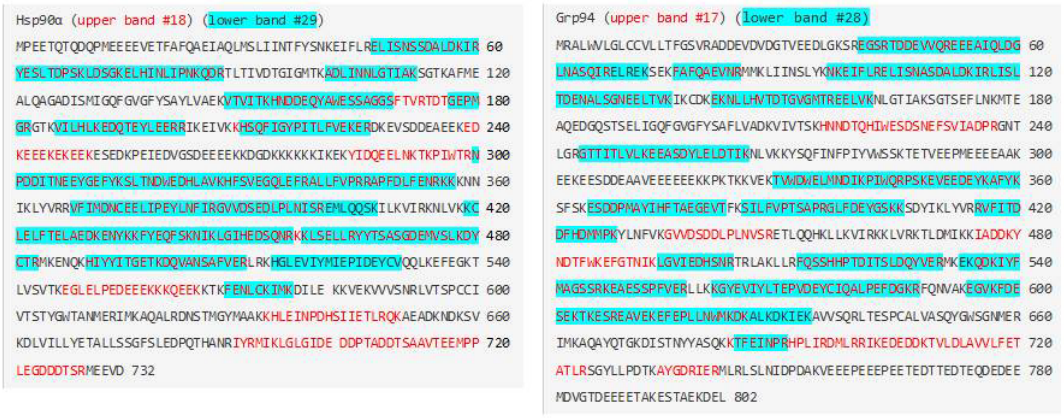

Figure 44: Amino acid MS coverage of Hsp90 and Grp94 C-terminal truncations

To test the elution at a more sensitive level, we probed the eluate for Hsp90, Grp94 and Trap1 by immunoblotting. Using this analysis, we examined the specificity of HS-10, HS-23, and PU-H39 and we observed that HS-10 exhibits the highest affinity for the different isoforms with HS-23 showing some selectivity and PU-H39 showing no selectivity for any of the Hsp90 isoforms (Figure 45).

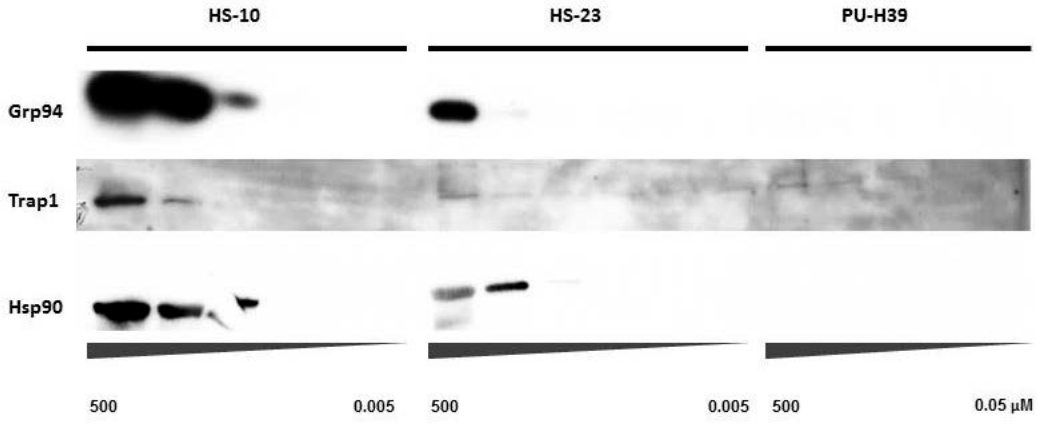

Figure 45: Grp94, TRAP1 and Hsp90 elution from ATP sepharose resin

To maximize the opportunity of PU-H39 binding to Grp94, we pretreated tissue lysates with DMSO, 10 μM PU-H71, or 10 μM PU-H39 before loading on the ATP-sepharose resin. All samples were eluted with a dose titration of PU-H71. As expected DMSO did not block the binding of Hsp90 and Grp94 and they were eluted demonstrating the typical elution pattern (Figure 46). Contrastingly, to DMSO, the pretreatment of PU-H71 competitively blocked the binding of Hsp90 and Grp94 to the ATP-sepharose and thus no protein was captured with the elution of PU-H71 (Figure 46). Interestingly, both Hsp90 and Grp94 were eluted (similar to DMSO) when pretreated with PU-H39 and eluted with PU-H71 (Figure 46).

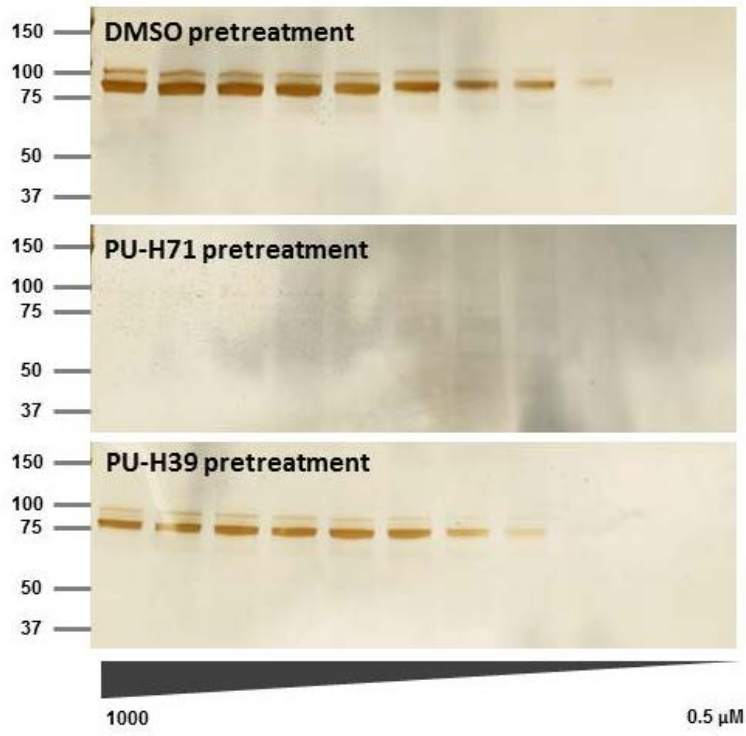

Figure 46: Hsp90 and Grp94 elution with PU-H71 titration with pretreatment

If PU-H39 is a bona fide selective inhibitor of Grp94, one would predict that Grp94 would be competitively blocked and only Hsp90 would be eluted using PU-H71. This evidence contradicts the earlier reports of PU-H39's nanomolar potency and selectivity[180].

5.2 Native Hsp90 and Grp94 purification

To perform more elegant biochemical experiments on the interaction of these inhibitors with Hsp90 and Grp94, we needed to isolate native protein. To achieve this goal, we devised a sequence of purifications and elutions using an Hsp90-selective affinity resin, the ATP-sepharose resin, and a pan-Hsp90 inhibitor. The schematic is diagramed in Figure 47. First, we added homogenized tissue to the Hsp90 selective resin Figure 47a) to deplete both Hsp90α and β. These proteins were eluted off the sepharose resin by reductively cleaving the linker using 25 mM sodium dithionite (Figure 47II). The ligand was dialyzed away using decreasing amounts of ATP until Hsp90 was unbound from the ligand and ATP. The flow through from the Hsp90-selective affinity resin (Figure 47I) was collected and loaded onto an ATP-sepharose resin (Figure 47b). After thoroughly washing the ATP-sepharose resin, proteins were eluted using a pan-Hsp90 inhibitor, HS-10. Because Hsp90 had been previously depleted, the only protein captured and identified by mass spectrometry was Grp94 (Figure 47III).

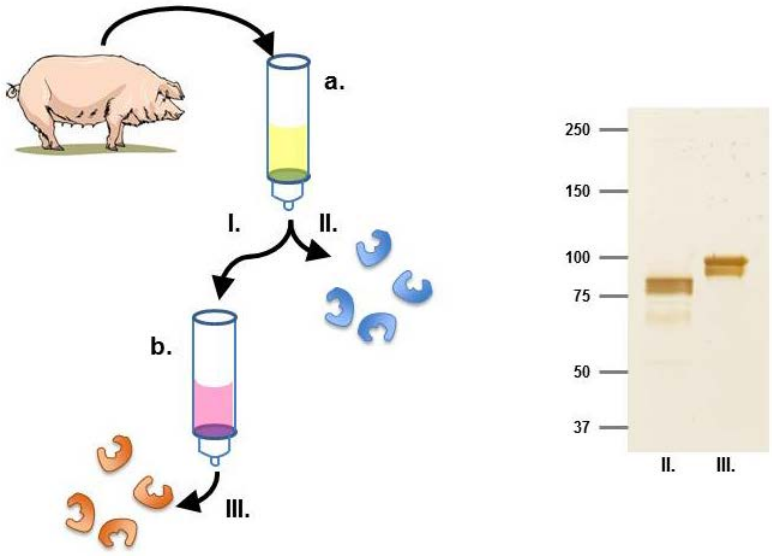

Figure 47: Schematic of native Hsp90 and Grp94 using affinity resin chromatography

5.3 Thermal Stability of Hsp90 and Grp94 reveals selective Hsp90 inhibitors

Once we confirmed that we had pure samples of Hsp90 and Grp94 by SDS-PAGE gel electrophoresis and mass spectrometry (Figure 47), we analyzed the thermal stability of these proteins in the presence of the different Hsp90 inhibitors. ATP competitive inhibitors typically confer thermal stability to purine binding proteins, and this often equates with affinity of the molecule for its protein target[183-185]. Using purified Hsp90 and Grp94, we observed an increase in melting temperature (T_m) using pan-Hsp90 inhibitors HS-10 and PU-H71 (Figure 48). However, the tethered Hsp90 inhibitors, HS-23 and HS-32, demonstrated selectivity for Hsp90 (Figure 48a), and no

stability was conferred upon Grp94 (Figure 48b). This confirms the results of previous assays that adding a tether to HS-10 to form HS-23 bestows selectivity for Hsp90 regardless of the chemical moiety on the distal end of the linker (Figure 49). These linkers and added chemical moieties come with a price as affinity is usually measured to be half as potent as the established pan-Hsp90 inhibitors in shifting the thermal stability. However, the affinity of these tethered Hsp90 inhibitors for Hsp90 is still in the submicromolar range. Next we examined the selectivity of PU-H39 under like conditions and thermal stability was not observed for Hsp90 or Grp94 (Figure 48c,d). We have therefore further demonstrated a lack of affinity and selectivity of PU-H39 for any of the native isoforms of Hsp90.

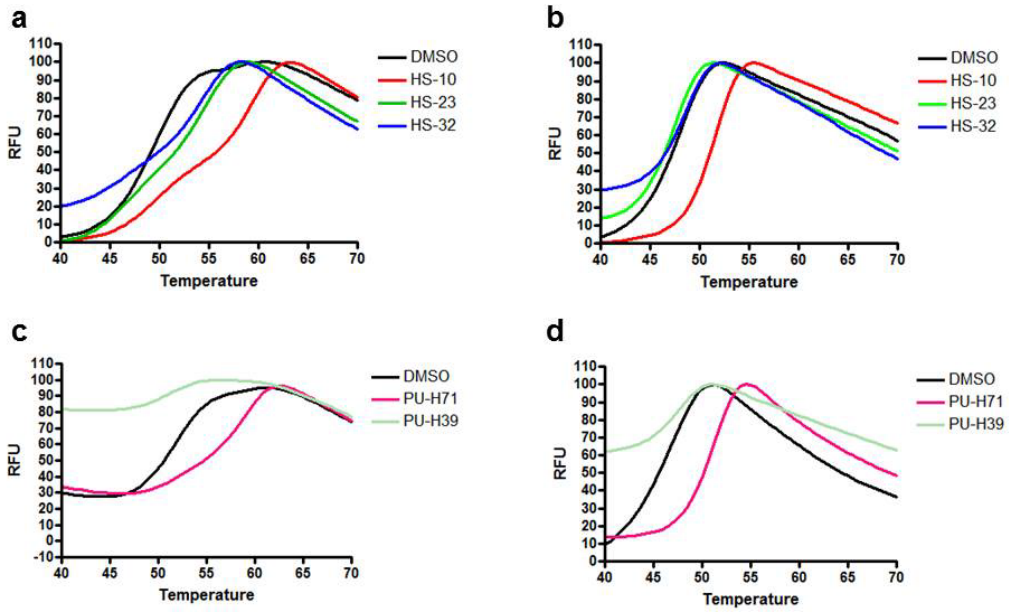

Figure 48: Thermal stability of Hsp90 and Grp94 in the presence of pan and selective Hsp90 inhibitors

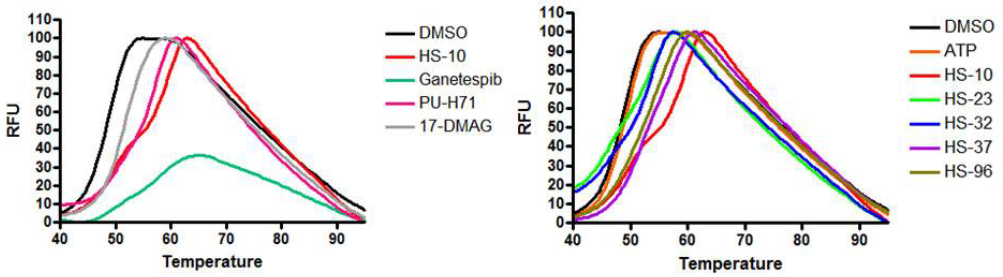

Figure 49: Thermal stability of Hsp90 in the presence of pan Hsp90 inhibitors and tethered Hsp90 inhibitors

5.4 In vivo biological activity of Hsp90 selective inhibitors

While some discrepancies exist between our findings and Patel et al, the biochemical affinity could be explained by the use of recombinant proteins and not native proteins. To evaluate the effects of these compounds in a biological context, we analyzed the classical client degradation of Her2 in BT474 cells and the well-characterized upregulation of Hsp70, both of which are associated with Hsp90 inhibition. After 12 hours of treatment with a dose titration, we found that pan-Hsp90 inhibitors exhibited potent degradation of Her2 and upregulation of Hsp70 at an $EC_{50} < 1$ μM (Figure 50a,b,e). Tethered Hsp90 inhibitors also demonstrated similar potency with the exception of HS-132, which contains a nIR fluorophore attached to the distal end of the linker, affecting its cellular bioavailability (Figure 50a,b,e). Intriguingly, the 60 μM EC_{50} correlates inversely with the fluorescent uptake measured intracellularly in the BT474 cells (Figure 50d). In contrast, no effects on Her2 and Hsp70 were observed upon

treatment with PU-H39 (Figure 50a,b,e). Additionally, none of the compounds exhibited deleterious effects on Hsp90 (Figure 50c,e). We also looked for an unfolded protein response as exhibited by an increase in Erdj3, a classical molecular marker of Grp94 inhibition. After 12 hours of treatment, no response was detected in cells treated with PU-H39 at 3 orders of magnitude higher than the reported K_d (Figure 51a,c)[180]. There was, however, a modest increase in Grp94 expression across all treatments including PU-H39 (Figure 51b,c). The decreases in protein expression with higher treatments of HS-32, the bis-ferrocene conjugated Hsp90 inhibitor, can be attributed to the ferrocene molecules and not Hsp90 inhibition because HS-10 treatments at these doses and for 12 hours did not exhibit deleterious effects on the cells (Figure 51d). Together these data demonstrate PU-H39's lack of potency at the biochemical level and lack of biological activity at the cellular level. However, we have demonstrated that tethered Hsp90 inhibitors can be used for biological and biochemical analyses of Hsp90. In addition, the effects seen in these studies can be confidently attributed to the mechanism of action of Hsp90, albeit the complexity largely remains. We also have devised a method to purify native Hsp90 and Grp94 from tissue using Hsp90 selective affinity chromatography, ATP-sepharose chromatography and pan-Hsp90 inhibitors. This method could facilitate the discovery of other truly potent and selective inhibitors of Grp94 and Hsp90.

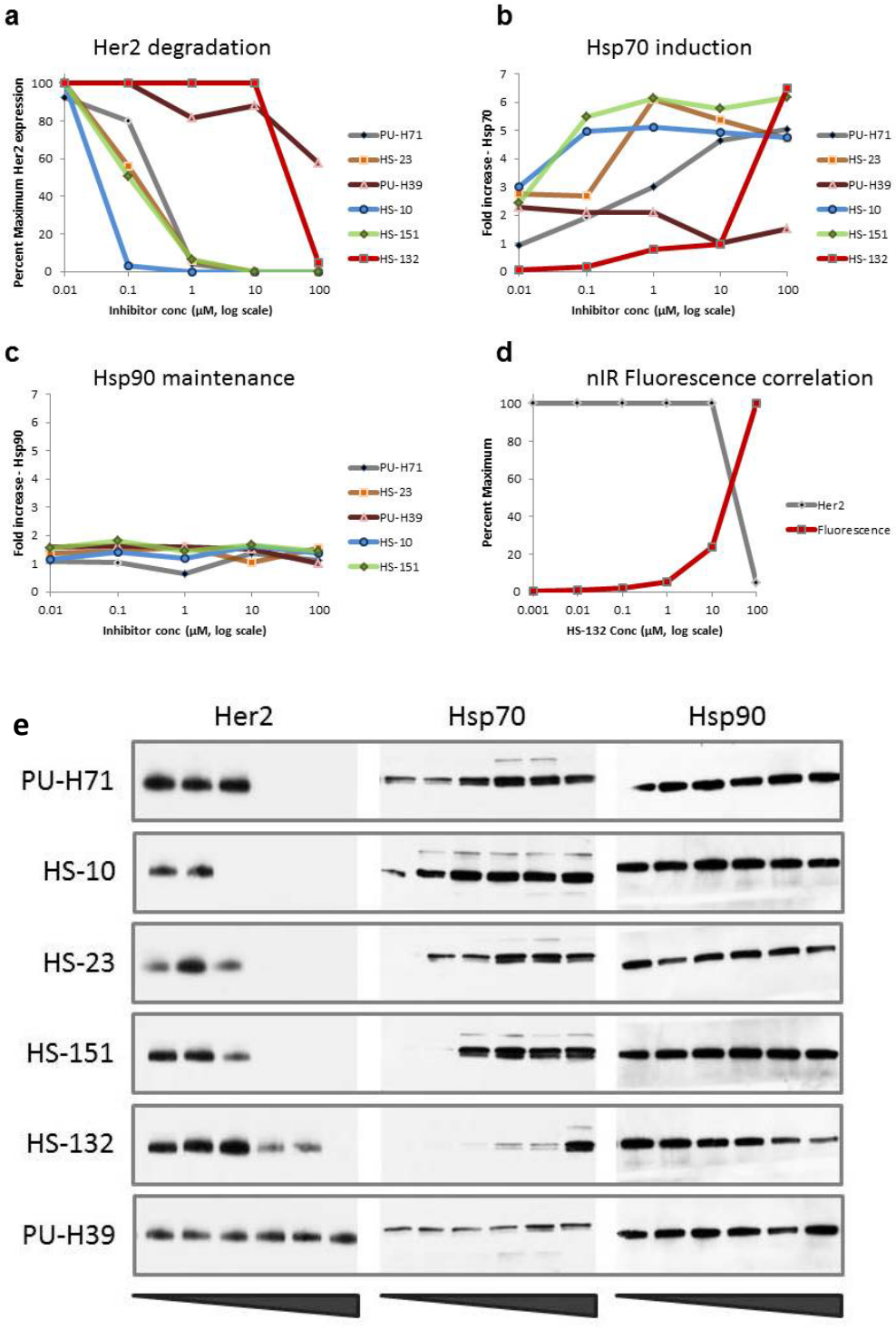

Figure 50: Biological activity of Hsp90 selective inhibitors

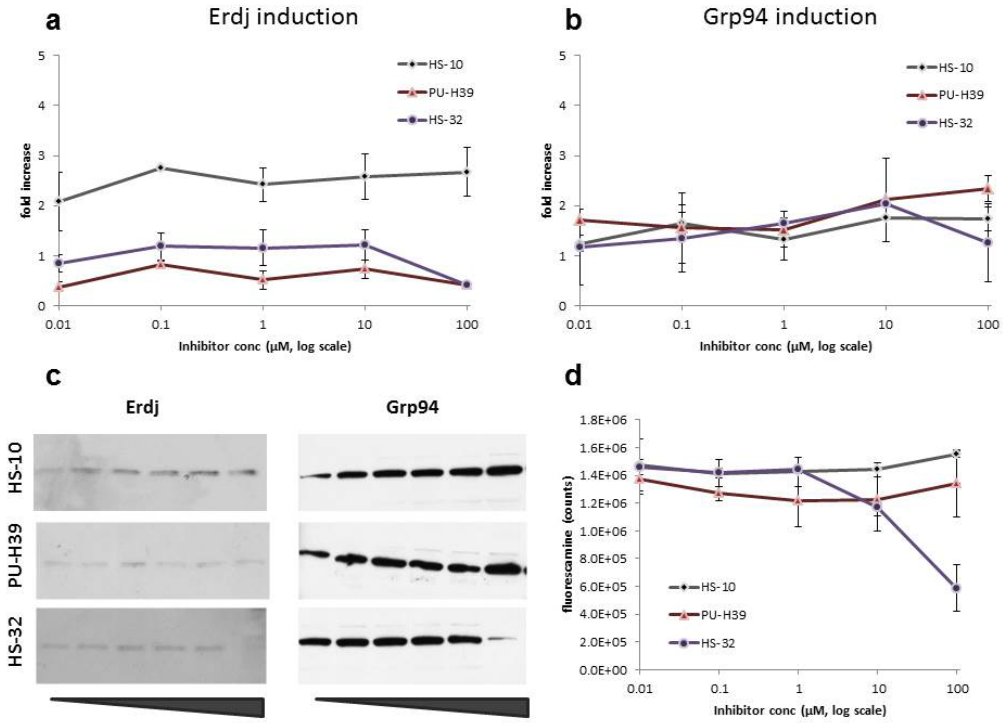

Figure 51: Detection of the unfolded protein response in MDA-MB-468 cells

5.5 Conclusions

There are on-going attempts to tease apart the mechanisms of the four isoforms of Hsp90, how each isoform uniquely contributes to cancer, and more importantly how each can be selectively targeted in cancer and not in normal tissues. Small molecule inhibitors that distinguish the different Hsp90 isoforms will greatly advance our understanding of this important field. Unfortunately, PU-H39 demonstrates neither the potency nor the selectivity as previously reported[180]. A number of reasons could explain the discrepancies. First, in the previous report, the screening of inhibitors involved a

tagged recombinant version of Grp94. Not only was the protein tagged, but it represented less than half of the protein (aa 66-337). Second, although we chose PU-H39 to synthesize and study based on the potency and selectivity reported, a number of PU analogues were reported and by chance, we selected a biologically inactive compound that does not bind native Grp94 in vitro. Lastly, the crystal structure remains enigmatic especially pertaining to the hinge in vicinity of the active site. We believe the crystallographic data to be artificial and using a truncated protein for this study further riddles this study with artifacts. In our own examination of the crystal structures of Hsp90 and Grp94 with various ligands, we saw no obvious clue as to why tethered Hsp90 inhibitors such as HS-23 would display a greater binding selectivity for Hsp90 over Grp94 and TRAP1 compared to the other known Hsp90 inhibitors. It may be that the hydration of the PEG linker in HS-23 gives rise to a relatively larger, more sterically demanding structure, which precludes binding to Grp94. The study supports evidence that selectivity between Hsp90 isoforms can be achieved and that native protein studies demonstrate advantages over recombinant proteins and reduce the risk of committing a type I error.

6. Unfolded Hsp90 in cancer cells

6.1 Introduction

Hsp90 facilitates many of the molecular steps in a tumors progression from being benign to becoming malignant and invasive. In order to undergo cell behavior that is implicated in metastatic tumors, one must envision molecular changes at the cell membrane. Indeed, Hsp90 is found on the surface of tumors and not on the surface of normal tissue[110]. Extracellular Hsp90 has been shown to stimulate migration and invasion of cancer cells[98]. We have used this unique phenomenon to design large, polar Hsp90 inhibitors tethered to fluorophores to detect and study extracellular expression in cancer cells[110]. In addition to the extracellular differences in Hsp90, we highlight new findings that there are seminal differences between cancer and normal tissue in Hsp90's stability found in these cells.

6.2 Normal tissue HS-27 affinity compared to breast cancer cells

In 2003, it was reported that Hsp90 exhibited a unique expression in cancer as a multimeric complex with other co-chaperones and that these complexes demonstrated higher affinity for inhibitors such as 17-AAG and higher ATPase activity[45]. We, however, have found that Hsp90 is devoid of its co-chaperones when retrieved using affinity ligand chromatography[47]. We have since tested the hypothesis that there are affinity differences between normal and tumor tissues. First, we optimized an assay using HS-27 binding to protein extracts and fluorescent detection in a 96-well plate to determine the

affinities for different tissues. Unbound HS-27 was washed thoroughly in a 96-well 10K kDa filter plate followed by elution of the protein samples through a pinhole into a catch plate. Using purified Hsp90, we added 1.14 μM, 11.4 μM or 114 μM HS-27 to a range (0.1 to 500 μg) of purified Hsp90 (Figure 52a). According to these results, we chose to focus more exclusively on the 10-100 μM range of HS-27, and then we performed competition experiments with HS-10 so as to demonstrate that any signal retained could be attributed to the binding of HS-27 to the protein. The competition experiments effectively reduced the signal (Figure 52b). Another important observation is that regardless of the increase in protein and the correlative increase in HS-27 retention as determined by fluorescence, the affinity remained constant (mean 340 nM, SEM ±38 nM) as determined by the apparent K_d equation[1] using the EC_{50} of the curves (mean 68.5 μM, SEM ±7.7 μM) (Figure 52).

[1] Apparent $K_d = EC_{50}/[1 + (\text{ATP concentration}/K_m)]$186. Haystead, T.A. The purinome, a complex mix of drug and toxicity targets. *Current topics in medicinal chemistry* **6**, 1117-1127 (2006).

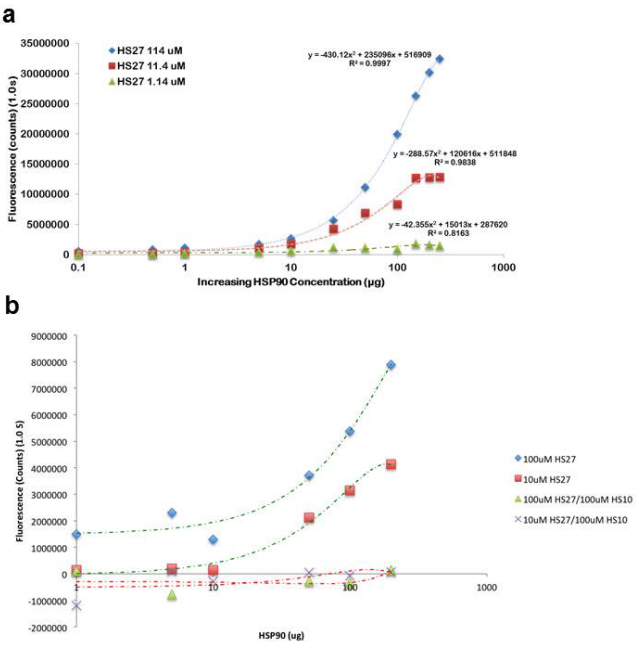

Figure 52: Optimization for Hsp90 affinity assay using HS-27

Based off these data, we determined that the optimal amount of Hsp90 per well is 50-100 µg. As Hsp90 is 2-3% of the total protein of a cell, we estimated that we would need about 2,000 µg of total protein in each well from the harvested mouse tissues and human breast cancer cells. We focused primarily on tissues that have exhibited high expression of Hsp90 in our past experiments, namely brain, kidney, liver, spleen and lung. Using this technique, we can measure both the relative abundance of Hsp90 and its affinity for Hsp90 inhibitors such as HS-27. We report that there is no disparity in affinity for Hsp90 and HS-27 between MDA-MB-468 breast cancer cells and the normal tissues harvested from mice (Figure 53).

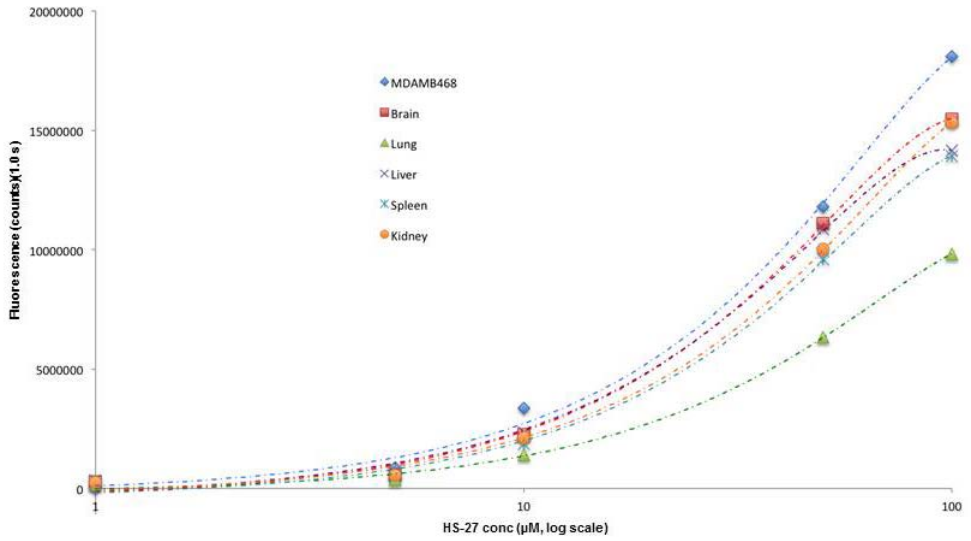

Figure 53: HS-27 affinity is the similar between cancer cells and normal tissues

6.3 The unfolded Hsp90 protein is unique to cancer cells

We have previously published that there is a fraction of intracellular Hsp90 that does not bind to our small molecule affinity chromatography resin and this is congruent with the Chiosis lab at Sloan-Kettering[46,110]. In our attempts to isolate the flow through pool and perform proteomic comparisons between the drug-binding pool and non-drug-binding pool, we came across an original observation that normal tissue from mice or pigs does not contain Hsp90 in the flow through after resin depletion. In other words, there is a population of Hsp90 that does not bind to affinity chromatography resins in cancer cells that is not found in normal tissues. We developed an in-plate assay for

analyzing many tissue sources in replicate and in parallel. To validate that a through-put assay could still discriminate between resin-bound Hsp90 and flow through Hsp90 after scaling down our samples, we looked at MDA-MB-468 and SKBr3 cells and observed the expected pattern of resin capture, followed by depletion and presence of Hsp90 in the flow through (Figure 54).

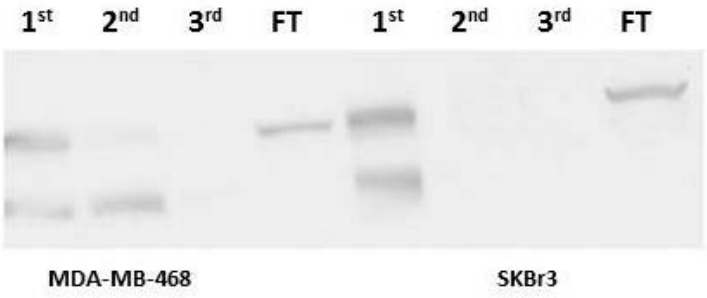

Figure 54: Resin depleted Hsp90 detected in breast cancer cell lines

However, when we assayed normal mouse tissues under the same conditions, we detected no Hsp90 in the flow through after the 3rd resin depletion pass (Figure 55).

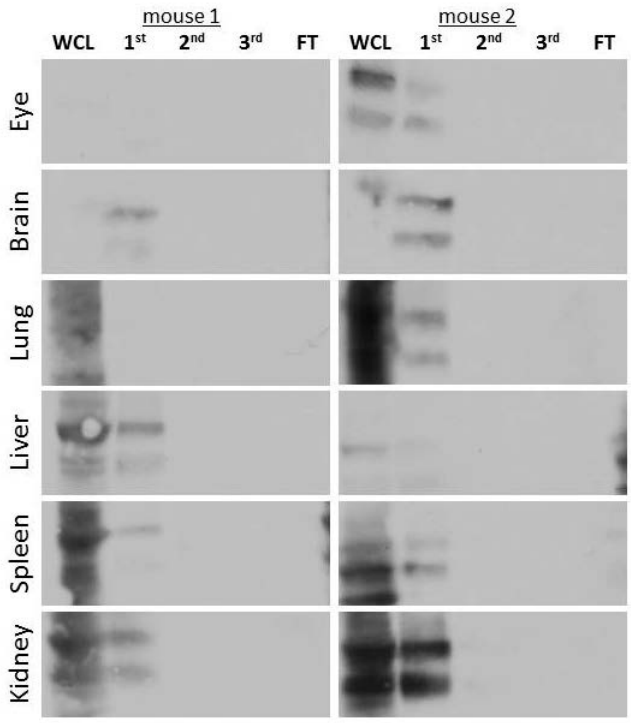

Figure 55: Hsp90 resin depletion reveals no Hsp90 in flow through for normal tissues

We found that cultured human breast cancer cells contained inactive Hsp90 and normal tissues from mice, such as eyes, brain, lung, liver, spleen and kidney did not. To validate that the flow through was not an artifact of in vitro culturing or harvesting, we took three human breast cancer xenografts from mice and observed that these tumors also exhibited a pool of Hsp90 that would not bind the affinity resin (Figure 56).

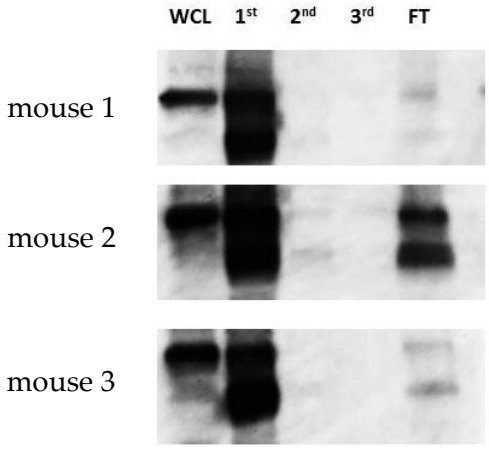

Figure 56: Resin depleted Hsp90 detected in breast cancer xenografts

6.4 Thermal stability reveals unfolded nature of resin depleted Hsp90

At this point, we questioned what the differences between these two pools of Hsp90 were. It is noted that the flow through Hsp90 is found primarily in its full length form and the truncated forms that have been observed have been confirmed to be missing the C-terminal end, which is opposite of the N-terminal ATP binding domain. There are two hypotheses: (1) either the ATP-binding domain is misfolded and that does not permit binding or (2) there is something bound in the binding pocket that precludes the binding of inhibitors. A thermal stability assay helped differentiate between these two possibilities. An increased shift in the transition temperature would support that something is bound and stabilizing the protein whereas a decreased shift in the transition melt temperature would suggest a less stable conformation of the protein that distorts the ATP binding pocket. In order to isolate the flow through Hsp90 from the

milieu of cell lysate proteins, we chromatographed inactive Hsp90 over a mono Q column. Wells were separated by gel electrophoresis and silver stained and suspected bands were analyzed by mass spectrometry and confirmed to be Hsp90. The corresponding wells were pooled and concentrated and thermofluor data was obtained. It was noted that the active pool of Hsp90 exhibited a transition melt temperature of 50°C which was increased 9°C by the presence of the small molecule inhibitor HS-10. However, the inactive Hsp90 demonstrated a 9°C shift to the left that was not rescued in the presence of HS-10, which supports the unstable conformation hypothesis (Figure 57).

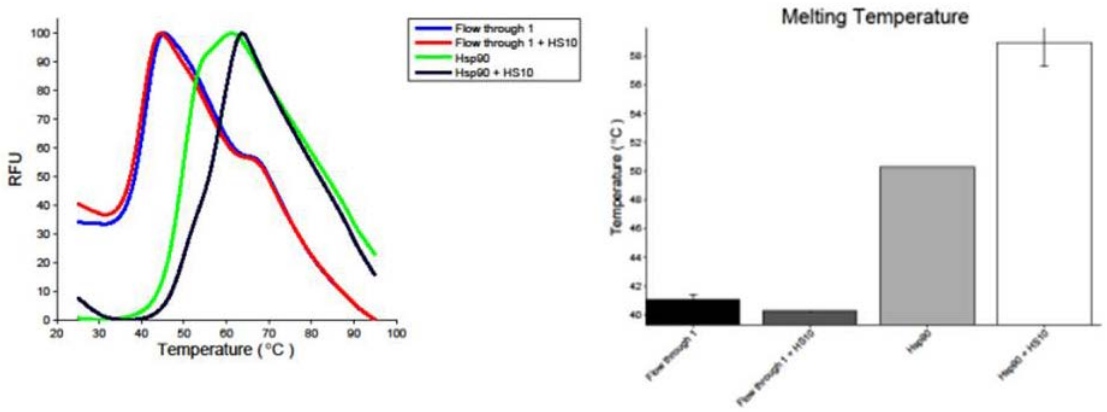

Figure 57: Thermal stability assay for active and inactive Hsp90

6.5 Conclusions

This discovery of misfolded chaperones in cancer is a novel finding and parallels the molecular mechanisms associated with neurodegenerative diseases such as Alzheimer's disease (AD). Indeed there are already several parallels between the aberrant signaling in cancer and in AD that incriminates Hsp90 chaperone function and

several research groups have proposed that patients with AD could benefit from Hsp90 inhibitor therapy[187]. Cancer is a complex conglomeration of signaling events that promote cell survival, growth, division, migration and invasion[2]. Alzheimer's disease is also very complicated demonstrating aberrant signaling cues from several hyperphosphorylated proteins. Neuronal cells promote survival in opposition to the accumulation of β-amyloid peptides and neurofibrillary tangles and the neuroinflammation of neighboring glial cells; however the upregulation of chaperones to buffer these cellular stresses most likely facilitates disease progression that leads to neuronal cell death[188].

Our novel finding that cancer has a pool of misfolded Hsp90 could also be linked to neurodegenerative diseases. Drawing upon the many parallels between AD and cancer, misfolded Hsp90 might be a cellular response to stress, which in turn facilitates Hsp90 for exosomal secretion. However, there are no reports of extracellular Hsp90 in neurodegenerative diseases, and rather than surviving like cancer cells in the harsh environmental stress associated within the microenvironment, neuronal cells die with increased kinase signaling and tau accumulation[189-191]. Neurodegenerative diseases, such as AD, could differentiate the impact that extracellular Hsp90 has on cell survival and migration, and whether misfolded protein is correlated to extracellular chaperone expression or simply a molecular cue of cellular stress.

The presence of Hsp90 on the surface of neuronal cells is not unprecedented. Over 20 years ago the Patsavoudi lab discovered Hsp90α in the membrane fraction of developing rat brains[192]. Using an antibody (4C5) specific for this protein, they followed up their study by demonstrating that Schwann cells were positive for surface Hsp90 following mechanical injury[193]. Schwann cell motility was significantly decreased when treated with the 4C5 antibody[194]. This cumulative data points to a physiological role for extracellular Hsp90 in neural morphogenesis and neuronal repair by promoting cell motility.

Embryonic morphogenesis shares more characteristics with cancer development than with neural degeneration. Thus it would not be alarming if Hsp90, in particular ectopic and misfolded Hsp90, were different between cancer and neurodegenerative diseases. Extracellular Hsp90 appears to play more of role that resembles epithelial to mesenchymal transformations (EMT), which is more of a tumor phenotype and will be discussed in the next chapter. Despite the incongruence of Hsp90 in cancer and AD, the young field of Hsp90 inhibition in neurodegenerative diseases is beginning to show some promise. Perhaps just as many doubted the relevance of Hsp90 inhibitors in cancer, so too will Hsp90 inhibitors blossom into a clinically significant therapeutics to treat complex neural diseases such as AD.

7. Mechanisms of internalization and secretion

7.1 Non-cancer mechanisms of receptor-mediated internalization of extracellular chaperones

While the importance of extracellular Hsp90 in cancer progression and detection has been highlighted, there are several unknown aspects concerning the mechanisms by which ectopic Hsp90 is internalized. Many comparisons can be made between the internalization and processing of antigens and chaperones in the cross-presentation pathway in antigen presentation cells (APCs) and the chaperone/inhibitor internalization in cancer.

Grp94 in particular has been studied for its participation in antigen presentation in several cancers, which activates the immune system to recognize and destroy tumor cells[195,196]. Chaperones, such as Grp94 and Hsp90α, are secreted from stressed cells and they enter professional APCs (e.g. dendritic cells and macrophages). Once internalized, the chaperones and their bound peptides undergo cross-presentation by forming complexes with the cell's major histocompatibility complex (MHC) class I. These antigen complexes enable $CD8^+$ cytotoxic T lymphocytes (CTL) recognition, and once activated, the CTL can search for the source of the antigen and destroy the cell[197-199]. Hsp90α is specifically implicated as a contributor to the antigen cross-presentation pathway in dendritic cells as Imai et al showed in in vitro and in vivo knock out studies[200].

Grp94 has been shown to be endocytosed by active receptor-mediated mechanisms as evidenced by colocalization studies with transferrin and electron micrograph images demonstrating the presence of the protein in endosomes. Additionally, some internalization was inhibited by DMA, which was attributed to fluid phase macropinocytosis but could also be explained by its inhibition on exosomal release[201].

Besides transferrin, there are other receptors that are more mechanistically linked to the internalization of extracellular chaperones. Stabilin-1 has been demonstrated to endocytose both Hsp90 and Hsp70 along with cargo, however, this internalization bypasses the steps of MHC receptor association[202]. Another potential receptor involved in endocytosis of Hsp90 is the scavenger receptor expressed by endothelial cells, SREC-1. SREC-1 has demonstrated the ability to internalize Hsp90-OVA polypeptide complexes through a Cdc42-dependent manner[203].

LRP1 is also implicated in the internalization of chaperone/antigen complexes in APCs because of the established interaction with several chaperones and the upregulation of pro-inflammatory cytokines such as IL-1β, TNF-α and IL-6 upon receptor stimulation with extracellular chaperones[204-206].

7.1.1 LRP1 is a potential receptor for exHsp90

LRP1 is a large endocytic receptor that belongs to the LDLR family. LRP1 binds and endocytoses over 30 distinct ligands including apolipoprotein, proteinases,

proteinase inhibitor complexes, extracellular matrix proteins, chaperone proteins and urokinase-type plasminogen activator[207,208]. There is an on-going debate on the function of LRP1 in cancer cell migration and invasion , whether LRP1 facilitates or hinders the processes that lead to metastasis[209-217]. In comparing these reports, it appears the results are cell specific, even within disease models and whether or not the studies are conducted in vitro or in vivo. Understanding that cancer cells require extracellular chaperones for migration and invasion in addition to the presence of LRP1, one could distinguish the difference between these reported discrepancies by implicating extracellular Hsp90 as a prerequisite for LRP1 to facilitate cancer progression.

In one study of interest, researchers found that Hsp90 secretion can result from TGFα stimulation through the exosome-secretion pathway. The secretion of Hsp90 translates into a promotility signaling cascade via the LRP1 receptor[98]. The middle domain and charged linker region are primarily implicated in LRP1 binding and cell migration, which suggests an ATPase-independent function for Hsp90[98]. One consistency found in several papers is that hypoxic conditions upregulate LRP1 through Hif-1α. Cells that have low levels of LRP1 in vitro show increased levels in in vivo xenografts in SCID mice[218]. Additionally, cells that express low levels of LRP1 show increased protein levels upon treatments that induce Hif-1α levels[218].

Without knowing the precise mechanism of Hsp90 internalization, it appears to play a pivotal role in the cross-presentation of antigens in APCs resulting in an

antitumor response. Despite the tumor-alerting role of extracellular chaperones in adaptive immunity, ectopic Hsp90 significantly enables tumors to survive and progress towards malignancy. Because of this dichotomous relationship, off target effects on T cell activation are seen as a minor trade for the increasing benefits of Hsp90 inhibition that negatively affect cancer growth, motility, metabolism and survival.

7.2 Non-cancer mechanisms of extracellular Hsp90 expression

Cancer is a master of mimicry, often by ectopic gene expression of established developmental signaling pathways. Wound healing is another process that draws numerous parallels with cancer signaling and progression. Indeed, extracellular Hsp90 plays a role in both processes, beneficially promoting cellular events in wound healing and on the other hand detrimentally facilitating events that lead to metastasis. Not surprisingly, LRP1 is also involved in both wound repair and cancer malignancy[219,220].

In addition to the similarities shared in the signaling axis of extracellular Hsp90 and LRP1, many features of the wound healing environment are analogous to the tumor microenvironment such as disrupted vasculature with its accompanied hypoxia and angiogenesis, inflammation, matrix remodeling and cell motility and invasion[221]. A key difference is not in the expression pattern of genes and proteins that lead to the array of cellular processes but the duration of expression. In wound healing the signaling events are acutely regulated, whereas in cancer the same pathways are persistently turned on. As stated earlier, Hsp90 appears to play a central role in these processes. While

intracellular Hsp90 facilitates many signaling aspects, it is the extracellular expression that is truly unique. Understanding the Hsp90 secretion mechanisms should give insight into the important pathways that regulate wound healing and cancer progression. Furthermore, if the cessation of extracellular Hsp90 is mechanistically correlated to the acute regulation of wound healing processes then we might have increased comprehension on how to impede tumor cellular activities that depend on extracellular Hsp90. So how does ectopic Hsp90 occur? Despite the lack of an extracellular signal peptide, Hsp90 is secreted from its normal cytoplasmic residence to the extracellular milieu by exosomal secretion[98,106,222,223]. Mechanisms regulating Hsp90 secretion have been reviewed and are linked to DNA damage, oxidative stress, chemotherapeutic agents , growth factors, heat stress and hypoxia[65].

Several studies have shown that posttranslational modifications are present on the extracellular Hsp90[14]. Some researchers suggest that the phosphorylation of T5 and T7 of Hsp90α is responsible for the translocation of Hsp90 to the cell membrane, and it has also been demonstrated that the secretion of Hsp90 was determined by the phosphorylation status at residue T90 and regulated by PKA and PP5[90,224]. While these modifications might be detected at the picogram level by immunoblotting, they might not be the biologically important driver of extracellular expression. In our lab, we have searched by mass spectrometry for these posttranslational modifications and no consensus on a driving modification can be made by our analysis. Another group

published that extracellular Hsp90 is present as a C-terminal truncated form that fits another group's model that only a segment of 115 amino acids in the middle domain is sufficient to stimulate cell migration in an in vitro assay[98,225]. While most of these studies underline the promotility function of Hsp90, the mechanism of secretion is poorly understood. Regardless of the uncertainty of the mechanism on how Hsp90 is excreted, there is a consensus that the secretion of Hsp90 is a prerequisite for pro-invasive functions and blocking the secreted Hsp90 results in significant inhibition of tumor migration and metastasis.

In the context of our data, the misfolded Hsp90 found in cancer may be the source of extracellular Hsp90. Both the misfolded protein and extracellular expression are unique to breast cancer. The extracellular functions of Hsp90 appear to act independently of ATP hydrolysis, which fits the data that this population of Hsp90 cannot be recovered on affinity chromatography resins. Misfolded Hsp90 might be more accessible to posttranslational modifications or display more exposed sequences that are preferentially loaded into exosomes. One way to test this hypothesis is to look for the presence of misfolded protein in exosomal extracts. The presence of misfolded Hsp90 in exosomes would suggest that they are targeted for exosomal secretion. This would support the model that the primary purpose of ectopic Hsp90 is to serve as a danger cue to the surrounding cells by activating promotility signaling pathways and activating cells in the adaptive immune system.

Even without a complete comprehension of Hsp90 secretion and internalization, extracellular Hsp90 can serve as a revolutionary cancer target for selective detection and treatment. The data we have shown using fluor-tethered Hsp90 inhibitors underscores the potential of such clinical applications.

Appendix A

Synthesis Procedures for Affinity Probes as detailed and performed by Dr. Hughes.

Reagents were obtained from commercial sources and used without further purification. Proton NMR spectra were obtained on Varian 400 and 500 MHz spectrometers. LC/MS were obtained on an Agilent ion-trap LC/MS system. HRMS results were obtained on an Agilent 6224 LCMS-TOF and are reported as an average of four runs.

HS-10

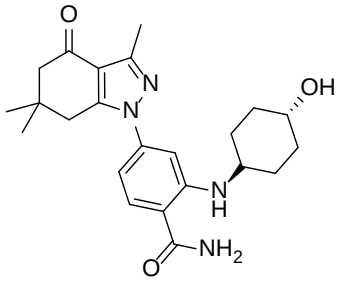

HS-10 was prepared as previously described[40,47].

HS-23

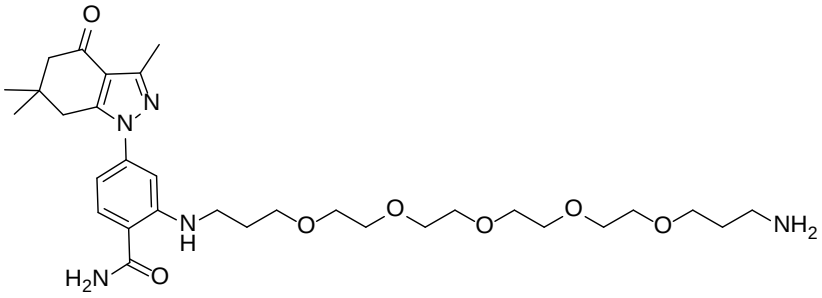

HS-23 was prepared as previously described[47].

HS-27

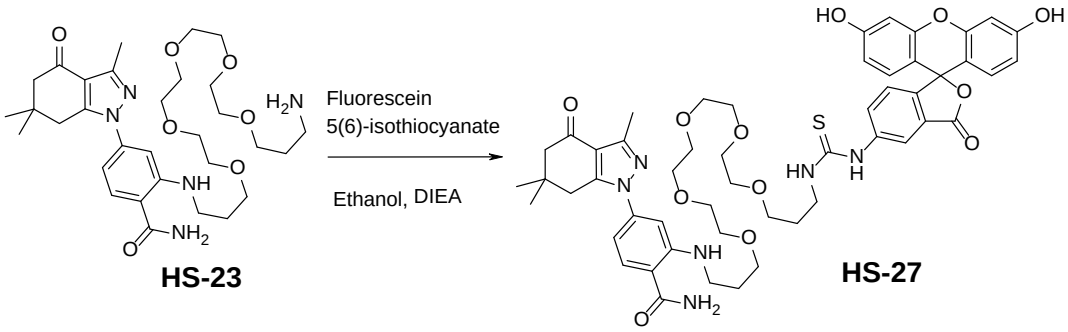

2-((1-((3',6'-dihydroxy-3-oxo-3H-spiro[isobenzofuran-1,9'-xanthen]-5-yl)amino)-1-thioxo-6,9,12,15,18-pentaoxa-2-azahenicosan-21-yl)amino)-4-(3,6,6-trimethyl-4-oxo-4,5,6,7-tetrahydro-1H-indazol-1-yl)benzamide (**HS-27**). Fluorescein 5(6)-isothiocyanate (35 mg, 90 μmol) was dissolved in ethanol (10 mL) and treated with amine **HS-23** (54.2 mg, 90 μmol) followed by Hunig's base (35 mg, 270 μmol) and stored in a drawer overnight. TLC (CH_2Cl_2/MeOH/AcOH : 4/1/0.1) showed formation of a new product. The reaction mixture was concentrated to a glass and dissolved in DMSO/water (4/1, 2.5 mL). About half of the product was purified in two injections by chromatography (5 to 100% MeOH, Agilent C-18 21.2 x 250 mm) to give the product (**HS-27**) (45 mg) as a yellow solid. TLC (4/0.9/0.1 : CH_2Cl_2/MeOH/NH3) Rf = 0.3; 1H NMR (DMSO-d6) δ 10.2 (br s, 2H), 8.40 (br t, 1H), 8.34 (br s, 1H), 8.23 (s, 1H), 7.92 (b s, 1H), 7.73 (d, J = 8.1 Hz, 2H), 7.26 (br s, 1H), 7.15 (d, J = 8.1 Hz, 1H), 6.76 (s, 1H), 6.67 (s, 1H), 6.65 (br s, 2H), 6.59 (d, J = 8.5 Hz, 2H), 6.54 (d, J = 8.5 Hz, 2H), 3.47 (m, 20H), 3.19 (m, 2H), 2.91 (s, 2H), 2.38 (s, 3H), 2.31 (s, 2H), 1.79 (m, 4H), 1.00 (s, 6H); 13C NMR (DMSO-d6) δ 13.57, 28.19, 29.01, 29.24, 35.79, 36.96, 40.13,

40.31, 41.86, 52.24, 68.38, 68.62, 70.01, 70.06, 70.17, 70.22, 70.26, 102.69, 105.56, 108.65, 110.20, 113.05, 113.37, 116.81, 124.47, 127.01, 129.47, 130.71, 141.83, 142.10, 147.53, 148.67, 149.92, 151.00, 152.34, 159.97, 168.97, 171.31, 180.85, 193.27; HRMS (ESI) [M+H]+ calcd for $C_{52}H_{61}N_6O_{12}S$, 993.4063; found 993.4065.

HS-32

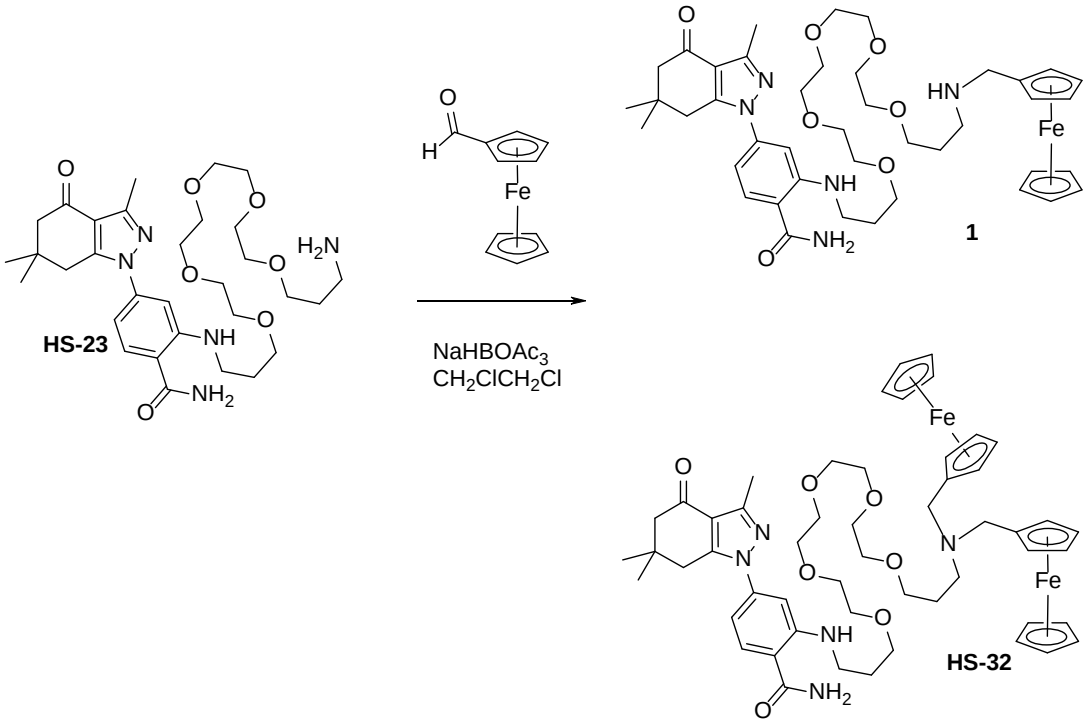

2-((19-(ferrocenemethylamino)-4,7,10,13,16-pentaoxanonadecyl)amino)-4-(3,6,6-trimethyl-4-oxo-4,5,6,7-tetrahydro-1H-indazol-1-yl)benzamide (**1**) and 2-((19,19-di(ferrocenemethylamino)-4,7,10,13,16-pentaoxanonadecyl)amino)-4-(3,6,6-trimethyl-4-oxo-4,5,6,7-tetrahydro-1H-indazol-1-yl)benzamide (**HS-32**). Amine **HS-23** (673 mg, 1.11 mmol) and ferrocene carboxaldehyde (239 mg, 1.11 mmol) were dissolved in

dichloroethane (5 mL) and treated with sodium triacetoxy-borohydride (283.5 mg, 1.34 mmol) followed by acetic acid (77 μL). The reaction mixture was stirred over the weekend. The mixture was adsorbed onto silica (3 g), added to a dry column (1.5 x 12 cm silica gel) and eluted with 100%, 19/1/0.1, then 9/1/0.1 : CH_2Cl_2/MeOH/NH4OH (300 mL ea.) to give the less polar product (~180 mg) and the more polar product (~650 mg), both as yellow glasses. The products were separately dissolved in DMSO and chromatographed by HPLC (Agilent Prep C-18, 2.5 x 25 cm, 5 to 100 % MeOH w/2% formic acid) to give 1 (490 mg, 54%) and **HS-32** (200 mg, 17%) as viscous yellow glasses.

1. TLC (9/0.9/0.1 CH_2Cl_2/MeOH/NH_3) Rf = 0.23; 1H NMR (CDCl3) δ 8.52 (s, 1H), 7.98 (br s, 1H), 7.51 (d, J= 8.1 Hz, 1H), 6.78 (d, J = 1.6 Hz, 1H), 6.59 (dd, J = 1.6, 8.1 Hz, 1H), 6.44 (br s, 1H), 4.3 (br s, 2H), 4.16 (br s, 2H), 4.11 (s, 5H), 3.91 (br s, 2H), 3.57 (br m, 20H), 3.28 (br s, 2H), 2.97 (br t, 2H), 2.79 (s, 2H), 5.52 (s, 3H), 2.37 (s, 2H), 1.91 (br m, 4H), 1.08 (s, 6H); 13C NMR (CDCl¬3) δ 193.60, 171.80, 167.86 (formate), 151.11, 149.85, 149.21, 142.54, 130.06, 117.15, 112.81, 108.95, 106.17, 77.43, 70.59, 70.57, 70.53, 70.51, 70.46, 70.34, 70.20, 70.09, 69.42, 68.99, 68.93, 68.88, 52.44, 46.72, 44.54, 40.20, 37.56, 35.88, 29.16, 28.46, 25.76, 13.50; MS (ESI): m/z 802.4 [M+H]+; HRMS (ESI) [M+H]+ calcd for $C_{42}H_{60}FeN_5O_7$, 802.3831; found 802.3846.

HS-32 TLC (9/0.9/0.1 CH_2Cl_2/MeOH/NH_3) Rf = 0.40; 1H NMR (CDCl¬3) δ 8.51 (s, 1H), 8.06 (br s, 1H), 7.51 (d, J = 8.4 Hz, 1H), 6.77 (d, J = 1.9 Hz, 1H), 6.59 (dd, J = 1.9, 8.4 Hz, 1H), 6.04 (v br s, 1H), 4.32 (br s, 4H), 4.21 (br s, 4H), 4.11 (s, 10 H), 3.88 (br s, 4 H), 3.54-

3.63 (m, 14H), 3.52 (m, 2H), 3.45 (m, 2H), 3.35 (t, J = 5.5 Hz, 2H), 3.28 (m, 2H), 2.79 (s, 2H), 2.70 (m, 2H), 2.51 (s, 3H), 2.37 (s, 2H), 1.93 (p, J = 6.1 Hz), 1.86 (m, 2H), 1.07 (s, 6H); 13C NMR (CDCl¬3) δ 193.56, 171.54, 167.71 (formate), 151.16, 149.84, 149.17, 142.54, 129.92, 117.15, 112.68, 108.89, 106.17, 75.49, 71.23, 70.60, 70.57, 70.56, 70.46, 70.36, 70.21, 69.57, 69.13, 69.06, 68.99, 68.92, 68.30, 52.44, 51.78, 47.22, 40.19, 37.56, 35.87, 29.20, 28.46, 24.82, 13.50; HRMS (ESI) [M+H]+ calcd for $C_{53}H_{70}Fe_2N_5O_7$, 1000.3969; found 1000.3978.

HS-42

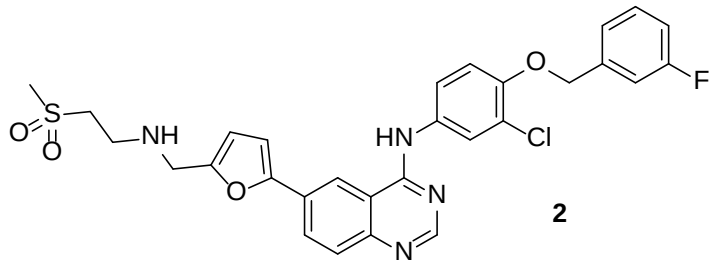

2

N-(3-chloro-4-((3-fluorobenzyl)oxy)phenyl)-6-(5-(((2-(methylsulfonyl)ethyl)amino)methyl)¬furan-2-yl)quinazolin-4-amine (**2**). Four lapatinib pills (assume 250 mg drug each) were partitioned between saturate sodium bicarbonate solution (100 mL) and ethyl acetate (100 mL) and vigorously stirred for 16 hours. The mixture was filtered to remove the solids, the layers separated and the aqueous layer washed with more ethyl acetate (50 mL). The combined organic layers were washed with brine (50 mL), dried ($NaSO_4$), filtered and concentrated to give the product (1.09 g) as a yellowish solid. The solid was dissolved in hot ethyl acetate and diluted with

hexanes, which quickly gave crystals. The mixture was stirred rapidly until cool and the solid was filtered off to give purified Lapatinib (**2**) (968 mg) as an off white solid.

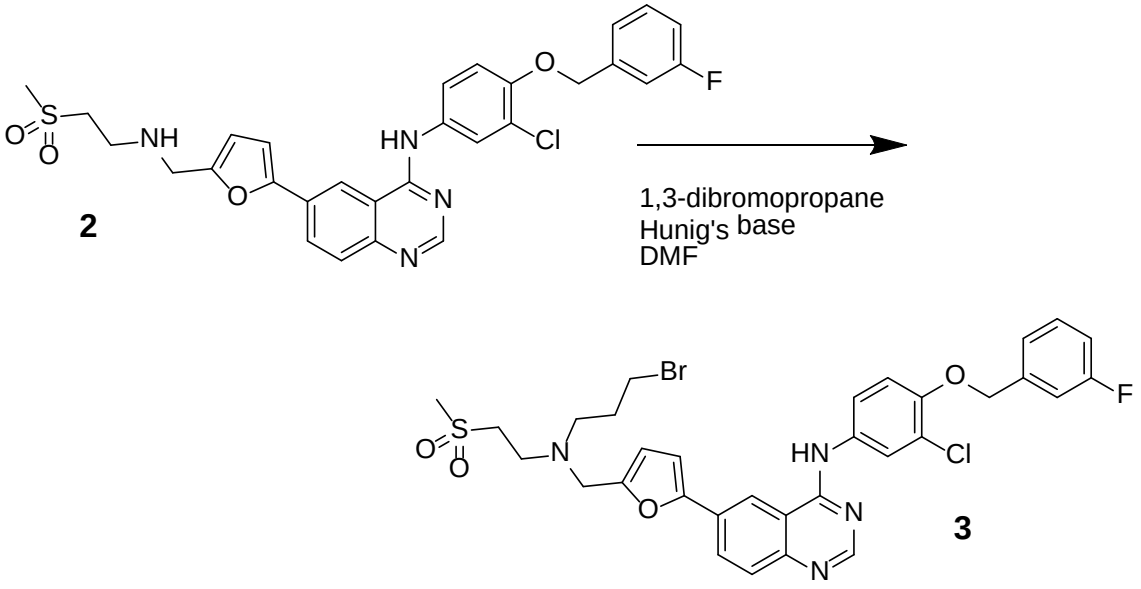

6-(5-(((3-bromopropyl)(2-(methylsulfonyl)ethyl)amino)methyl)furan-2-yl)-N-(3-chloro-4-((3-fluorobenzyl)oxy)phenyl)quinazolin-4-amine (3). Lapatinib (2) (500 mg, 860 μmol) was dissolved in DMF (2 mL) and treated with 1,3-dibromopropane (2.6 g, 12.9 mmol) and Hunig's base (450 μL) and stirred at RT for 4 days. The mixture was partitioned between water (30 mL) and ethyl acetate (60 mL). The resulting emulsion was filtered to give separation. The aqueous layer was re-extracted with ethyl acetate (30 mL) and the combined organic layers washed with brine (30 mL). The organic layer was treated with silica gel (2.5 g) and concentrated to a powder. The powder was added to a column and

chromatographed (silica gel 18 x 2.5 cm, EtOAc) to give product which was recrystallized in hexane/ethyl acetate to give 11 (174 mg, 29%) as a yellow solid. 1H NMR (DMSO-d6) δ 9.88 (s, 1H), 8.74 (s, 1H), 8.55 (s,1H), 8.13 (d, J = 8.8 Hz, 1H), 8.02 (d, J = 2.4 Hz, 1H), 7.79 (d, J = 8.8 Hz, 1H), 7.74 (dd, J = 2.4, 8.8 Hz, 1H), 7.47 (q, J = 8 Hz, 1H), 7.33 (d, J = 8 Hz, 1H), 7.28 (d, J = 8 Hz), 7.17 (dt, J = 2.8, 1H), 7.08 (d, J = 3.3 Hz, 1H), 6.57 (d, J = 3.3 Hz, 1H), 5.25 (s, 2H), 3.79 (s, 2H), 3.57 (t, J = 6.9 Hz, 2H), 3.37 (t, J = 6.9 Hz, 2H), 3.05 (s, 3H), 2.93 (t, J = 6.7 Hz, 2H), 2.63 (t, J = 6.9 Hz, 2H), 2.00 (p, J = 6.8 Hz, 2H); 13C NMR (DMSO-d6) δ 163.80, 160.58, 157.57, 152.48, 151.96, 149.81, 139.68, 139.57, 130.60, 130.49, 128.29, 124.33, 123.34, 123.29, 122.52, 121.04, 115.30, 114.82, 114.54, 114.30, 114.16, 113.87, 111.64, 107.84, 69.39, 51.13, 51.09, 49.02, 46.79, 41.49, 33.08, 29.81; HRMS (ESI) [M+H]+ calcd for $C_{32}H_{32}BrClFN_4O_4S$, 701.1007; found 701.1003.

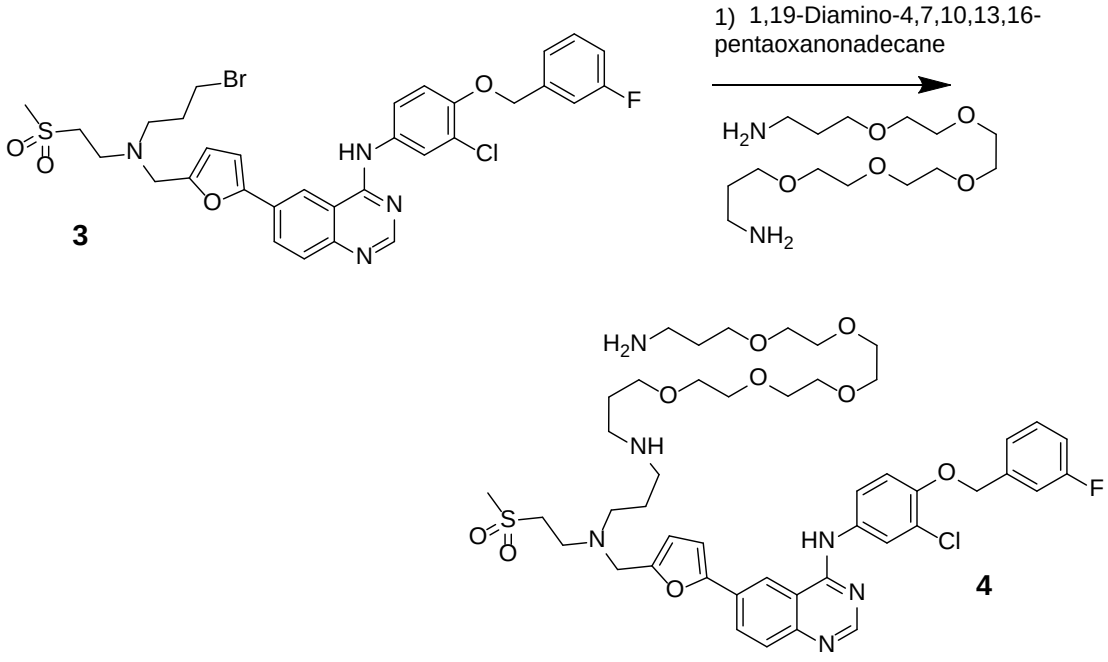

N1-(3-(((5-(4-((3-chloro-4-((3-fluorobenzyl)oxy)phenyl)amino)quinazolin-6-yl)furan-2-yl)methyl)(2-(methylsulfonyl)ethyl)amino)propyl)-4,7,10,13,16-pentaoxanonadecane-1,19-diamine (**4**). Bromide (3) (100 mg, 142 μmol) was treated with 1,19-diamino-4,7,10,13,16-pentaoxanonadecane (439 mg, 1.42 mmol) followed by DMSO (400 μL) with vigorous stirring. After 40 m, the entire reaction mixture was injected on the Prep HPLC (5 to 100% methanol, 20 mL/m, Agilent C-18, 21.1 x 25 cm) to give amine (**4**) (48 mg, 36%) as a yellow glass. 1H NMR (DMSO-d6) δ 8.82 (s, 1H), 8.53 (s, 1H), 8.31 (s, formate), 8.12 (dd, J = 1.5, 8.8 Hz, 1H), 8.02 (d, J = 2.5, 1H), 7.78 (d, J = 8.8 Hz, 1H), 7.74 (dd, J = 2.5, 8.8 Hz, 1H), 7.45 (dt, J = 6.3, 8.0 , 1H), 7.32 (d, J = 6.9 Hz, 1H), 7.30 (dm, J = 8.8 Hz, 1H), 7.24 (d, J = 8 Hz, 1H), 7.15 (tm, J = 8.8 Hz, 1H), 7.07 (d, J = 3.3 Hz, 1H), 6.56 (d, J = 3.3 Hz, 1H), 5.24 (s, 2H), 3.78 (s, 2H), 3.39-3.52 (m, 18H), 3.36 (t, J = 6.2 Hz, 2H), 3.02 (s, 3H), 2.87-2.98 (m, 6H), 2.83 (t, J = 7.1 Hz, 2H), 2.57 (bt, J = 6.2 Hz, 2H), 1.86 (m, 2H), 1.78 (m, 4H); 13C NMR (DMSO-d6) δ 164.90 (formate), 163.90, 160.67, 157.73, 152.22, 152.18, 149.82, 148.94, 139.78, 139.68, 133.26, 130.68, 130.57, 128.29, 124.47, 123.37, 123.33, 122.66, 121.11, 115.51, 114.29, 114.20, 113.91, 111.95, 107.87, 69.79, 69.66, 69.49, 67.49, 67.43, 50.89, 50.24, 48.48, 46.57, 45.35, 44.64, 41.47, 39.52, 36.83, 27.25, 25.95, 23.32; HRMS (ESI) [M+H]+ calcd for $C_{46}H_{63}ClFN_6O_9S$, 929.4044; found 929.4045.

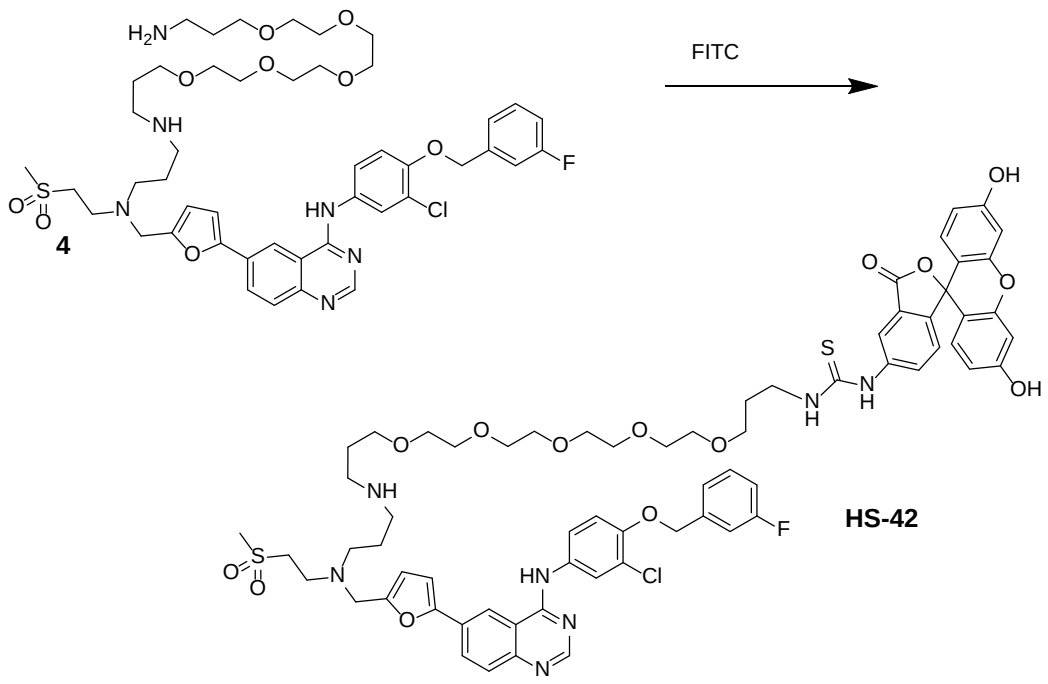

2-((1-((3',6'-dihydroxy-3-oxo-3H-spiro[isobenzofuran-1,9'-xanthen]-5-yl)amino)-1-thioxo-6,9,12,15,18-pentaoxa-2-azahenicosan-21-yl)amino)-4-(3,6,6-trimethyl-4-oxo-4,5,6,7-tetrahydro-1H-indazol-1-yl)benzamide (**HS-42**). Amine (4) (24 mg, 34 μmol) was dissolved in ethanol (1 mL) and treated with fluorescein isothiocyanate (13.3 mg, 34.2 μmol) followed by Hunig's base (9 mg) and stirred for 3 days. The mixture was diluted with DMSO and ethanol, then concentrated to an oil and injected on the prep HPLC (5 to 100% methanol, 20 mL/m, Agilent C-18, 21.1 x 25 cm). The product was collected and concentrated to give the fluorescein derivative (**HS-42**) (14 mg, 31%) as a yellow glass.

(ESI): base peak at m/z 1317.0 [M]-.

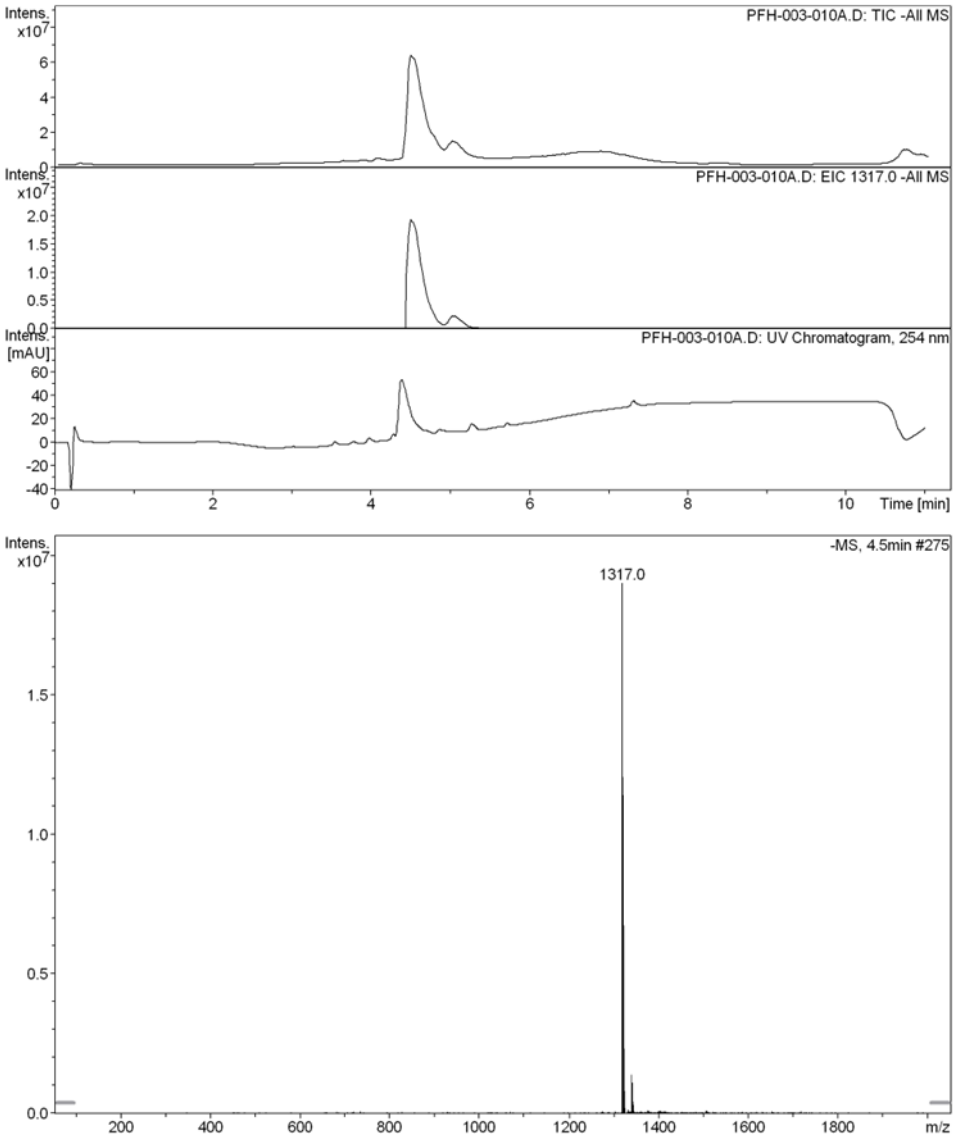

HS-66

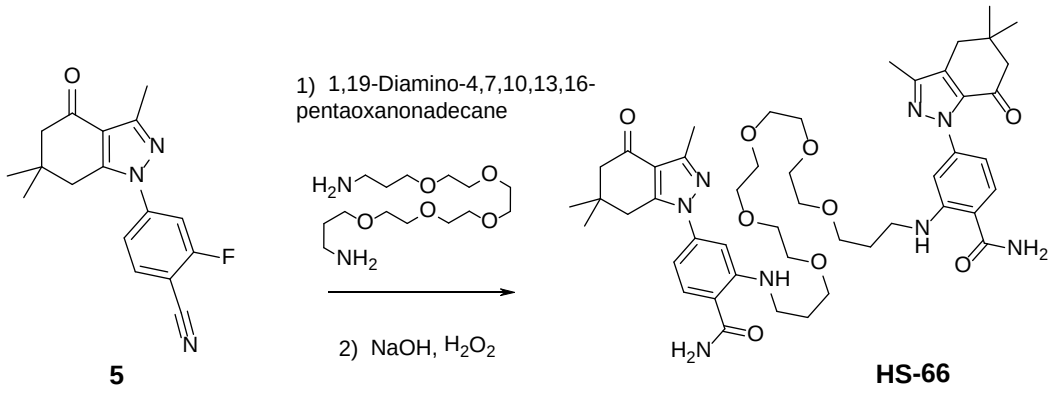

Synthesis of **HS-10** has been previously described[47].

2-((19-((2-carbamoyl-5-(3,5,5-trimethyl-7-oxo-4,5,6,7-tetrahydro-1H-indazol-1-yl)phenyl)amino)-4,7,10,13,16-pentaoxanonadecyl)amino)-4-(3,6,6-trimethyl-4-oxo-4,5,6,7-tetrahydro-1H-indazol-1-yl)benzamide HS-66. A mixture of 2-fluoro-4-(3,6,6-trimethyl-4-oxo-4,5,6,7-tetrahydro-1H-indazol-1-yl)benzonitrile 5 (500 mg, 1.6 mmol), 1,19-diamino-4,7,10,13,16-pentaoxanonadecane (260 mg, 840 µmol) and Hunig's base (520 mg, 4.0 mmol) in DMSO (1 ml) in a 60 mL EPA vial was stirred at 40°C for 2 days. The mixture was then diluted with ethanol (10 mL), heated to 90°C and treated with 10 drops of 50% sodium hydroxide followed by very slowly addition of 10 drops of 30% hydrogen peroxide. TLC (4/0.9/0.1 : CH_2Cl_2/MeOH/NH_3) showed complete conversion to new products. The mixture was adsorbed onto silica gel (3 g), concentrated to a solid, added to a column and chromatographed (3.5 x 20 cm, CH_2Cl_2 (200 mL), CH_2Cl_2/MeOH 19/1 (300 mL), 9/1 (300 mL) and 4/1 (200 mL)) to give product as a glass. The glass was

recrystallized in ethyl acetate/hexanes to give the product **HS-66** (360 mg, 47 %) as a white powder. TLC (4/0.9/0.1 : CH_2Cl_2/MeOH/NH_3) Rf = 0.33; ^{1}H NMR (DMSO-d6) δ 8.42 (t, J = 5.3 Hz, 2H), 7.92 (br s, 2H), 7.73 (d, J = 8.5 Hz, 2H), 7.25 (br s, 2H), 6.7602 (d, J = 2.0 Hz, 2H), 6.66 (dd, J = 2.0, 8.5 Hz, 2H), 3.41-3.51 (m, 20H), 3.19 (dd, J = 6.5, 12.2 Hz, 4H), 2.9046 (s, 4H), 2.38 (s, 6H), 2.30 (s, 4H), 1.79 (p, J = 6.4 Hz, 4H), 0.99 (s, 12H); 13C NMR (DMSO-d6) δ 192.77, 170.84, 150.54, 149.44, 148.19, 141.64, 130.24, 116.35, 112.89, 108.17, 105.09, 69.77, 69.73, 69.69, 69.59, 67.90, 51.77, 36.49, 35.32, 28.78, 27.72, 13.09 ; HRMS (ESI) $[M+H]^+$ calcd for $C_{48}H_{67}N_8O_9$, 899.5026; found 899.5029.

HS-69

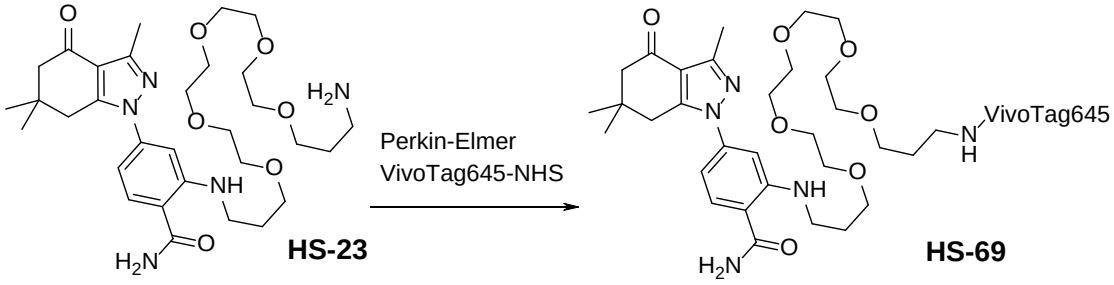

HS-23 **HS-69**

VivoTag 645 compound (**HS-69**). Amine **HS-23** (4.5 mg, 7.45 μmol) was dissolved in DMSO (200 μL) and added to VivoTag 645 (Perkin Elmer, 2.5 mg, 1.8 μmol) in its original container and placed back into the freezer overnight. The sample was purified in 3 portions by reverse-phase chromatography and concentrated to give VivoTag 645 compound (**HS-69**) (~3 mg) as a blue solid. MS (ESI): m/z 1577.5 [M^-].

LC/MS

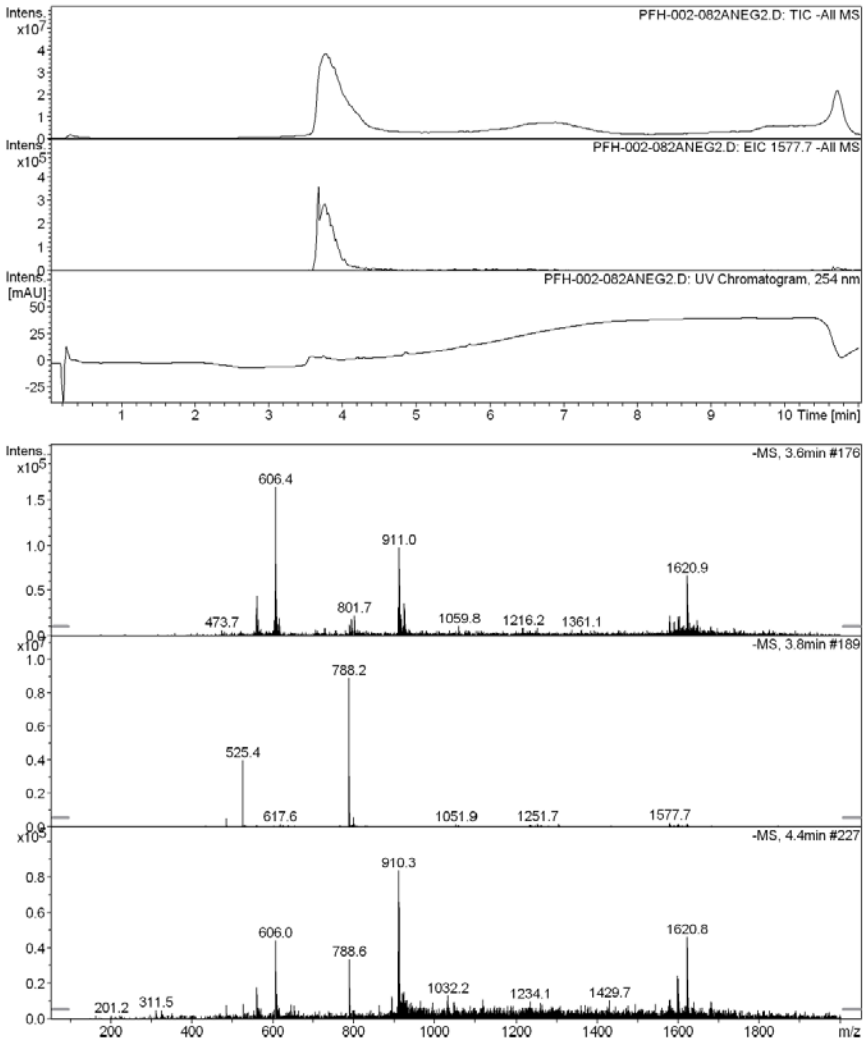

HPLC (C-18, 0 to 100% acetonitrile w/ 1% TFA over 30 min, hold at 100% 10 min.).

Fluorescent traces were obtained by collection of 15 sec fractions into a microtiter plate followed by buffering the wells to pH 7.4 and counting in a plate reader.

UV trace (254 nm)

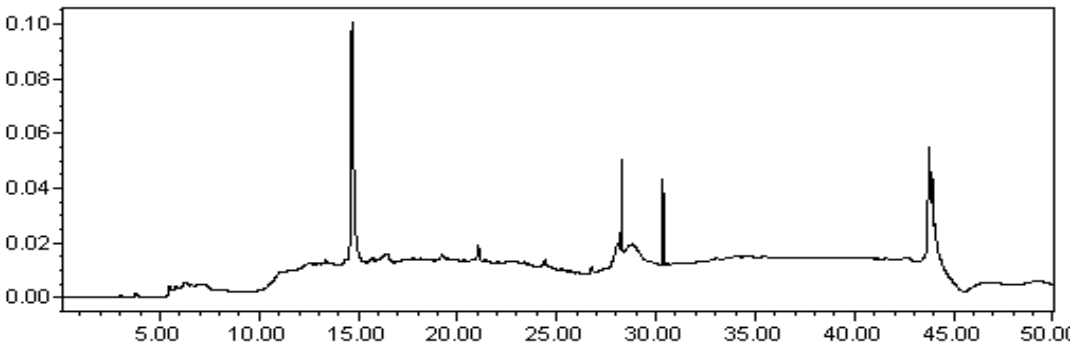

Fluorescence trace

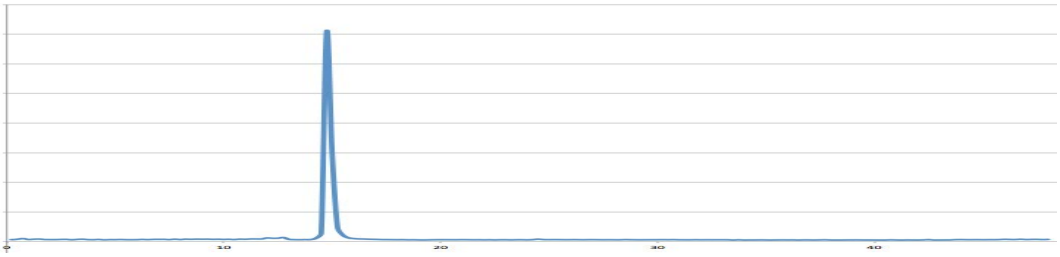

HS-70

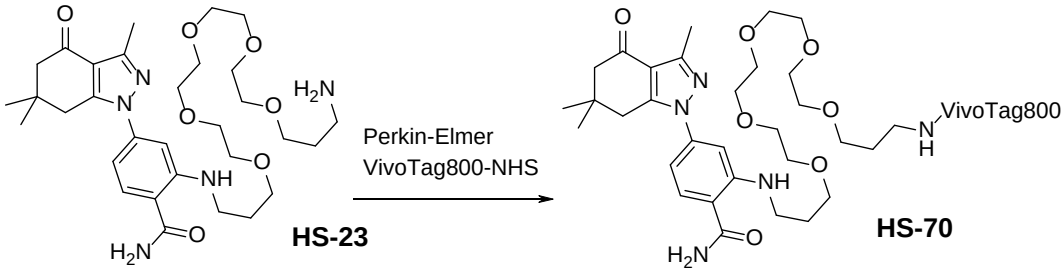

VivoTag 800 compound (**HS-70**). Amine **HS-23** (4.3 mg, 7.2 µmol) was dissolved in DMSO (100 µL) and treated with Hunig's base (10 µL) and added to VivoTag 800 (Perkin Elmer, 5 mg, 3.42 µmol) in its original container. The starting material vial was washed

twice with DMSO (100 µL), which was added to the reaction mixture. The mixture was left in an aluminum bag at RT for 30 minutes, then placed back into the freezer for the 3 days. The sample was purified in 3 portions by reverse-phase chromatography and concentrated to give VivoTag 800 compound (**HS-70**) (~9 mg) as a blue solid. MS (ESI): m/z 823.7 $[M-2]^{2-}$.

LC/MS

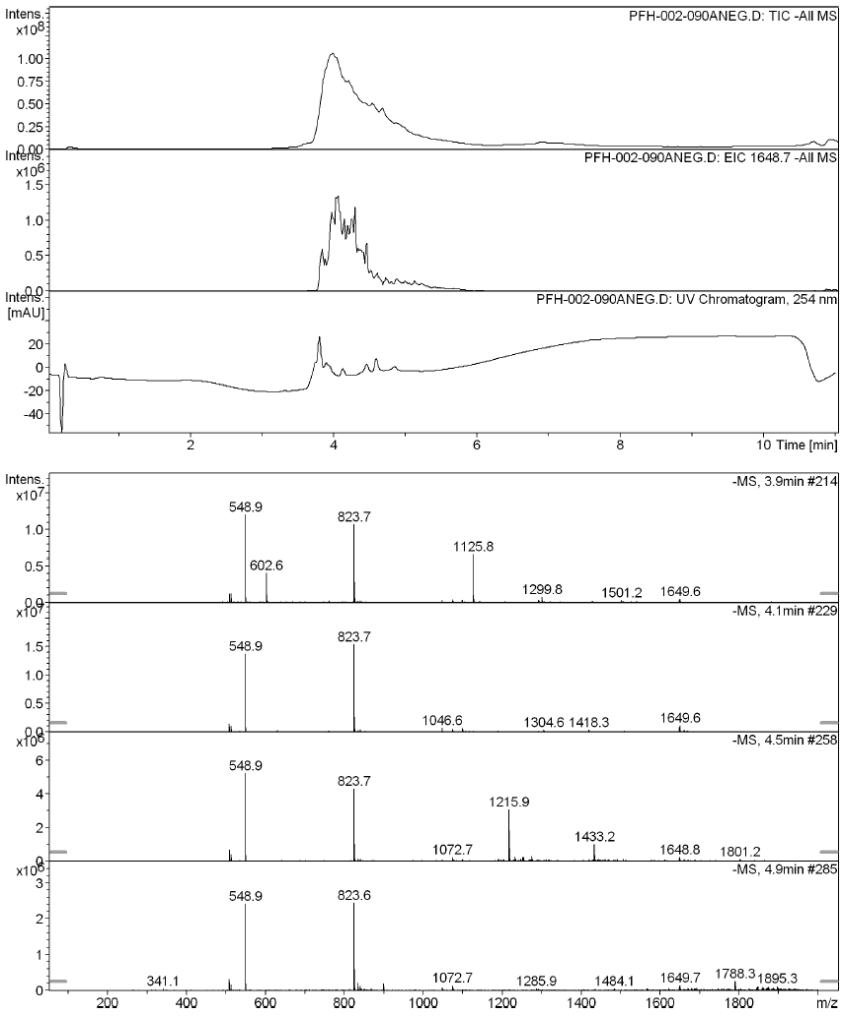

UV trace

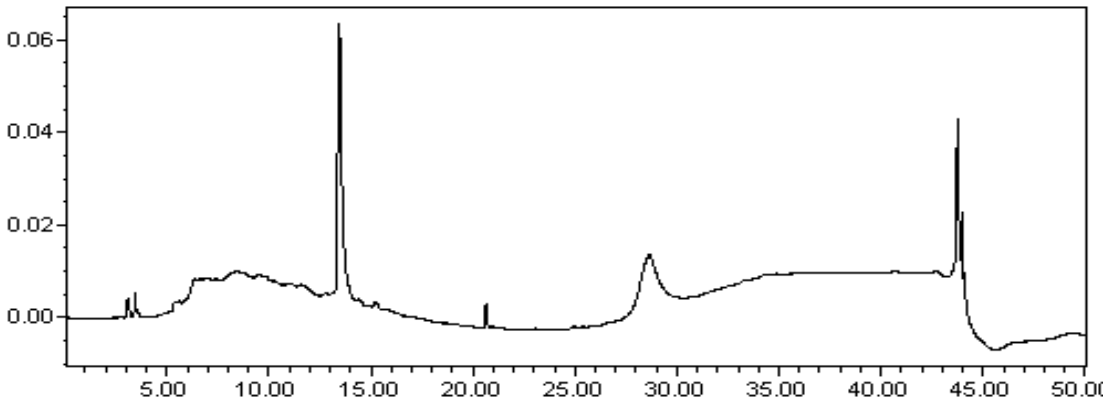

Fluorescence trace

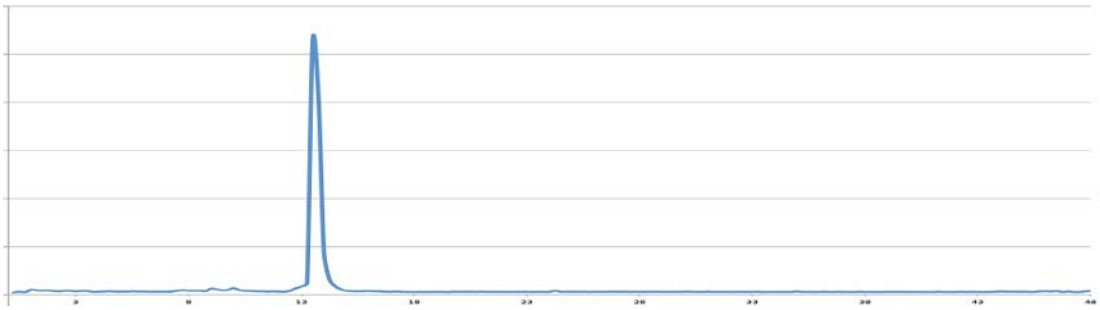

HS-96

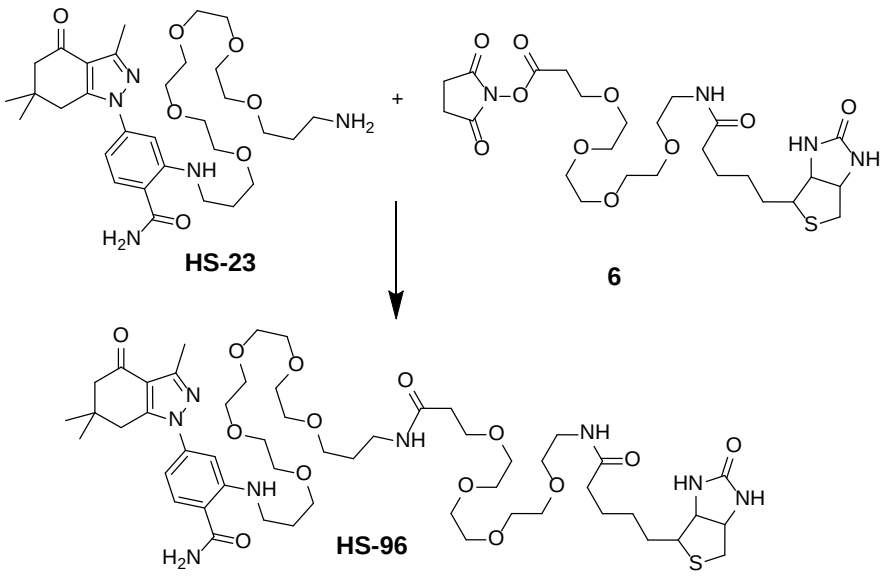

A solution of NHS-dPEG® **4**-biotin 6 (Quanta Biodesign Pt # 10200, 13.3 mg, 22.4 µmol) in DMF (200 µL) was added to **HS-23** (13.6 mg, 22.5 µmol) and Hunig's base (15 mg, 110 µmol). TLC (2/0.9/0.1 CH_2Cl_2/MeOH/NH_3) showed pretty clean formation of a new product so the entire reaction mixture was injected on the Prep HPLC (5 to 100% methanol, 20 mL/m, Agilent C-18, 21.1 x 25 cm) and the product collected and concentrated to give **HS-96** (16 mg. 67%) as a clear glass. MS (ESI): m/z 1077.7 $[M+H]^+$.

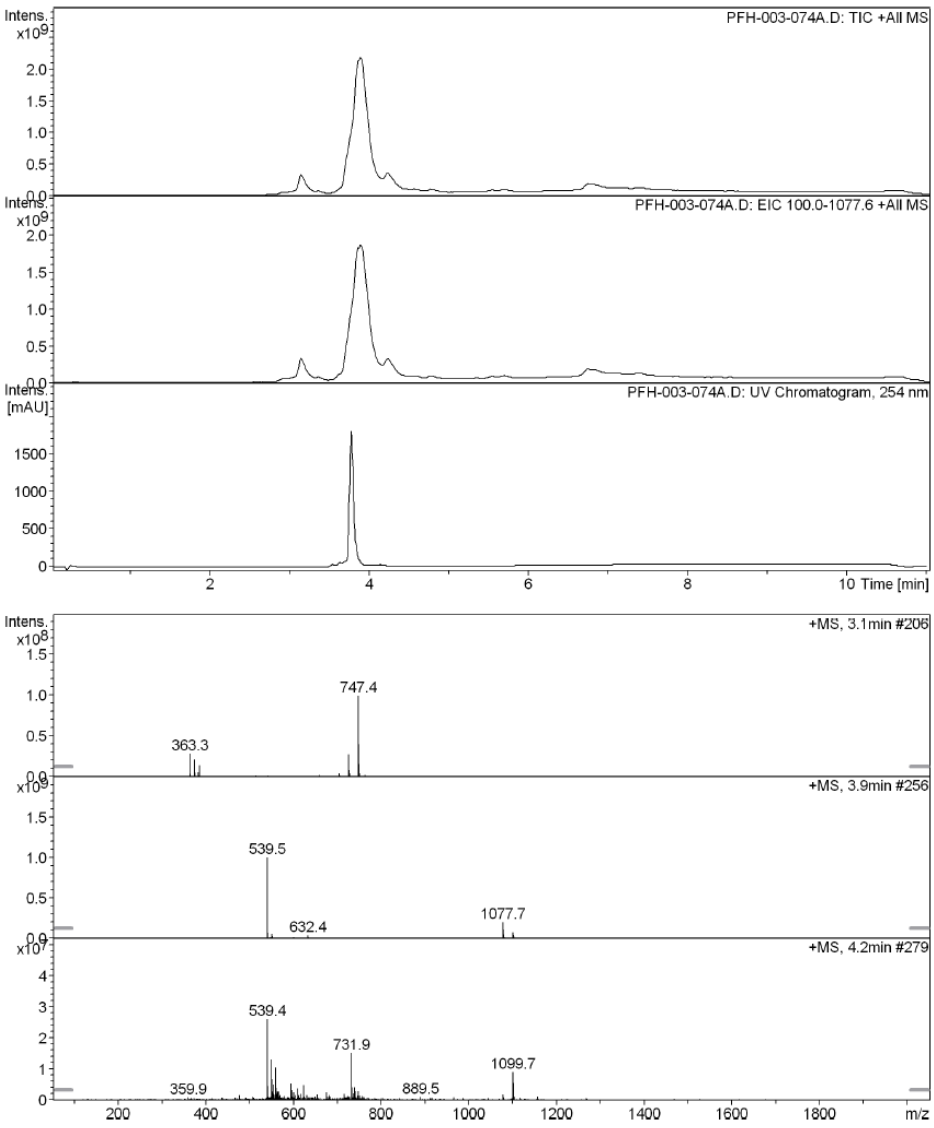
PFH-003-074A.D: TIC +All MS
PFH-003-074A.D: EIC 100.0-1077.6 +All MS
PFH-003-074A.D: UV Chromatogram, 254 nm
Time [min]
+MS, 3.1min #206
747.4
363.3
+MS, 3.9min #256
539.5
632.4
1077.7
+MS, 4.2min #279
539.4
731.9
1099.7
359.9
889.5
m/z

HS-105

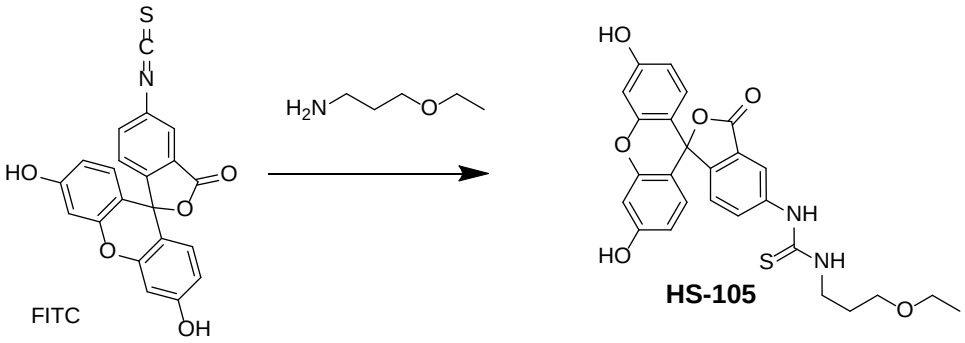

1-(3',6'-dihydroxy-3-oxo-3H-spiro[isobenzofuran-1,9'-xanthen]-5-yl)-3-(3-ethoxypropyl)thiourea **HS-105**. FITC (75 mg, 193 µmol) was slurried in methylene chloride (4 mL) and treated with 3-ethoxypropylamine (80 mg, 770 µmol) with rapid stirring for 30 m. The mixture was concentrated then chromatographed (silica gel 2.5 x 20 cm, CH_2Cl_2 (100mL), then CH_2Cl_2/MeOH/AcOH : 9/1/0.05 (400 mL)) to give an orange glass (82 mg). The glass was dissolved in some ethanol and diluted with water to effect solidification. Some of the ethanol was removed and the solid filtered off and air dried to give the product **HS-105** (62 mg, 65%) as an orange powder. ^{1}H NMR (CDCl¬3) δ 10.12 (s, 2H), 9.89 (br s, 1H), 8.20 (s, 1H), 8.06 (br s, 1H), 7.73 (d, J = 8 Hz, 1H), 7.18 (d, J = 8 Hz, 1H), 6.68 (d, J = 2.3 Hz, 2H), 6.61 (d, J = 8.7 Hz, 2H), 6.56 (dd, J = 2.3, 8.7 Hz, 2H), 3.56 (br m, 2H), 3.44 (d, J = 7 Hz, 2H), 3.43 (q, J = 7 Hz, 2H), 1.81 (p, J = 7 Hz, 2H), 1.11 (t, J = 7 Hz, 2H). ^{13}C NMR (CDCl¬3) δ 180.44, 168.45, 159.44, 159.19, 151.82, 128.96, 124.05, 120.64, 119.61, 119.38, 112.51, 109.74, 102.24, 102.22, 83.05, 67.65, 65.4, 41.53, 28.69, 15.18; HRMS (ESI) $[M+H]^+$ calcd for $C_{26}H_{25}N_2O_6S$, 493.1428; found 493.1438.

HS-111

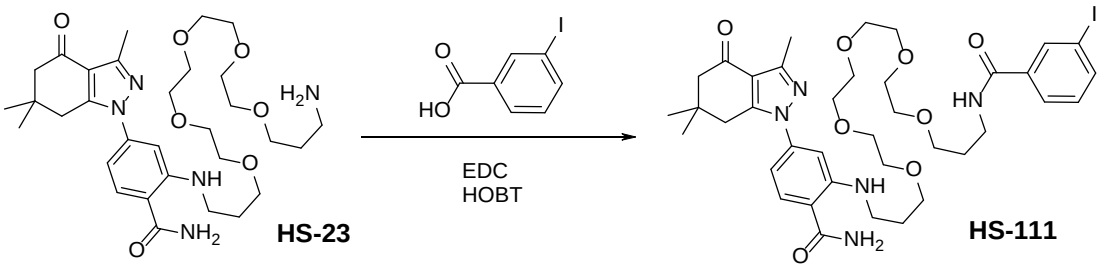

N-(19-((2-carbamoyl-5-(3,6,6-trimethyl-4-oxo-4,5,6,7-tetrahydro-1H-indazol-1-yl)phenyl)amino)-4,7,10,13,16-pentaoxanonadecyl)-3-iodobenzamide **HS-111**. The free amine, 2-((19-amino-4,7,10,13,16-pentaoxanonadecyl)amino)-4-(3,6,6-trimethyl-4-oxo-4,5,6,7-tetrahydro-1H-indazol-1-yl)benzamide HS-23 (55 mg, 91 μmol), 3-iodobenzoic acid (23 mg, 92 μmol), EDC (27 mg, 137 μmol), HOBT (12 mg, 91 μmol) and Hunig's base (20 μL) were dissolved in DMSO (400 μL) and stirred at RT for one hour. The reaction mixture injected onto the HPLC (30 to 100% methanol, 20 mL/m, Agilent C-18, 21.1 x 25 cm) to give purified product HS-111 (38 mg, 50%) as a clear glass. TLC (9/1 : CH_2Cl_2/MeOH) Rf = 0.51; ^{1}H NMR (CDCl3) δ 8.10 (t, J = 1.6 Hz, 1H), 7.96 (br t, J = 4.7 Hz, 1H), 7.74 (d m, J = 7.6 Hz, 1H), 7.73)d m, J = 7.6 Hz, 1H), 7.47 (d, J = 8.3 Hz, 1H), 7.32 (br t, J = 4.7 Hz, 1H), 7.11 (t, J = 7.6 Hz, 1H), 6.76 (d, J = 2.0 Hz, 1H), 6.57 (dd, J = 2.0, 8.3 Hz, 1H), 6.01 (br s, 1H), 3.48-3.63 (m, 22H), 3.26 (br q, 2H), 2.78 (s, 2H), 2.50 (s, 3H), 2.37 (s, 2H), 1.9 (p, J = 6 Hz, 2H), 1.84 (p, J = 6 Hz, 2H), 1.06 (s, 6H); ^{13}C NMR (CDCl3) δ 193.66, 171.49, 165.87, 151.18, 150.07, 149.29, 142.77, 140.17, 137.07, 136.27, 130.32, 129.76, 126.46, 117.32, 112.83, 109.09, 106.44, 94.31, 77.65, 77.23, 76.81, 70.79, 70.69, 70.68, 70.67, 70.61,

70.60, 70.49, 70.49, 70.40, 69.12, 52.57, 40.45, 39.26, 37.72, 36.01, 29.26, 28.85, 28.59, 13.61; HRMS (ESI) $[M+H]^+$ calcd for $C_{38}H_{53}IN_5O_8$, 834.2933; found 834.3195.

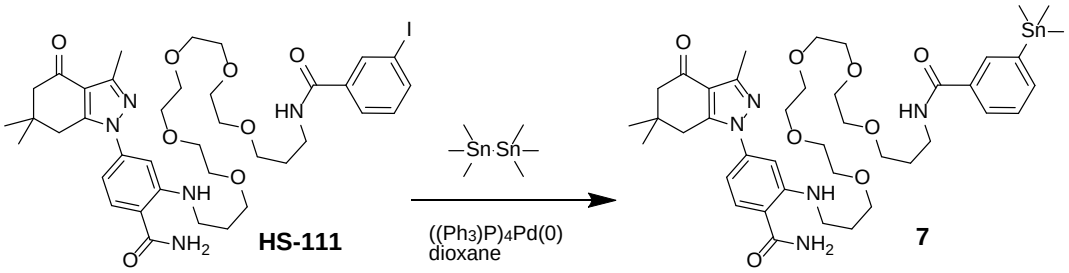

This procedure was adapted from published procedures[226,227].

N-(19-((2-carbamoyl-5-(3,6,6-trimethyl-4-oxo-4,5,6,7-tetrahydro-1H-indazol-1-yl)phenyl)amino)-4,7,10,13,16-pentaoxanonadecyl)-3-(trimethylstannyl)benzamide (7). N-(19-((2-carbamoyl-5-(3,6,6-trimethyl-4-oxo-4,5,6,7-tetrahydro-1H-indazol-1-yl)phenyl)amino)-4,7,10,13,16-pentaoxanonadecyl)-3-iodobenzamide (**HS-111**) (92.7 mg, 111 μmol), hexamethylditin (40 mg, 122 μmol) and tetrakis triphenylphosphine palladium(0) (2.6 mg 2.22 μmol) were slurried in dioxane (2 mL), purged with nitrogen and heated to 100 °C for 1 h, then 80 °C for 16h. The reaction mixture was concentrated then added to a column and chromatographed (silica gel, 2.5 x 25, CH_2Cl_2 (100 mL), CH_2Cl_2/MeOH : 19/1 (250 mL), CH_2Cl_2/MeOH : 9/1 (250 mL)) to give the product (7) (91.8 mg, 95%) as a slightly yellowish oil. TLC (9/1 CH2Cl2/MeOH) Rf = 0.46; ^{1}H NMR (CDCl3) δ 7.97 (bt, 1H), 7.92 (sm, 1H), 7.64 (dm, J = 7.2 Hz, 1H), 7.55 (dm, J = 7.2 Hz, 1H), 7.47 (d, J = 8.3 Hz, 1H), 7.32 (tm, J = 7.2 Hz, 1H), 7.12 (brt, 1H), 6.76 (d, J = 2 Hz, 1H), 6.57 (dd, J = 2,8.3 Hz, 1H), 5.94 (vbrs, 1H), 3.49-3.62 (m, 22 H), 3.26 (q, J = 6.5 Hz, 2H), 2.78 (s,

2H), 2.50 (s, 3H), 2.36 (s, 2H), 1.91 (p, J = 6.2 Hz, 2H), 1.85 (p, J = 6.2 Hz, 2H), 1.07 (s, 6H), 0.27 (s, 9H). ^{13}C NMR (CDCl3) δ 193.69, 171.45, 168.10, 151.19, 150.08, 149.29, 143.13, 142.78, 138.84, 134.70, 129.75, 128.60, 127.98, 126.62, 117.33, 112.84, 109.09, 106.45, 70.68 3C), 70.63 (2C), 70.59, 70.51, 70.47, 70.39, 69.13, 52.57, 40.45, 38.79, 37.72, 36.02, 29.25, 29.11, 28.59, 13.61, -9.27; (ESI): base peak at m/z 858.4 $[M]^+$. HRMS (ESI) $[M+H]^+$ calcd for $C_{41}H_{61}N_5O_8116Sn$, 868.3626; found 868.3623.

^{125}I-HS-111

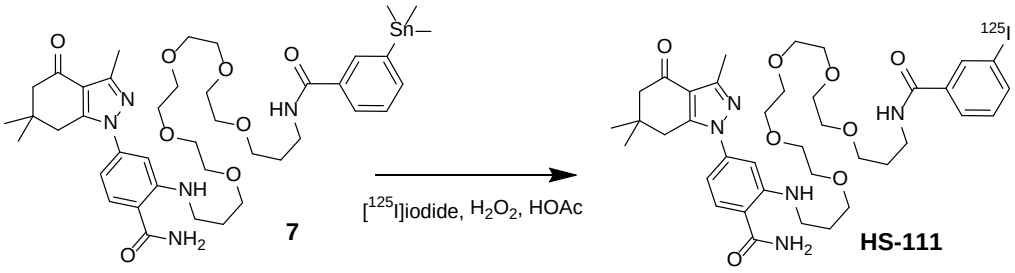

Sodium [^{125}I]iodide (2200 Ci/mmol) as a solution in 0.1N NaOH was procured from Perkin Elmer Life and Analytical Sciences (Boston, MA). High-pressure liquid chromatography (HPLC) was performed using a Beckman Gold HPLC system equipped with a Model 126 programmable solvent module, a Model 166 NM variable wavelength detector, a Model 170 radioisotope detector and a Beckman System Gold remote interface module SS420X; data was acquired using the 32 Karat® software. Reversed-phase HPLC was performed using a Waters 4.6 × 250-mm XTerra RP18 (5 :m) column. It was eluted at a flow rate of 1 ml/min with a gradient consisting of 0.1% TFA in water (solvent A) and 0.1% TFA in acetonitrile (solvent B). The proportion of solvent B was

linearly increased from 30% to 100% in 30 min and held at 100% for the next 5 min before restoring to original conditions.

Compound 7 was dissolved in methanol (2.5 mg/ml) and a 10 µl aliquot of this was transferred to a small conical glass vial, and methanol was evaporated with a gentle stream of argon. A solution of [^{125}I]iodide in 0.1N NaOH (2 µl, about 500 µCi) was added to 7 (25 µg; 28.7 nmol) followed by a 5 µl of a solution of H2O2 (30% w/v) in acetic acid (1:3 v/v). The vial with the contents was briefly sonicated (~20 sec) and the entire reaction mixture was injected onto a reversed-phase HPLC column eluted with the gradient conditions described above. Under these conditions, the product (^{125}I-HS-111) eluted with a tR of 15.3 min. HPLC fractions containing [^{125}I]HS-111 were pooled and most acetonitrile from them was evaporated with a gentle stream of argon and diluted with the addition of 10 ml of water. This was passed through a C18 Seppak cartridge (Waters), which was pre-activated by eluting with 2 ml each of methanol and water. The cartridge was eluted with 2 × 5 ml water followed by 0.25 ml portions of methanol. Methanol fractions containing most of the radioactivity (typically 3-5) were pooled and methanol evaporated with argon. The residual radioactivity was reconstituted in PBS.

Compound 7 was radioiodinated to obtain [^{125}I]-HS-111 in an average radiochemical yield of 64.5 ± 5.6% (n = 4). The product co-eluted with an authentic standard of **HS-111** (see Figure 1. for HPLC) and had a radiochemical purity of greater than 98%. No co-eluting peaks were seen in the HPLC profile of the reaction mixture

and thus the specific activity of the product is assumed to be that of starting radioiodide (2200 Ci/mmol).

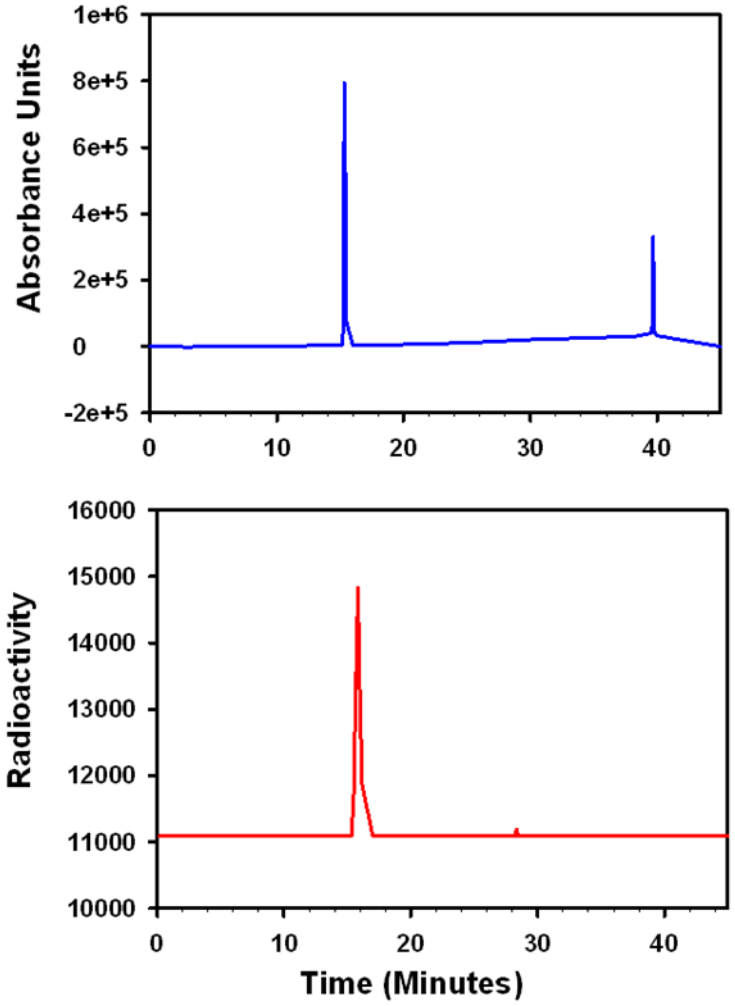

Quality control HPLC of [^{125}I]HS-111: Final formulated [^{125}I]HS-111 was co-injected onto the HPLC with an authentic standard of **HS-111**. Upper-UV; Lower-Gamma

References

1. Koboldt, D.C., *et al.* Comprehensive molecular portraits of human breast tumours. *Nature* (2012).

2. Hanahan, D. & Weinberg, R.A. Hallmarks of cancer: the next generation. *Cell* **144**, 646-674 (2011).

3. Passarino, G., *et al.* Molecular variation of human HSP90alpha and HSP90beta genes in Caucasians. *Human mutation* **21**, 554-555 (2003).

4. Urban, J.D., Budinsky, R.A. & Rowlands, J.C. An evaluation of single nucleotide polymorphisms in the human heat shock protein 90 kDa alpha and beta isoforms. *Drug metabolism and pharmacokinetics* **27**, 268-278 (2012).

5. Komarova, N.L. & Wodarz, D. Drug resistance in cancer: principles of emergence and prevention. *Proceedings of the National Academy of Sciences of the United States of America* **102**, 9714-9719 (2005).

6. Bozic, I., Allen, B. & Nowak, M.A. Dynamics of targeted cancer therapy. *Trends in molecular medicine* **18**, 311-316 (2012).

7. Pao, W., *et al.* Acquired resistance of lung adenocarcinomas to gefitinib or erlotinib is associated with a second mutation in the EGFR kinase domain. *PLoS medicine* **2**, e73 (2005).

8. Ying, W., *et al.* Ganetespib, a unique triazolone-containing Hsp90 inhibitor, exhibits potent antitumor activity and a superior safety profile for cancer therapy. *Molecular cancer therapeutics* **11**, 475-484 (2012).

9. Proia, D.A., *et al.* Synergistic activity of the Hsp90 inhibitor ganetespib with taxanes in non-small cell lung cancer models. *Investigational new drugs* **30**, 2201-2209 (2012).

10. Acquaviva, J., *et al.* Targeting KRAS-Mutant Non-Small Cell Lung Cancer with the Hsp90 Inhibitor Ganetespib. *Molecular cancer therapeutics* **11**, 2633-2643 (2012).

11. Wiech, H., Buchner, J., Zimmermann, R. & Jakob, U. Hsp90 chaperones protein folding in vitro. *Nature* **358**, 169-170 (1992).

12. Pearl, L.H. & Prodromou, C. Structure and mechanism of the Hsp90 molecular chaperone machinery. *Annu Rev Biochem* **75**, 271-294 (2006).

13. Sawarkar, R., Sievers, C. & Paro, R. Hsp90 globally targets paused RNA polymerase to regulate gene expression in response to environmental stimuli. *Cell* **149**, 807-818 (2012).

14. Mollapour, M. & Neckers, L. Post-translational modifications of Hsp90 and their contributions to chaperone regulation. *Biochimica et biophysica acta* **1823**, 648-655 (2012).

15. Owens-Grillo, J.K., Stancato, L.F., Hoffmann, K., Pratt, W.B. & Krishna, P. Binding of immunophilins to the 90 kDa heat shock protein (hsp90) via a tetratricopeptide repeat domain is a conserved protein interaction in plants. *Biochemistry* **35**, 15249-15255 (1996).

16. Ratajczak, T. & Carrello, A. Cyclophilin 40 (CyP-40), mapping of its hsp90 binding domain and evidence that FKBP52 competes with CyP-40 for hsp90 binding. *The Journal of biological chemistry* **271**, 2961-2965 (1996).

17. Young, J.C., Obermann, W.M. & Hartl, F.U. Specific binding of tetratricopeptide repeat proteins to the C-terminal 12-kDa domain of hsp90. *The Journal of biological chemistry* **273**, 18007-18010 (1998).

18. Chen, S., Sullivan, W.P., Toft, D.O. & Smith, D.F. Differential interactions of p23 and the TPR-containing proteins Hop, Cyp40, FKBP52 and FKBP51 with Hsp90 mutants. *Cell stress & chaperones* **3**, 118-129 (1998).

19. Smith, D.F., Baggenstoss, B.A., Marion, T.N. & Rimerman, R.A. Two FKBP-related proteins are associated with progesterone receptor complexes. *The Journal of biological chemistry* **268**, 18365-18371 (1993).

20. Silverstein, A.M., *et al.* Protein phosphatase 5 is a major component of glucocorticoid receptor.hsp90 complexes with properties of an FK506-binding immunophilin. *The Journal of biological chemistry* **272**, 16224-16230 (1997).

21. Jiang, J., *et al.* CHIP is a U-box-dependent E3 ubiquitin ligase: identification of Hsc70 as a target for ubiquitylation. *The Journal of biological chemistry* **276**, 42938-42944 (2001).

22. Panaretou, B., *et al.* Activation of the ATPase activity of hsp90 by the stress-regulated cochaperone aha1. *Molecular cell* **10**, 1307-1318 (2002).

23. Lotz, G.P., Lin, H., Harst, A. & Obermann, W.M. Aha1 binds to the middle domain of Hsp90, contributes to client protein activation, and stimulates the ATPase activity of the molecular chaperone. *The Journal of biological chemistry* **278**, 17228-17235 (2003).

24. Gray, P.J., Jr., Prince, T., Cheng, J., Stevenson, M.A. & Calderwood, S.K. Targeting the oncogene and kinome chaperone CDC37. *Nature reviews. Cancer* **8**, 491-495 (2008).

25. Taipale, M., *et al.* Quantitative analysis of hsp90-client interactions reveals principles of substrate recognition. *Cell* **150**, 987-1001 (2012).

26. Johnson, J.L. & Toft, D.O. A novel chaperone complex for steroid receptors involving heat shock proteins, immunophilins, and p23. *The Journal of biological chemistry* **269**, 24989-24993 (1994).

27. Johnson, J.L. & Toft, D.O. Binding of p23 and hsp90 during assembly with the progesterone receptor. *Mol Endocrinol* **9**, 670-678 (1995).

28. Cox, M.B. & Miller, C.A., 3rd. Cooperation of heat shock protein 90 and p23 in aryl hydrocarbon receptor signaling. *Cell stress & chaperones* **9**, 4-20 (2004).

29. Forsythe, H.L., Jarvis, J.L., Turner, J.W., Elmore, L.W. & Holt, S.E. Stable association of hsp90 and p23, but Not hsp70, with active human telomerase. *The Journal of biological chemistry* **276**, 15571-15574 (2001).

30. Trinklein, N.D., Chen, W.C., Kingston, R.E. & Myers, R.M. Transcriptional regulation and binding of heat shock factor 1 and heat shock factor 2 to 32 human heat shock genes during thermal stress and differentiation. *Cell stress & chaperones* **9**, 21-28 (2004).

31. Bagatell, R., *et al.* Induction of a heat shock factor 1-dependent stress response alters the cytotoxic activity of hsp90-binding agents. *Clinical cancer research : an official journal of the American Association for Cancer Research* **6**, 3312-3318 (2000).

32. Felts, S.J., *et al.* The hsp90-related protein TRAP1 is a mitochondrial protein with distinct functional properties. *The Journal of biological chemistry* **275**, 3305-3312 (2000).

33. Tsutsumi, S., *et al.* Hsp90 charged-linker truncation reverses the functional consequences of weakened hydrophobic contacts in the N domain. *Nature structural & molecular biology* **16**, 1141-1147 (2009).

34. Dollins, D.E., Warren, J.J., Immormino, R.M. & Gewirth, D.T. Structures of GRP94-nucleotide complexes reveal mechanistic differences between the hsp90 chaperones. *Molecular cell* **28**, 41-56 (2007).

35. Frey, S., Leskovar, A., Reinstein, J. & Buchner, J. The ATPase cycle of the endoplasmic chaperone Grp94. *The Journal of biological chemistry* **282**, 35612-35620 (2007).

36. Leskovar, A., Wegele, H., Werbeck, N.D., Buchner, J. & Reinstein, J. The ATPase cycle of the mitochondrial Hsp90 analog Trap1. *The Journal of biological chemistry* **283**, 11677-11688 (2008).

37. Chiosis, G. & Neckers, L. Tumor selectivity of Hsp90 inhibitors: the explanation remains elusive. *ACS chemical biology* **1**, 279-284 (2006).

38. Bachleitner-Hofmann, T., *et al.* Antitumor activity of SNX-2112, a synthetic heat shock protein-90 inhibitor, in MET-amplified tumor cells with or without resistance to selective MET Inhibition. *Clinical cancer research : an official journal of the American Association for Cancer Research* **17**, 122-133 (2011).

39. Chandarlapaty, S., *et al.* SNX2112, a synthetic heat shock protein 90 inhibitor, has potent antitumor activity against HER kinase-dependent cancers. *Clinical cancer research : an official journal of the American Association for Cancer Research* **14**, 240-248 (2008).

40. Huang, K.H., *et al.* Discovery of novel 2-aminobenzamide inhibitors of heat shock protein 90 as potent, selective and orally active antitumor agents. *Journal of medicinal chemistry* **52**, 4288-4305 (2009).

41. Fadden, P., *et al.* Application of chemoproteomics to drug discovery: identification of a clinical candidate targeting hsp90. *Chemistry & biology* **17**, 686-694 (2010).

42. Eiseman, J.L., *et al.* Pharmacokinetics and pharmacodynamics of 17-demethoxy 17-[[(2-dimethylamino)ethyl]amino]geldanamycin (17DMAG, NSC 707545) in C.B-17 SCID mice bearing MDA-MB-231 human breast cancer xenografts. *Cancer chemotherapy and pharmacology* **55**, 21-32 (2005).

43. Vilenchik, M., *et al.* Targeting wide-range oncogenic transformation via PU24FCl, a specific inhibitor of tumor Hsp90. *Chemistry & biology* **11**, 787-797 (2004).

44. Zhou D, T.F., Liu Y, Ye J, Ying W, Shin Ogawa L, Inoue T, Lee W, Adjiri-Awere A, Kolodzieyski L, Tatsuta N, Wada Y, Sonderfan AJ. Associating retinal drug exposure and retention with the ocular toxicity profiles of Hsp90 inhibitors. *Journal Clinical Oncology* **30**(2012).

45. Kamal, A., Lia Thao, John Sensintaffar, Lin Zhang, Marcus F. Boehm, & Burrows, L.C.F.F.J. A high-affinity conformation of Hsp90 confers tumour selectivity on Hsp90 inhibitors. *Nature* **425**, 407-410 (2003).

46. Moulick, K., *et al.* Affinity-based proteomics reveal cancer-specific networks coordinated by Hsp90. *Nature chemical biology* **7**, 818-826 (2011).

47. Hughes, P.F., *et al.* A highly selective Hsp90 affinity chromatography resin with a cleavable linker. *Bioorganic & medicinal chemistry* **20**, 3298-3305 (2012).

48. Li, Y., Zhang, T., Schwartz, S.J. & Sun, D. New developments in Hsp90 inhibitors as anti-cancer therapeutics: mechanisms, clinical perspective and more potential. *Drug resistance updates : reviews and commentaries in antimicrobial and anticancer chemotherapy* **12**, 17-27 (2009).

49. Powers, M.V. & Workman, P. Inhibitors of the heat shock response: biology and pharmacology. *FEBS letters* **581**, 3758-3769 (2007).

50. Chiosis, G., Caldas Lopes, E. & Solit, D. Heat shock protein-90 inhibitors: a chronicle from geldanamycin to today's agents. *Current opinion in investigational drugs* **7**, 534-541 (2006).

51. Workman, P., Burrows, F., Neckers, L. & Rosen, N. Drugging the cancer chaperone HSP90: combinatorial therapeutic exploitation of oncogene addiction and tumor stress. *Annals of the New York Academy of Sciences* **1113**, 202-216 (2007).

52. Neckers, L. & Workman, P. Hsp90 molecular chaperone inhibitors: are we there yet? *Clinical cancer research : an official journal of the American Association for Cancer Research* **18**, 64-76 (2012).

53. Trepel, J., Mollapour, M., Giaccone, G. & Neckers, L. Targeting the dynamic HSP90 complex in cancer. *Nature reviews. Cancer* **10**, 537-549 (2010).

54. Welch, W.J. & Feramisco, J.R. Purification of the major mammalian heat shock proteins. *The Journal of biological chemistry* **257**, 14949-14959 (1982).

55. Sahu, D., *et al.* A potentially common peptide target in secreted heat shock protein-90alpha for hypoxia-inducible factor-1alpha-positive tumors. *Molecular biology of the cell* **23**, 602-613 (2012).

56. Whitesell, L. & Lindquist, S.L. HSP90 and the chaperoning of cancer. *Nature reviews. Cancer* **5**, 761-772 (2005).

57. Zagouri, F., *et al.* Hsp90 in the continuum of breast ductal carcinogenesis: Evaluation in precursors, preinvasive and ductal carcinoma lesions. *BMC cancer* **10**, 353 (2010).

58. Pick, E., *et al.* High HSP90 expression is associated with decreased survival in breast cancer. *Cancer research* **67**, 2932-2937 (2007).

59. Cheng, Q., *et al.* Amplification and high-level expression of heat shock protein 90 marks aggressive phenotypes of human epidermal growth factor receptor 2 negative breast cancer. *Breast cancer research : BCR* **14**, R62 (2012).

60. Becker, B., *et al.* Induction of Hsp90 protein expression in malignant melanomas and melanoma metastases. *Experimental dermatology* **13**, 27-32 (2004).

61. Flandrin, P., *et al.* Significance of heat-shock protein (HSP) 90 expression in acute myeloid leukemia cells. *Cell stress & chaperones* **13**, 357-364 (2008).

62. Kubota, H., *et al.* Increased expression of co-chaperone HOP with HSP90 and HSC70 and complex formation in human colonic carcinoma. *Cell stress & chaperones* **15**, 1003-1011 (2010).

63. Burgess, E.F., *et al.* Prostate cancer serum biomarker discovery through proteomic analysis of alpha-2 macroglobulin protein complexes. *Proteomics. Clinical applications* **2**, 1223 (2008).

64. Zhong, L., *et al.* Antibodies to HSP70 and HSP90 in serum in non-small cell lung cancer patients. *Cancer detection and prevention* **27**, 285-290 (2003).

65. Li, W., Sahu, D. & Tsen, F. Secreted heat shock protein-90 (Hsp90) in wound healing and cancer. *Biochimica et biophysica acta* **1823**, 730-741 (2012).

66. Samant, R.S., Clarke, P.A. & Workman, P. The expanding proteome of the molecular chaperone HSP90. *Cell cycle* **11**, 1301-1308 (2012).

67. Prince, T. & Neckers, L. A network of its own: the unique interactome of the Hsp90 cochaperone, Sba1/p23. *Molecular cell* **43**, 159-160 (2011).

68. Echeverria, P.C., Bernthaler, A., Dupuis, P., Mayer, B. & Picard, D. An interaction network predicted from public data as a discovery tool: application to the Hsp90 molecular chaperone machine. *PloS one* **6**, e26044 (2011).

69. Carbone, D.L., Doorn, J.A., Kiebler, Z., Ickes, B.R. & Petersen, D.R. Modification of heat shock protein 90 by 4-hydroxynonenal in a rat model of chronic alcoholic liver disease. *The Journal of pharmacology and experimental therapeutics* **315**, 8-15 (2005).

70. Scroggins, B.T., *et al.* An acetylation site in the middle domain of Hsp90 regulates chaperone function. *Molecular cell* **25**, 151-159 (2007).

71. Kovacs, J.J., *et al.* HDAC6 regulates Hsp90 acetylation and chaperone-dependent activation of glucocorticoid receptor. *Molecular cell* **18**, 601-607 (2005).

72. Yang, Y., *et al.* Role of acetylation and extracellular location of heat shock protein 90alpha in tumor cell invasion. *Cancer research* **68**, 4833-4842 (2008).

73. Murphy, P.J., Morishima, Y., Kovacs, J.J., Yao, T.P. & Pratt, W.B. Regulation of the dynamics of hsp90 action on the glucocorticoid receptor by acetylation/deacetylation of the chaperone. *The Journal of biological chemistry* **280**, 33792-33799 (2005).

74. Bali, P., *et al.* Inhibition of histone deacetylase 6 acetylates and disrupts the chaperone function of heat shock protein 90: a novel basis for antileukemia activity of histone deacetylase inhibitors. *The Journal of biological chemistry* **280**, 26729-26734 (2005).

75. Kekatpure, V.D., Dannenberg, A.J. & Subbaramaiah, K. HDAC6 modulates Hsp90 chaperone activity and regulates activation of aryl hydrocarbon receptor signaling. *The Journal of biological chemistry* **284**, 7436-7445 (2009).

76. Wandinger, S.K., Suhre, M.H., Wegele, H. & Buchner, J. The phosphatase Ppt1 is a dedicated regulator of the molecular chaperone Hsp90. *EMBO J* **25**, 367-376 (2006).

77. Duval, M., Le Boeuf, F., Huot, J. & Gratton, J.P. Src-mediated phosphorylation of Hsp90 in response to vascular endothelial growth factor (VEGF) is required for VEGF receptor-2 signaling to endothelial NO synthase. *Molecular biology of the cell* **18**, 4659-4668 (2007).

78. Kurokawa, M., Zhao, C., Reya, T. & Kornbluth, S. Inhibition of apoptosome formation by suppression of Hsp90beta phosphorylation in tyrosine kinase-induced leukemias. *Molecular and cellular biology* **28**, 5494-5506 (2008).

79. Lees-Miller, S.P. & Anderson, C.W. Two human 90-kDa heat shock proteins are phosphorylated in vivo at conserved serines that are phosphorylated in vitro by casein kinase II. *The Journal of biological chemistry* **264**, 2431-2437 (1989).

80. Mollapour, M., Tsutsumi, S. & Neckers, L. Hsp90 phosphorylation, Wee1 and the cell cycle. *Cell cycle* **9**, 2310-2316 (2010).

81. Mollapour, M., *et al.* Swe1Wee1-dependent tyrosine phosphorylation of Hsp90 regulates distinct facets of chaperone function. *Molecular cell* **37**, 333-343 (2010).

82. Mollapour, M., *et al.* Threonine 22 phosphorylation attenuates Hsp90 interaction with cochaperones and affects its chaperone activity. *Molecular cell* **41**, 672-681 (2011).

83. Mollapour, M., Tsutsumi, S., Kim, Y.S., Trepel, J. & Neckers, L. Casein kinase 2 phosphorylation of Hsp90 threonine 22 modulates chaperone function and drug sensitivity. *Oncotarget* **2**, 407-417 (2011).

84. Xu, W., *et al.* Dynamic tyrosine phosphorylation modulates cycling of the HSP90-P50(CDC37)-AHA1 chaperone machine. *Molecular cell* **47**, 434-443 (2012).

85. Quanz, M., *et al.* Heat shock protein 90alpha (Hsp90alpha) is phosphorylated in response to DNA damage and accumulates in repair foci. *The Journal of biological chemistry* **287**, 8803-8815 (2012).

86. Lees-Miller, S.P. & Anderson, C.W. The human double-stranded DNA-activated protein kinase phosphorylates the 90-kDa heat-shock protein, hsp90 alpha at two NH2-terminal threonine residues. *The Journal of biological chemistry* **264**, 17275-17280 (1989).

87. Adinolfi, E., Kim, M., Young, M.T., Di Virgilio, F. & Surprenant, A. Tyrosine phosphorylation of HSP90 within the P2X7 receptor complex negatively regulates P2X7 receptors. *The Journal of biological chemistry* **278**, 37344-37351 (2003).

88. Old, W.M., *et al.* Functional proteomics identifies targets of phosphorylation by B-Raf signaling in melanoma. *Molecular cell* **34**, 115-131 (2009).

89. Huang, S.Y., Tsai, M.L., Chen, G.Y., Wu, C.J. & Chen, S.H. A systematic MS-based approach for identifying in vitro substrates of PKA and PKG in rat uteri. *Journal of proteome research* **6**, 2674-2684 (2007).

90. Wang, X., *et al.* The regulatory mechanism of Hsp90alpha secretion and its function in tumor malignancy. *Proceedings of the National Academy of Sciences of the United States of America* **106**, 21288-21293 (2009).

91. Lei, H., Venkatakrishnan, A., Yu, S. & Kazlauskas, A. Protein kinase A-dependent translocation of Hsp90 alpha impairs endothelial nitric-oxide synthase activity in high glucose and diabetes. *The Journal of biological chemistry* **282**, 9364-9371 (2007).

92. Martinez-Ruiz, A., *et al.* S-nitrosylation of Hsp90 promotes the inhibition of its ATPase and endothelial nitric oxide synthase regulatory activities. *Proceedings of the National Academy of Sciences of the United States of America* **102**, 8525-8530 (2005).

93. Retzlaff, M., *et al.* Hsp90 is regulated by a switch point in the C-terminal domain. *EMBO reports* **10**, 1147-1153 (2009).

94. Blank, M., Mandel, M., Keisari, Y., Meruelo, D. & Lavie, G. Enhanced ubiquitinylation of heat shock protein 90 as a potential mechanism for mitotic cell death in cancer cells induced with hypericin. *Cancer research* **63**, 8241-8247 (2003).

95. Sidera, K. & Patsavoudi, E. Extracellular HSP90: conquering the cell surface. *Cell cycle* **7**, 1564-1568 (2008).

96. Eustace, B.K., *et al.* Functional proteomic screens reveal an essential extracellular role for hsp90 alpha in cancer cell invasiveness. *Nature cell biology* **6**, 507-514 (2004).

97. Tsutsumi, S. & Neckers, L. Extracellular heat shock protein 90: a role for a molecular chaperone in cell motility and cancer metastasis. *Cancer science* **98**, 1536-1539 (2007).

98. Cheng, C.F., *et al.* Transforming growth factor alpha (TGFalpha)-stimulated secretion of HSP90alpha: using the receptor LRP-1/CD91 to promote human skin cell migration against a TGFbeta-rich environment during wound healing. *Molecular and cellular biology* **28**, 3344-3358 (2008).

99. Li, W., *et al.* Extracellular heat shock protein-90alpha: linking hypoxia to skin cell motility and wound healing. *EMBO J* **26**, 1221-1233 (2007).

100. Ullrich, S.J., Robinson, E.A., Law, L.W., Willingham, M. & Appella, E. A mouse tumor-specific transplantation antigen is a heat shock-related protein. *Proceedings of the National Academy of Sciences of the United States of America* **83**, 3121-3125 (1986).

101. Sidera, K., Samiotaki, M., Yfanti, E., Panayotou, G. & Patsavoudi, E. Involvement of cell surface HSP90 in cell migration reveals a novel role in the developing nervous system. *The Journal of biological chemistry* **279**, 45379-45388 (2004).

102. Saito, K., Dai, Y. & Ohtsuka, K. Enhanced expression of heat shock proteins in gradually dying cells and their release from necrotically dead cells. *Experimental cell research* **310**, 229-236 (2005).

103. Yerbury, J.J., Stewart, E.M., Wyatt, A.R. & Wilson, M.R. Quality control of protein folding in extracellular space. *EMBO reports* **6**, 1131-1136 (2005).

104. Sims, J.D., McCready, J. & Jay, D.G. Extracellular heat shock protein (Hsp)70 and Hsp90alpha assist in matrix metalloproteinase-2 activation and breast cancer cell migration and invasion. *PloS one* **6**, e18848 (2011).

105. Nickel, W. The mystery of nonclassical protein secretion. A current view on cargo proteins and potential export routes. *European journal of biochemistry / FEBS* **270**, 2109-2119 (2003).

106. McCready, J., Sims, J.D., Chan, D. & Jay, D.G. Secretion of extracellular hsp90alpha via exosomes increases cancer cell motility: a role for plasminogen activation. *BMC cancer* **10**, 294 (2010).

107. Stellas, D., El Hamidieh, A. & Patsavoudi, E. Monoclonal antibody 4C5 prevents activation of MMP2 and MMP9 by disrupting their interaction with extracellular HSP90 and inhibits formation of metastatic breast cancer cell deposits. *BMC cell biology* **11**, 51 (2010).

108. Dowling, P., Walsh, N. & Clynes, M. Membrane and membrane-associated proteins involved in the aggressive phenotype displayed by highly invasive cancer cells. *Proteomics* **8**, 4054-4065 (2008).

109. Taiyab, A. & Rao Ch, M. HSP90 modulates actin dynamics: inhibition of HSP90 leads to decreased cell motility and impairs invasion. *Biochimica et biophysica acta* **1813**, 213-221 (2011).

110. Barrott, J.J., *et al.* Optical and radioiodinated tethered hsp90 inhibitors reveal selective internalization of ectopic hsp90 in malignant breast tumor cells. *Chemistry & biology* **20**, 1187-1197 (2013).

111. Wong, K., *et al.* An open-label phase II study of the Hsp90 inhibitor ganetespib (STA-9090) as monotherapy in patients with advanced non-small cell lung cancer (NSCLC). *Journal Clinical Oncology* **29**(2011).

112. Sjoblom, T., *et al.* The consensus coding sequences of human breast and colorectal cancers. *Science* **314**, 268-274 (2006).

113. Greenman, C., *et al.* Patterns of somatic mutation in human cancer genomes. *Nature* **446**, 153-158 (2007).

114. Gerlinger, M., *et al.* Intratumor heterogeneity and branched evolution revealed by multiregion sequencing. *The New England journal of medicine* **366**, 883-892 (2012).

115. Garraway, L.A. & Janne, P.A. Circumventing cancer drug resistance in the era of personalized medicine. *Cancer discovery* **2**, 214-226 (2012).

116. Shimamura, T. & Shapiro, G.I. Heat shock protein 90 inhibition in lung cancer. *Journal of thoracic oncology : official publication of the International Association for the Study of Lung Cancer* **3**, S152-159 (2008).

117. Holmes, J.L., Sharp, S.Y., Hobbs, S. & Workman, P. Silencing of HSP90 cochaperone AHA1 expression decreases client protein activation and increases cellular sensitivity to the HSP90 inhibitor 17-allylamino-17-demethoxygeldanamycin. *Cancer research* **68**, 1188-1197 (2008).

118. Gray, P.J., Jr., Stevenson, M.A. & Calderwood, S.K. Targeting Cdc37 inhibits multiple signaling pathways and induces growth arrest in prostate cancer cells. *Cancer research* **67**, 11942-11950 (2007).

119. McDowell, C.L., Bryan Sutton, R. & Obermann, W.M. Expression of Hsp90 chaperone [corrected] proteins in human tumor tissue. *International journal of biological macromolecules* **45**, 310-314 (2009).

120. Au, Q., Zhang, Y., Barber, J.R., Ng, S.C. & Zhang, B. Identification of inhibitors of HSF1 functional activity by high-content target-based screening. *Journal of biomolecular screening* **14**, 1165-1175 (2009).

121. Dai, C., *et al.* Loss of tumor suppressor NF1 activates HSF1 to promote carcinogenesis. *The Journal of clinical investigation* **122**, 3742-3754 (2012).

122. Schmitt, E., *et al.* Heat shock protein 70 neutralization exerts potent antitumor effects in animal models of colon cancer and melanoma. *Cancer research* **66**, 4191-4197 (2006).

123. Ray, R. & Haystead, T.A. Phosphoproteome analysis in yeast. *Methods in enzymology* **366**, 95-103 (2003).

124. Brown, J.Q., *et al.* Quantitative optical spectroscopy: a robust tool for direct measurement of breast cancer vascular oxygenation and total hemoglobin content in vivo. *Cancer research* **69**, 2919-2926 (2009).

125. Palmer, G.M. & Ramanujam, N. Monte-Carlo-based model for the extraction of intrinsic fluorescence from turbid media. *Journal of biomedical optics* **13**, 024017 (2008).

126. Liu, C., *et al.* Experimental validation of an inverse fluorescence Monte Carlo model to extract concentrations of metabolically relevant fluorophores from

turbid phantoms and a murine tumor model. *Journal of biomedical optics* **17**, 077012 (2012).

127. Palmer, G.M., *et al.* Non-invasive monitoring of intra-tumor drug concentration and therapeutic response using optical spectroscopy. *Journal of controlled release : official journal of the Controlled Release Society* **142**, 457-464 (2010).

128. Konishi, M. & Watanabe, M. Molecular size-dependent leakage of intracellular molecules from frog skeletal muscle fibers permeabilized with beta-escin. *Pflugers Archiv : European journal of physiology* **429**, 598-600 (1995).

129. Osada, T., Morse, M.A., Lyerly, H.K. & Clay, T.M. Ex vivo expanded human CD4+ regulatory NKT cells suppress expansion of tumor antigen-specific CTLs. *Int Immunol* **17**, 1143-1155 (2005).

130. Smith, R.A., Cokkinides, V., Brooks, D., Saslow, D. & Brawley, O.W. Cancer screening in the United States, 2010: a review of current American Cancer Society guidelines and issues in cancer screening. *CA: a cancer journal for clinicians* **60**, 99-119 (2010).

131. Esserman, L., Shieh, Y. & Thompson, I. Rethinking screening for breast cancer and prostate cancer. *JAMA : the journal of the American Medical Association* **302**, 1685-1692 (2009).

132. Warning, K., Hildebrandt, M.G., Kristensen, B. & Ewertz, M. Utility of 18FDG-PET/CT in breast cancer diagnostics--a systematic review. *Danish medical bulletin* **58**, A4289 (2011).

133. Barrott, J.J. & Haystead, T.A. Hsp90, an Unlikely Ally in the War on Cancer. *The FEBS journal* (2013).

134. Neckers, L., Mollapour, M. & Tsutsumi, S. The complex dance of the molecular chaperone Hsp90. *Trends in biochemical sciences* **34**, 223-226 (2009).

135. Vaughan, C.K., Neckers, L. & Piper, P.W. Understanding of the Hsp90 molecular chaperone reaches new heights. *Nature structural & molecular biology* **17**, 1400-1404 (2010).

136. Chiosis, G., *et al.* Development of purine-scaffold small molecule inhibitors of Hsp90. *Current cancer drug targets* **3**, 371-376 (2003).

137. Csermely, P., Tamás Schnaider, Csaba S ti, Zoltán Prohászka and Gábor Nardai. The 90-kDa Molecular Chaperone Family: Structure, Function, and Clinical Applications. A Comprehensive Review. *Pharmacol. Ther.* **79**, 129-168 (1998).

138. Kim, Y.S., *et al.* Update on Hsp90 Inhibitors in Clinical Trial. *Current topics in medicinal chemistry* **9**, 1479-1492 (2009).

139. Wang, Y., Trepel, J.B., Neckers, L.M. & Giaccone, G. STA-9090, a small-molecule Hsp90 inhibitor for the potential treatment of cancer. *Current opinion in investigational drugs* **11**, 1466-1476 (2010).

140. Tsutsumi, S., *et al.* A small molecule cell-impermeant Hsp90 antagonist inhibits tumor cell motility and invasion. *Oncogene* **27**, 2478-2487 (2008).

141. Grenert, J.P., William P. Sullivan, Patrick Fadden, Timothy A. J. Haystead,, Jenny Clark, E.M., Henry Krutzsch, Hans-Joachim Ochel, & Theodor W. Schulte, E.S., Leonard M. Neckers, and David O. Toft. The Amino-terminal Domain of Heat Shock Protein 90 (hsp90) That Binds Geldanamycin Is an ATP/ADP Switch Domain That Regulateshsp90 Conformation. *Journal of Biological Chemistry* **272**, 23843-23850 (1997).

142. Neve, R.M., *et al.* A collection of breast cancer cell lines for the study of functionally distinct cancer subtypes. *Cancer cell* **10**, 515-527 (2006).

143. Koga, F., Kihara, K. & Neckers, L. Inhibition of cancer invasion and metastasis by targeting the molecular chaperone heat-shock protein 90. *Anticancer research* **29**, 797-807 (2009).

144. Ide, M. & Suzuki, Y. Is whole-body FDG-PET valuable for health screening? For. *European journal of nuclear medicine and molecular imaging* **32**, 339-341 (2005).

145. Schoder, H. & Gonen, M. Screening for cancer with PET and PET/CT: potential and limitations. *Journal of nuclear medicine : official publication, Society of Nuclear Medicine* **48 Suppl 1**, 4S-18S (2007).

146. Yin, X., *et al.* BIIB021, a novel Hsp90 inhibitor, sensitizes head and neck squamous cell carcinoma to radiotherapy. *International journal of cancer. Journal international du cancer* **126**, 1216-1225 (2010).

147. Sidera, K., El Hamidieh, A., Mamalaki, A. & Patsavoudi, E. The 4C5 cell-impermeable anti-HSP90 antibody with anti-cancer activity, is composed of a single light chain dimer. *PloS one* **6**, e23906 (2011).

148. Xu, W., *et al.* Surface charge and hydrophobicity determine ErbB2 binding to the Hsp90 chaperone complex. *Nature structural & molecular biology* **12**, 120-126 (2005).

149. Graves, P.R. & Haystead, T.A. Molecular biologist's guide to proteomics. *Microbiology and molecular biology reviews : MMBR* **66**, 39-63; table of contents (2002).

150. Whitesell, L., Mimnaugh, E.G., De Costa, B., Myers, C.E. & Neckers, L.M. Inhibition of heat shock protein HSP90-pp60v-src heteroprotein complex formation by benzoquinone ansamycins: essential role for stress proteins in oncogenic transformation. *Proceedings of the National Academy of Sciences of the United States of America* **91**, 8324-8328 (1994).

151. He, H., *et al.* Identification of potent water soluble purine-scaffold inhibitors of the heat shock protein 90. *Journal of medicinal chemistry* **49**, 381-390 (2006).

152. Verhelst, S.H., Fonovic, M. & Bogyo, M. A mild chemically cleavable linker system for functional proteomic applications. *Angew Chem Int Ed Engl* **46**, 1284-1286 (2007).

153. Yang, Y.Y., Grammel, M., Raghavan, A.S., Charron, G. & Hang, H.C. Comparative analysis of cleavable azobenzene-based affinity tags for bioorthogonal chemical proteomics. *Chemistry & biology* **17**, 1212-1222 (2010).

154. Schulte, T.W. & Neckers, L.M. The benzoquinone ansamycin 17-allylamino-17-demethoxygeldanamycin binds to HSP90 and shares important biologic activities with geldanamycin. *Cancer chemotherapy and pharmacology* **42**, 273-279 (1998).

155. Graves, P.R., *et al.* Discovery of novel targets of quinoline drugs in the human purine binding proteome. *Molecular pharmacology* **62**, 1364-1372 (2002).

156. Janecke, A.R., *et al.* Mutations in RDH12 encoding a photoreceptor cell retinol dehydrogenase cause childhood-onset severe retinal dystrophy. *Nature genetics* **36**, 850-854 (2004).

157. Thompson, D.A., *et al.* Retinal degeneration associated with RDH12 mutations results from decreased 11-cis retinal synthesis due to disruption of the visual cycle. *Human molecular genetics* **14**, 3865-3875 (2005).

158. Morisseau, C. & Hammock, B.D. Epoxide hydrolases: mechanisms, inhibitor designs, and biological roles. *Annual review of pharmacology and toxicology* **45**, 311-333 (2005).

159. Bucci, M., Roviezzo, F., Cicala, C., Sessa, W.C. & Cirino, G. Geldanamycin, an inhibitor of heat shock protein 90 (Hsp90) mediated signal transduction has anti-

inflammatory effects and interacts with glucocorticoid receptor in vivo. *British journal of pharmacology* **131**, 13-16 (2000).

160. Rice, J.W., *et al.* Small molecule inhibitors of Hsp90 potently affect inflammatory disease pathways and exhibit activity in models of rheumatoid arthritis. *Arthritis and rheumatism* **58**, 3765-3775 (2008).

161. Cala, S.E. & Jones, L.R. GRP94 resides within cardiac sarcoplasmic reticulum vesicles and is phosphorylated by casein kinase II. *The Journal of biological chemistry* **269**, 5926-5931 (1994).

162. Srivastava, P.K. Peptide-binding heat shock proteins in the endoplasmic reticulum: role in immune response to cancer and in antigen presentation. *Advances in cancer research* **62**, 153-177 (1993).

163. Marzec, M., Eletto, D. & Argon, Y. GRP94: An HSP90-like protein specialized for protein folding and quality control in the endoplasmic reticulum. *Biochimica et biophysica acta* **1823**, 774-787 (2012).

164. Reed, R.C. & Nicchitta, C.V. Chaperone-mediated cross-priming: a hitchhiker's guide to vesicle transport (review). *International journal of molecular medicine* **6**, 259-264 (2000).

165. Ma, Y. & Hendershot, L.M. The role of the unfolded protein response in tumour development: friend or foe? *Nature reviews. Cancer* **4**, 966-977 (2004).

166. Ni, M. & Lee, A.S. ER chaperones in mammalian development and human diseases. *FEBS letters* **581**, 3641-3651 (2007).

167. Luo, B. & Lee, A.S. The critical roles of endoplasmic reticulum chaperones and unfolded protein response in tumorigenesis and anticancer therapies. *Oncogene* **32**, 805-818 (2013).

168. Reddy, R.K., Lu, J. & Lee, A.S. The endoplasmic reticulum chaperone glycoprotein GRP94 with Ca(2+)-binding and antiapoptotic properties is a novel proteolytic target of calpain during etoposide-induced apoptosis. *The Journal of biological chemistry* **274**, 28476-28483 (1999).

169. Song, H.Y., Dunbar, J.D., Zhang, Y.X., Guo, D. & Donner, D.B. Identification of a protein with homology to hsp90 that binds the type 1 tumor necrosis factor receptor. *The Journal of biological chemistry* **270**, 3574-3581 (1995).

170. Maddalena, F., *et al.* Resistance to paclitxel in breast carcinoma cells requires a quality control of mitochondrial antiapoptotic proteins by TRAP1. *Molecular oncology* **7**, 895-906 (2013).

171. Cechetto, J.D. & Gupta, R.S. Immunoelectron microscopy provides evidence that tumor necrosis factor receptor-associated protein 1 (TRAP-1) is a mitochondrial protein which also localizes at specific extramitochondrial sites. *Experimental cell research* **260**, 30-39 (2000).

172. Takemoto, K., Miyata, S., Takamura, H., Katayama, T. & Tohyama, M. Mitochondrial TRAP1 regulates the unfolded protein response in the endoplasmic reticulum. *Neurochemistry international* **58**, 880-887 (2011).

173. Kang, B.H., *et al.* Regulation of tumor cell mitochondrial homeostasis by an organelle-specific Hsp90 chaperone network. *Cell* **131**, 257-270 (2007).

174. Chen, C.F., *et al.* A new member of the hsp90 family of molecular chaperones interacts with the retinoblastoma protein during mitosis and after heat shock. *Molecular and cellular biology* **16**, 4691-4699 (1996).

175. Landriscina, M., *et al.* Mitochondrial chaperone Trap1 and the calcium binding protein Sorcin interact and protect cells against apoptosis induced by antiblastic agents. *Cancer research* **70**, 6577-6586 (2010).

176. Masuda, Y., *et al.* Involvement of tumor necrosis factor receptor-associated protein 1 (TRAP1) in apoptosis induced by beta-hydroxyisovalerylshikonin. *The Journal of biological chemistry* **279**, 42503-42515 (2004).

177. Montesano Gesualdi, N., *et al.* Tumor necrosis factor-associated protein 1 (TRAP-1) protects cells from oxidative stress and apoptosis. *Stress* **10**, 342-350 (2007).

178. Leav, I., *et al.* Cytoprotective mitochondrial chaperone TRAP-1 as a novel molecular target in localized and metastatic prostate cancer. *The American journal of pathology* **176**, 393-401 (2010).

179. Costantino, E., *et al.* TRAP1, a novel mitochondrial chaperone responsible for multi-drug resistance and protection from apoptotis in human colorectal carcinoma cells. *Cancer letters* **279**, 39-46 (2009).

180. Patel, P.D., *et al.* Paralog-selective Hsp90 inhibitors define tumor-specific regulation of HER2. *Nature chemical biology* **9**, 677-684 (2013).

181. Kang, B.H., *et al.* Combinatorial drug design targeting multiple cancer signaling networks controlled by mitochondrial Hsp90. *The Journal of clinical investigation* **119**, 454-464 (2009).

182. Siegelin, M.D., *et al.* Exploiting the mitochondrial unfolded protein response for cancer therapy in mice and human cells. *The Journal of clinical investigation* **121**, 1349-1360 (2011).

183. Cummings, M.D., Farnum, M.A. & Nelen, M.I. Universal screening methods and applications of ThermoFluor. *Journal of biomolecular screening* **11**, 854-863 (2006).

184. Niesen, F.H., Berglund, H. & Vedadi, M. The use of differential scanning fluorimetry to detect ligand interactions that promote protein stability. *Nature protocols* **2**, 2212-2221 (2007).

185. Pantoliano, M.W., *et al.* High-density miniaturized thermal shift assays as a general strategy for drug discovery. *Journal of biomolecular screening* **6**, 429-440 (2001).

186. Haystead, T.A. The purinome, a complex mix of drug and toxicity targets. *Current topics in medicinal chemistry* **6**, 1117-1127 (2006).

187. Luo, W., Rodina, A. & Chiosis, G. Heat shock protein 90: translation from cancer to Alzheimer's disease treatment? *BMC neuroscience* **9 Suppl 2**, S7 (2008).

188. Salminen, A., Ojala, J., Kaarniranta, K., Hiltunen, M. & Soininen, H. Hsp90 regulates tau pathology through co-chaperone complexes in Alzheimer's disease. *Progress in neurobiology* **93**, 99-110 (2011).

189. Shen, Y., He, P., Zhong, Z., McAllister, C. & Lindholm, K. Distinct destructive signal pathways of neuronal death in Alzheimer's disease. *Trends in molecular medicine* **12**, 574-579 (2006).

190. Sekine, Y., Takeda, K. & Ichijo, H. The ASK1-MAP kinase signaling in ER stress and neurodegenerative diseases. *Current molecular medicine* **6**, 87-97 (2006).

191. Monaco, E.A., 3rd. Recent evidence regarding a role for Cdk5 dysregulation in Alzheimer's disease. *Current Alzheimer research* **1**, 33-38 (2004).

192. Thomaidou, D. & Patsavoudi, E. Identification of a novel neuron-specific surface antigen in the developing nervous system, by monoclonal antibody 4C5. *Neuroscience* **53**, 813-827 (1993).

193. Thomaidou, D., Yfanti, E. & Patsavoudi, E. Expression of the 4C5 antigen during development and after injury of the rat sciatic nerve. *Journal of neuroscience research* **46**, 24-33 (1996).

194. Yfanti, E., Sidera, K., Margaritis, L.H. & Patsavoudi, E. The 4C5 antigen is associated with Schwann cell migration during development and regeneration of the rat peripheral nervous system. *Glia* **45**, 39-53 (2004).

195. Basu, S. & Srivastava, P.K. Calreticulin, a peptide-binding chaperone of the endoplasmic reticulum, elicits tumor- and peptide-specific immunity. *The Journal of experimental medicine* **189**, 797-802 (1999).

196. Tamura, Y., Peng, P., Liu, K., Daou, M. & Srivastava, P.K. Immunotherapy of tumors with autologous tumor-derived heat shock protein preparations. *Science* **278**, 117-120 (1997).

197. Binder, R.J. & Srivastava, P.K. Peptides chaperoned by heat-shock proteins are a necessary and sufficient source of antigen in the cross-priming of CD8+ T cells. *Nature immunology* **6**, 593-599 (2005).

198. Suto, R. & Srivastava, P.K. A mechanism for the specific immunogenicity of heat shock protein-chaperoned peptides. *Science* **269**, 1585-1588 (1995).

199. Blachere, N.E., *et al.* Heat shock protein-peptide complexes, reconstituted in vitro, elicit peptide-specific cytotoxic T lymphocyte response and tumor immunity. *The Journal of experimental medicine* **186**, 1315-1322 (1997).

200. Imai, T., *et al.* Heat shock protein 90 (HSP90) contributes to cytosolic translocation of extracellular antigen for cross-presentation by dendritic cells. *Proceedings of the National Academy of Sciences of the United States of America* **108**, 16363-16368 (2011).

201. Wassenberg, J.J., Dezfulian, C. & Nicchitta, C.V. Receptor mediated and fluid phase pathways for internalization of the ER Hsp90 chaperone GRP94 in murine macrophages. *Journal of cell science* **112 (Pt 13)**, 2167-2175 (1999).

202. Theriault, J.R., Adachi, H. & Calderwood, S.K. Role of scavenger receptors in the binding and internalization of heat shock protein 70. *J Immunol* **177**, 8604-8611 (2006).

203. Murshid, A., Gong, J. & Calderwood, S.K. Heat shock protein 90 mediates efficient antigen cross presentation through the scavenger receptor expressed by endothelial cells-I. *J Immunol* **185**, 2903-2917 (2010).

204. Basu, S., Binder, R.J., Suto, R., Anderson, K.M. & Srivastava, P.K. Necrotic but not apoptotic cell death releases heat shock proteins, which deliver a partial maturation signal to dendritic cells and activate the NF-kappa B pathway. *Int Immunol* **12**, 1539-1546 (2000).

205. Pawaria, S. & Binder, R.J. CD91-dependent programming of T-helper cell responses following heat shock protein immunization. *Nature communications* **2**, 521 (2011).

206. Zhou, Y.J., Messmer, M.N. & Binder, R.J. Establishment of Tumor-Associated Immunity Requires Interaction of Heat Shock Proteins with CD91. *Cancer immunology research* **2**, 217-228 (2014).

207. Herz, J. & Strickland, D.K. LRP: a multifunctional scavenger and signaling receptor. *The Journal of clinical investigation* **108**, 779-784 (2001).

208. Herz, J. & Bock, H.H. Lipoprotein receptors in the nervous system. *Annu Rev Biochem* **71**, 405-434 (2002).

209. Sid, B., *et al.* Human thyroid carcinoma cell invasion is controlled by the low density lipoprotein receptor-related protein-mediated clearance of urokinase plasminogen activator. *The international journal of biochemistry & cell biology* **38**, 1729-1740 (2006).

210. Dedieu, S., *et al.* LRP-1 silencing prevents malignant cell invasion despite increased pericellular proteolytic activities. *Molecular and cellular biology* **28**, 2980-2995 (2008).

211. Kancha, R.K., Stearns, M.E. & Hussain, M.M. Decreased expression of the low density lipoprotein receptor-related protein/alpha 2-macroglobulin receptor in invasive cell clones derived from human prostate and breast tumor cells. *Oncology research* **6**, 365-372 (1994).

212. Li, Y., Wood, N., Grimsley, P., Yellowlees, D. & Donnelly, P.K. In vitro invasiveness of human breast cancer cells is promoted by low density lipoprotein receptor-related protein. *Invasion & metastasis* **18**, 240-251 (1998).

213. Wijnberg, M.J., Quax, P.H., Nieuwenbroek, N.M. & Verheijen, J.H. The migration of human smooth muscle cells in vitro is mediated by plasminogen activation and can be inhibited by alpha2-macroglobulin receptor associated protein. *Thrombosis and haemostasis* **78**, 880-886 (1997).

214. Chazaud, B., *et al.* Promigratory effect of plasminogen activator inhibitor-1 on invasive breast cancer cell populations. *The American journal of pathology* **160**, 237-246 (2002).

215. Catasus, L., *et al.* Low-density lipoprotein receptor-related protein 1 is associated with proliferation and invasiveness in Her-2/neu and triple-negative breast carcinomas. *Human pathology* **42**, 1581-1588 (2011).

216. Catasus, L., *et al.* Low-density lipoprotein receptor-related protein 1 (LRP-1) is associated with highgrade, advanced stage and p53 and p16 alterations in endometrial carcinomas. *Histopathology* **59**, 567-571 (2011).

217. Li, Y. & Reynolds, R.C. A Tumor and Metastasis Promoter or Suppressor? 1:e121. doi:10.4172/2167-0501.1000e121. *Biochem Pharmacol* **1**(2012).

218. Montel, V., Gaultier, A., Lester, R.D., Campana, W.M. & Gonias, S.L. The low-density lipoprotein receptor-related protein regulates cancer cell survival and metastasis development. *Cancer research* **67**, 9817-9824 (2007).

219. Song, H., Li, Y., Lee, J., Schwartz, A.L. & Bu, G. Low-density lipoprotein receptor-related protein 1 promotes cancer cell migration and invasion by inducing the expression of matrix metalloproteinases 2 and 9. *Cancer research* **69**, 879-886 (2009).

220. Woodley, D.T.*, et al.* Participation of the lipoprotein receptor LRP1 in hypoxia-HSP90alpha autocrine signaling to promote keratinocyte migration. *Journal of cell science* **122**, 1495-1498 (2009).

221. Hance, M.W., Nolan, K.D. & Isaacs, J.S. The double-edged sword: conserved functions of extracellular hsp90 in wound healing and cancer. *Cancers* **6**, 1065-1097 (2014).

222. Clayton, A., Turkes, A., Navabi, H., Mason, M.D. & Tabi, Z. Induction of heat shock proteins in B-cell exosomes. *Journal of cell science* **118**, 3631-3638 (2005).

223. Yu, X., Harris, S.L. & Levine, A.J. The regulation of exosome secretion: a novel function of the p53 protein. *Cancer research* **66**, 4795-4801 (2006).

224. Hance, M.W.*, et al.* Secreted Hsp90 is a novel regulator of the epithelial to mesenchymal transition (EMT) in prostate cancer. *The Journal of biological chemistry* **287**, 37732-37744 (2012).

225. Cheng, C.F.*, et al.* A fragment of secreted Hsp90alpha carries properties that enable it to accelerate effectively both acute and diabetic wound healing in mice. *The Journal of clinical investigation* **121**, 4348-4361 (2011).

226. Chun, J.H. & Pike, V.W. Regiospecific syntheses of functionalized diaryliodonium tosylates via [hydroxy(tosyloxy)iodo]arenes generated in situ from (diacetoxyiodo)arenes. *The Journal of organic chemistry* **77**, 1931-1938 (2012).

227. Koziorowski, J., Henssen, C. & Weinreich, R. A new convenient route to radioiodinated N-succinimidyl 3- and 4-iodobenzoate, two reagents for radioiodination of proteins. *Appl Radiat Isotopes* **49**, 955-959 (1998).

Biography

Place and Date of Birth

St. Anthony, Idaho
September 17, 1981

Education

2014 Duke University – Doctor of Philosophy
2008 Brigham Young University – Masters of Science
2006 Brigham Young University-Idaho – Bachelors of Science

Publications

Optical and Radioiodinated Tethered Hsp90 Inhibitors Reveal Selective Internalization of Ectopic Hsp90 in Malignant Breast Tumor Cells. Cell Chem Bio. 2013.

Hsp90, an unlikely ally in the war on cancer. FEBS Journal. 2013.

A highly selective Hsp90 affinity chromatography resin with a cleavable linker. Bioorganic Medicinal Chemistry. 2012.

Deletion of mouse Porcn blocks Wnt ligand secretion and reveals an ectodermal etiology of human focal dermal hypoplasia/Goltz syndrome. PNAS. 2011.

Honors and Awards

Robert J. Fitzgerald Scholar Award